University of Reading
Department of Mathematics and Statistics

Unstable Periodic Orbits: a language to interpret the complexity of chaotic systems

Candidate: Chiara Cecilia Maiocchi
Supervisors: Valerio Lucarini, Andrey Gritsun

A thesis submitted in partial fulfillment of the requirements for the degree of
Doctor of Philosophy in Mathematics, October 2022

Dedication

A Cerri, che è con me ancora ogni giorno.

Contents

Abstract

Unstable periodic orbits (UPOs), exact periodic solutions of the evolution equation, offer a very powerful framework for studying chaotic dynamical systems, as they allow one to dissect their dynamical structure. UPOs can be considered the skeleton of chaotic dynamics, its essential building blocks. In fact, it is possible to prove that in a chaotic system, UPOs are dense in the attractor, meaning that it is always possible to find a UPO arbitrarily near any chaotic trajectory. We can thus think of the chaotic trajectory as being approximated by different UPOs as it evolves in time, jumping from one UPO to another as a result of their instability.

In this thesis we provide a contribution towards the use of UPOs as a tool to understand and distill the dynamical structure of chaotic dynamical systems. We will focus on two models, characterised by different properties, the Lorenz-63 and Lorenz-96 model.

The process of approximation of a chaotic trajectory in terms of UPOs will play a central role in our investigation. In fact, we will use this tool to explore the properties of the attractor of the system under the lens of its UPOs.

In the first part of the thesis we consider the Lorenz-63 model with the classic parameters' value. We investigate how a chaotic trajectory can be approximated using a complete set of UPOs up to symbolic dynamics' period 14. At each instant in time, we rank the UPOs according to their proximity to the position of the orbit in the phase space. We study this process from two different perspectives. First, we find that longer period UPOs overwhelmingly provide the best local approximation to the trajectory. Second, we construct a finite-state Markov chain by studying the scattering of the trajectory between the neighbourhood of the various UPOs. Each UPO and its neighbourhood are taken as a possible state of the system. Through the analysis of the subdominant eigenvectors of the corresponding stochastic matrix we provide a different interpretation of the mixing processes occurring in the system by taking advantage of the concept of quasi-invariant sets.

In the second part of the thesis we provide an extensive numerical investigation of the variability of the dynamical properties across the attractor of the much studied Lorenz '96 dynamical system. By combining the Lyapunov analysis of the tangent space with the study of the shadowing of the chaotic trajectory performed by a very large set of unstable periodic orbits, we show that the observed variability in the number of unstable dimensions, which shows a

serious breakdown of hyperbolicity, is associated with the presence of a substantial number of finite-time Lyapunov exponents that fluctuate about zero also when very long averaging times are considered.

Chapter 1

Introduction

1.1 Motivation and Objectives

Until the 19th century it was commonly believed that an unpredictable behaviour could not arise from deterministic systems. Instead, even deterministic systems, as simple as a double pendulum, can exhibit a sensitive dependence on the initial condition, meaning that trajectories associated with imperceptibly different starting points can end up with extremely different outcomes. From a practical level, this observation implies that every prediction based on a chaotic model will turn to be exponentially wrong in time, since any measurement of the current state is intrinsically associated to some uncertainty.

It seems that, within this context, the quest for an accurate prediction would represent an almost impossible challenge. A statistical approach comes to the rescue: if, instead of focusing on single trajectories, one moves the attention to the evolution of densities, it is possible to gain the sought predictive power. A breakthrough in the understanding of chaotic dynamics was represented by a shift of perspective in the way of looking at complex chaotic systems. From this perspective, dynamics can be interpreted as a walk through repeating shapes. More formally, this repeating patterns are exact periodic solutions of the evolution equations, the unstable periodic orbits of the system (UPOs), islets of order in the sea of chaos, and can

be used to reconstruct the statistical features of a dynamical system [1, 2, 3]. In fact, under particular assumptions that will be later discussed (see chapter 2), UPOs can be proved to be dense in the attractor of the system, which, roughly speaking, is the set of states toward which a system tends to evolve. Such topological property implies that it is always possible to find a UPO arbitrarily near the chaotic trajectory up to any arbitrary accuracy. We can thus think of the chaotic trajectory as being approximated by different UPOs as it evolves in time, jumping from one UPO to another as a result of their instability.

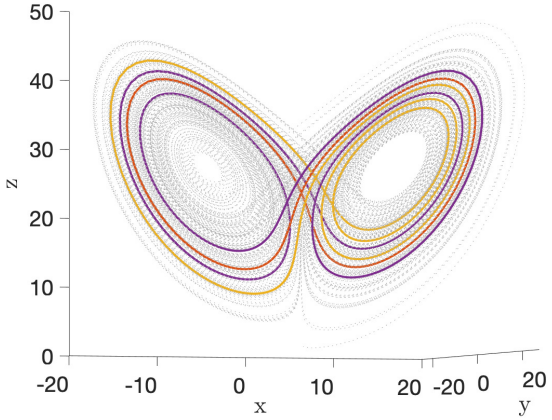

Figure 1.1: Example of UPOs in the attractor of the Lorenz-63 system (see chapter 3 for more details on the model). A typical chaotic trajectory (dotted in gray) can be approximated by UPOs (we represented three different UPOs in solid purple, orange and yellow) in different points of its evolution. The property of density of the UPOs in the attractor allows to choose a UPO arbitrarly close to the chaotic trajectory.

For a specific class of "well behaved" chaotic systems characterised by the presence of expanding and contracting direction of the derivative, the Uniformly Hyperbolic and Axiom A systems (see chapter 2 for more details), there exists a rigorous theory where UPOs are used as a mean to calculate the statistical properties of the system. Namely, through the so-called trace formulas, it is possible to write ergodic averages of observables as weighted sums over the full set of UPOs. In this sense, UPOs can be seen as a rigid skeleton hidden in the chaos of the dynamics [4, 5, 6].

A formal extension of a UPO based analysis of spatio-temporal chaos and high dimensional systems is still a far-reaching goal, but promising steps have been made in this direction, allowing to successfully understand and characterise macroscopic features in turbulent flows in terms of UPOs [7, 8, 9, 10].

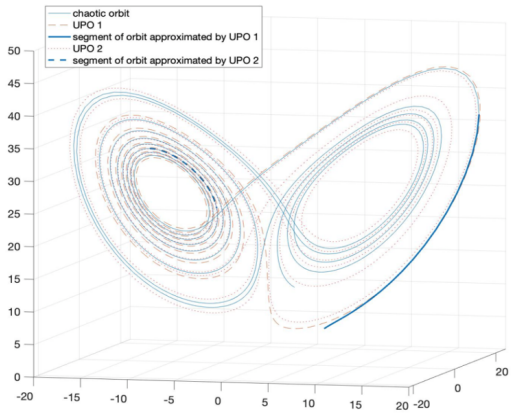

(a)

Figure 1.2: Shadowing of a segment of chaotic trajectory in the Lorenz-63 model. The chaotic trajectory is approximated in different instant of times by two different UPOs, chosen so that they would minimise the distance with the chaotic trajectory among all orbits of the database.

The aim of this thesis is to use the language of UPOs to provide a description of the geometrical (quasi-invariant set, tangent space) and statistical (ergodic averages of observables) properties of the system. Through the use of this language it is in fact possible to develop a duality between the local, topological, short time dynamically invariant compact sets (equilibria, UPOs) and the global long-time evolution of densities of trajectories. Specifically, we will look at the Lorenz-63 model and, building up in complexity, at the Lorenz-96 model.

Central in the investigation of both model will be the process of approximation of a chaotic trajectory in terms of UPOs (ranked shadowing). It is in fact our chosen way to explore the geometry of the attractor under the lens of its UPOs. At each instant of time the trajectory can be best approximated by a UPO of the database, and as it evolves in time it jumps from one UPO to the other because of their instability. In this sense the rank shadowing can be seen as a scattering process where the scatterers are the UPOs (Fig 1.2 and 1.3).

The Lorenz-63 model with classical parameters' value is an example of an almost everywhere uniformly hyperbolic system in a three dimensional phase space. In the first part of the thesis we show that UPOs can be used to distill the dynamical and statistical properties of the sys-

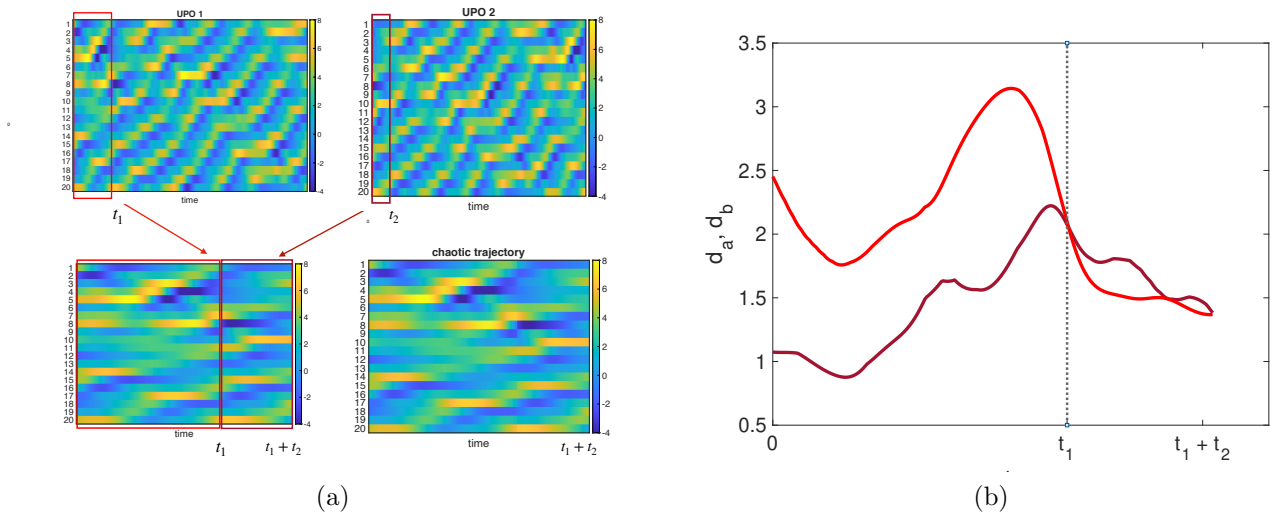

(a) (b)

Figure 1.3: Panel (a): Ranked shadowing of a segment of chaotic trajectory shadowed by two different UPOs (here UPO1 and UPO2) in the Lorenz-96 model (See chapter 4 for an extensive discussion). We represent the segment of trajectory with a space-time diagram, where the value assumed by each component over time is represented with different colours. UPO1 (UPO2) have period $T_1 = 10.8748$ ($T_2 = 10.7626$) and possesses 5 (4) positive LEs. Their space-time diagram over the full period showed in the first row. The chaotic trajectory (second row, right side) is shadowed by UPO1 (bright red) for a time duration $t_1 = 1.78$ and then by UPO2 (dark red) for a time duration $t_2 = 0.87$. It is possible to see how the pattern of the shadowing UPOs within the shadowing window resembles the space pattern of the chaotic trajectory. Panel (b): distance between the chaotic trajectory and the two UPOs.

tem. By assuming this perspective on the problem, we show that, on the one side, longer UPOs have the lion's share in reproducing the invariant measure on the system. On the other side, we construct a finite-state Markov chain where each UPO and its immediate neighborhood are considered as a possible state of the system and the scattering represents transitions between states. Through the study of the spectral properties of the discretised transfer operator, we obtain a partition of the phase space in different bundle of UPOs, each one identifying a quasi-invariant set, showing that UPOs can represent a valid tool to investigate diffusion properties of the system.

In the second part of the project we extend this analysis to the more complex Lorenz-96 system, characterised by higher dimension and variability in the number of unstable dimensions (characteristic that because of the constraint imposed by dimensionality and chaoticity was not present in the Lorenz-63 model). The fact that different regions of the phase space might

be characterised by different dimensions of the unstable manifold represents a breakdown of the hyperbolicity condition through the so called mechanism of unstable dimension variability (UDV) [11, 12, 13]. We first show that, as expected, UDV manifests itself through the presence of certain Finite Time Lyapunov exponents that exhibit large fluctuations between positive and negative values. We successively provide an interpretation of such variability in terms of UPOs, bridging the gap between local and global properties of the system. Namely, we found that anomalously unstable UPOs preferentially populates regions of the attractor which are detected to be anomalously unstable through Lyapunov analysis.

Our motivation stems from climate studies. We believe that periodic orbit theory represents a valid investigation tool in the realm of climate systems. Lucarini and Gritsun already showed that different regimes of motion in a baroclinic model of the atmosphere, blocking vs zonal, can be characterised by UPOs having different stability properties. Specifically, they found that blocked states are associated with conditions of higher instability of the atmosphere, in agreement with a separate line of evidence [14]. In further studies, we would like to address the techniques developed in this thesis to more realistic and complex atmospheric models and analyse the connection between UPOs and linear response of the system to external perturbations.

1.2 Outline of the thesis

This thesis is structured as follow. Chapter 2 is devoted to the introduction of the mathematical framework necessary to describe the main results of this work. We describe general features of chaotic dynamics and introduce relevant dynamical tools. We discuss the evolution and applications of periodic orbit theory and present numerical methods that were instrumental in the development of the results presented in this thesis. In chapter 3 we consider the model Lorenz-63 and investigate how a long forward chaotic trajectory can be approximated using a complete set of UPOs up to symbolic dynamics' period 14. We will show that such process helps elucidate how a generic ensamble of initial conditions converges to the invariant measure

through diffusion and provides a new interpretation of quasi-invariant sets of the systems in terms of UPOs. In chapter 4 we investigate the heterogeneity of the attractor of the Lorenz-96 model. We present evidence of unstable dimension variability through the extraction of a database of UPO that exhibits very different stability properties. Such variability is reflected in the behaviour of some Finite Time Lyapunov exponents, that oscillates between positive and negative values. We will explain this variability in terms of UPOs. In chapter 5 we summarise the main results and outline perspectives for future research.

1.3 Statement of Originality and Publications

I declare that this thesis is my own work and that work by others has been properly referenced.

The thesis is based on the following publications:

- Chiara Cecilia Maiocchi, Valerio Lucarini, and Andrey Gritsun. *Decomposing the dynamics of the lorenz 1963 model using unstable periodic orbits: Averages, transitions, and quasi-invariant sets.* Chaos: An Interdisciplinary Journal of Nonlinear Science, 32(3):033129, 2022.

- Chiara Cecilia Maiocchi, Valerio Lucarini, Andrey Gritsun, and Yuzuru Sato. *Heterogeneity of the attractor of the Lorenz'96 model.* In preparation, 2022

Chapter 2

Background theory

2.1 Chaotic dynamics

A deterministic system is defined as a system whose present state is in principle fully determined by its initial conditions. This is in contrast to stochastic systems, where the initial condition only partially determines the future state: the present state is in fact obtained as image of the past initial condition plus a particular realisation of the noise encountered along the way. With the discovery of deterministic chaos, it appeared clear that the behaviour of a deterministic system could resemble the unpredictable behaviour typical of stochastic systems. So how do we define chaos exactly? The attribute *chaotic* refers to the fact that the system obeys a deterministic law of evolution, but at the same time exhibits sensitive dependence to initial conditions, meaning that given two imperceptibly close points in phase space, their relative trajectory will separate exponentially fast in time. Such property has dramatic consequences over the predictability of the system. In fact, during a finite time, the separation of the trajectories attains a distance which is comparable to the "size" of the attractor, resulting in the impossibility of making prediction over a finite time horizon.

The other essential condition that characterises deterministic chaos is mixing. In a mixing system, any open set of initial conditions will overlap with any other finite region in a finite time, spreading entirely over the phase space. In a chaotic system the trajectories separate locally,

but the asymptotic dynamics remains confined in a finite region of the space, constraining the separated trajectories to be folded and to get back again, infinitely many times. We can think of this process as the one necessary to prepare puff pastry: a block of butter needs to be finely layered inside a dough ball and to do so, the dough is stretched and folded back many times. The butter uniformly diffuses inside the dough and initially close sections of butter and dough separates exponentially. From this perspective, the quest of predicting the future state of individual trajectories is out of reach, but a new, statistical, view on the problem is developed, shifting our attention from trajectories to evolution of densities. Namely, with periodic orbit theory [1], the precise prediction of individual trajectories - doomed to fail due to the chaoticity of the system - is replaced by the study of the evolution of densities, intended as averages over the space of all possible outcomes. The dynamics of densities of trajectories is then described in terms of evolution operators. In the evolution operator formalism, such averages are given by exact formulas, the so called trace formulas (see later discussion).

In this section we introduce the essential concepts of nonlinear and chaotic dynamics, necessary to develop the language in which the results of this thesis are described. We review different mathematical frameworks that have been designed to contain and describe chaotic behaviour that provide different degrees of stringency on the chaotic behaviour of the system. We will be interested in the long term dynamics after chaotic transients, that happens on a closed subset such that for "many" choices of initial points, the system will evolve towards to. Such set is the so-called *attractor*. We formally introduce the notion of chaotic attractor and present different methods to quantify its size. Since we will be interested in averages, we define the weights used for the averaging, introducing the concept of invariant measure. In particular we will describe the properties of a special class of measures, which is particularly relevant for the study of systems of practical physical interest. We then introduce the transfer operator, instrumental for describing how densities evolves in the phase space. Finally, we define the Lyapunov exponents and their finite time counterpart, dynamical indicators that quantify the sensitive dependence on the initial conditions of the system.

2.1.1 Dynamical Systems

Dynamical systems describe the evolution of a physical system in time. The goal of dynamics, broadly speaking, is to describe the asymptotic evolution of a system for which only an "infinitesimal" evolution rule is known. With asymptotic evolution we refer to the long-term behaviour of the system as time goes to infinity, it is the behaviour that the system approaches as it settles into a steady state. More precisely, a dynamical system is defined by the pair $(\mathcal{M}, \phi)$, where $\mathcal{M}$ is a manifold describing all the admissible states of the system and $\phi^t : \mathcal{M} \to \mathcal{M}$ is an evolution rule, that indicates where a point $x \in \mathcal{M}$ lands in $\mathcal{M}$ after a time interval t. In this thesis we will consider continuous autonomous dynamical systems that can be described by a set of ordinary differential equations (ODE):

$$\dot{x} = \frac{dx}{dt} = f(x). \tag{2.1}$$

The time parameter is a real variable $t \in \mathbb{R}$, and f depends only implicitly on the time t.

The evolution in time of an initial condition $x_0 = x(0)$ at time $t_0 = 0$ is traced out in phase space by the solution of the ODEs system. It can be conveniently expressed through the evolution operator S^t as

$$S^t : x_0 \to x(x_0, t) \tag{2.2}$$

that describes the evolution of the point x_0 at time t. We call *orbit* of x_0 the totality of states that can be reached from x_0. An orbit can be *stationary*, if $S^t(x) = x \ \forall t$, *periodic*, if $S^t(x) = S^{t+T_p}(x)$ for a given minimum period T_p, or *aperiodic* if $S^t(x) \neq S^{t'}(x) \ \forall t \neq t'$. An orbit is an example of dynamically invariant notion, in fact its points are only shifted as we move through time, but the set remains unchanged.

In general, the concept of invariant set is very relevant in dynamical systems, as they provide a way to understand its long-term behaviour. An invariant set is a subset of the state space of the system that is preserved under its evolution. This implies that if a point in the set is initially in the set, it will remain in the set for all future times. Examples of invariant sets include fixed points, periodic orbits and strange attractors. The study of the existence, stability and

location of such sets can be instrumental in gaining an insight into the long-term dynamics of the system: for instance, the stability of a fixed point can determine whether the system converges to a particular state or oscillates around it.

2.1.2 Different frameworks to describe chaotic behaviour

In Chapter 4 of his book Science and Méthode [15], Poincaré proposed for the first time the concept of sensitive dependence of the evolution of a system on its initial conditions, making also explicit reference to the relevance of this issue in the context of Meteorology [16]. Poincaré in fact understood that the local instability of trajectories is closely related to the statistical properties of the system. A "typical" trajectory of chaotic systems distributes over the phase space in a very ravelled and complex way, so that trajectories are forced to mix (but never cross). Successively, Hadamard returned onto these ideas by investigating the properties of geodesic flows on surfaces of negative curvature [17]. Historically, the idea of hyperbolicity was given by associating the behaviour nearby any fixed trajectory to the one characteristic of trajectories nearby a saddle point [18]. Throughout the thirties of last century Hedlund [19], Hopf [20] and others continued the study on geodesic flows on some types of compact Riemannian manifolds with negative curvature, this time having ergodicity properties as their main focus, and confirming the relevant role played by the instability of trajectories in the characterisation of the system. The condition of hyperbolicity was finally formulated for the first time by Anosov [21] and used as basic assumption for further results: hyperbolic behaviour was specified by providing infinitesimal conditions on the differential of the dynamical system, according to which in an uniformly hyperbolic system the tangent space can be decomposed at every point $x \in \mathcal{M}$ in two subspaces E_{1x} and E_{2x} (if the system is a flow an additional subspace corresponding to the direction of the direction of the motion should be added) so that the differential maps of the flow restricted to the subspaces E_{1x} and E_{2x} are a contraction and an expansion with coefficients that are uniform with respect to the phase space. In particular, Anosov proved the ergodicity of such flows, which were later named after him as "Anosov flows". Uniform hyperbolicity, as defined by Anosov, was conjectured to be the default condition for

systems featuring sensitive dependence on initial conditions [22, 23, 21]. This idea stems from the fact that hyperbolic dynamics is robust with respect to perturbations [24]. More precisely, Smale and others, conjectured that any chaotic dynamical systems could be transformed into an hyperbolic system by applying an appropriate perturbation. As a result of this conjecture, it would be possible to identify any chaotic behaviour emerging in a mathematical model of a physical process with a uniformly hyperbolic system. The study of uniformly hyperbolic dynamics that stemmed after the seminal results of Pesin and Anosov was incredibly useful for the development of the theoretical structure and toolset needed to describe and study chaotic dynamics. However, the definition of Anosov diffeomorfism was way too stringent for it to realistically capture the variety of "chaotic" behaviour present in the applications. In fact, from the point of view of the applications, the theoretical and practical relevance of the phenomenon of sensitive dependence on initial conditions and its compatibility with the presence of orbits contained in a compact set became apparent arguably through the seminal contributions by Lorenz [25], Ruelle and Takens [26], and Li and Yorke [27]. Since then, there has been a great effort in creating sophisticated mathematical frameworks for chaotic systems able to include, at the same time, phenomenology of practical relevance in science and engineering. One of the first generalisations of the concept of uniformly hyperbolic dynamics is to consider systems that present exponential contraction and expansion without necessary admitting a uniform bounds in the rates of growth and decay.

Such systems are known as nonuniform hyperbolic systems and they are subject of the study of the so-called Pesin's theory [18]. Pesin's theory had a huge impact in the applications, since it provides a characterisation of nonuniformly hyperbolic system in terms of their Lyapunov exponents ([18], Def. 1.5), which became later accessible thanks to the contribution of Benettin et al. [28] Many of the properties of uniformly hyperbolic systems are retained by nonuniformly hyperbolic systems, such as positive entropy and strong ergodic properties.

Another way to generalise the notion of uniform hyperbolicity entails introducing a nontrivial centre manifold in the tangent space where expansion or contraction are extremely slow, thus removing hyperbolicity. The so-defined partial hyperbolic systems can be further generalized by allowing for nonuniformity outside the centre manifold: the continuous-time nonuniform

partially hyperbolic systems feature more than one zero Lyapunov exponents [29].

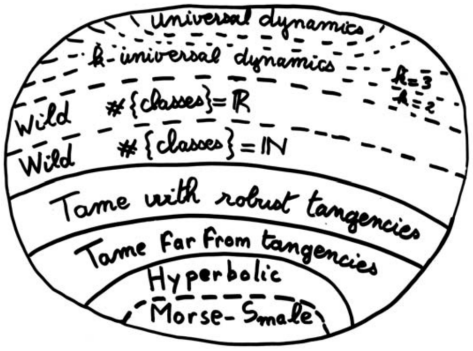

Figure 2.1: Conjectural map of $Diff(\mathcal{M})$. Figure and caption are from [30].

Yet another revolution took place in the last decades, with the ambitious goal of building a theory for "most" dynamical systems. A very influential attempt at creating a powerful paradigm of chaos beyond uniform hyperbolicity has been presented by Bonatti et al. [31]. According to such a paradigm, chaos can originate from very different mechanisms, such as heterodimensional cycles or homoclinic tangencies, originating different types of "non-hyperbolicity". As compared to uniformly hyperbolic systems, these more general systems are less understood and advances have been mainly made on discrete dynamical systems, because of the simpler structure of the phase space [22], hence numerical approaches play an important role in shedding light on the global organisation of phase space [32]. Generalli speaking, Bonatti [30] conjectures that the space of universal dynamics ($Diff(\mathcal{M})$) can be divided into 8 disjoint regions (C^1-open subsets) whose union is C^1-dense (Fig. 2.1).

Uniformly hyperbolic dynamics

Uniformly hyperbolic dynamics exhibits the characteristic behaviour of stretching and folding of trajectories described in the introduction. In fact, as we mentioned earlier, the derivative is characterised by the presence of both contracting and expanding directions that, together with the instability of trajectories, have the effect of creating chaotic motions in a deterministic dynamical systems.

Let [33] $\phi : \mathcal{M} \to \mathcal{M}$ be a diffeomorphism. We say that ϕ is uniformly hyperbolic if for every

$x \in \mathcal{M}$ there is a splitting of the tangent space $T_x\mathcal{M} = E^s(x) \oplus E^u(x)$ and there are constants $C > 0$ and $\lambda \in (0, 1)$ such that for every $n \in \mathbb{N}$ one has

- $||D\phi^n(v) \leq C\lambda^n||v||$, for $v \in E^s(x)$
- $||D\phi^{-n}(v)|| \leq C\lambda^n||v||$, for $v \in E^u(x)$.

where D is the differential of ϕ. The subspaces $E^s(x)$ and $E^u(x)$ are called the stable and unstable subspaces at x. It is worth noticing that as a consequence on this definition the stable and unstable subspaces depends continuously on the point x and are invariant with respect to the flow.

Uniformly hyperbolic diffeomorphism belong to the larger class of Axiom A diffeomorphism. Namely, we say that the diffeomorphism $\phi : \mathcal{M} \to \mathcal{M}$ is an axiom A diffeomorphism [34] if the following two holds:

- the *nonwandering* set of ϕ, $\Gamma(f)$ is a hyperbolic compact set,
- The set of periodic points of ϕ is dense in $\Gamma(f)$.

Axiom A systems are well understood, both from a statistical and geometrical standpoint [31], and a remarkable successful theory has been developed since Smale's first results in the early '60s. We will see in later chapters more example of the relevance of such types of system.

2.1.3 Chaotic attractors

In this thesis we will focus on the study of long term dynamics of chaotic *dissipative systems* ($\nabla \cdot f < 0$) in a finite dimensional phase space. In such systems, the phase space volumes are contracted by time evolution and the dynamics happens on an invariant set called *attractor*. In particular we assume that there is an open set $U \in \mathcal{M}$ which is asymptotically contracted by the time evolution of the system to a compact set Ω. We say that Ω is an *attracting set* (alternatively an *attractor*) with fundamental neighbourhood U if

- there exist a t_0 so that for $t > t_0$, $\forall$ open set $V \supset \Omega$ we have that $S^t U \subset \Omega$;

- $S^t \Omega = \Omega$.

The attractor of a system could also be defined operationally as the set on which experimental points $S^t x$ accumulate for large values of t. When the system is chaotic, the contraction only happens to some directions, while others are stretched at the same time. An attractor characterised by such separation of trajectories (sensitive dependence on the initial conditions) is called *strange attractor*.

One of the most important characterisation of the attractor is its dimension. While in the case of a point, line, area, etc., the definition of dimension is intuitive and straightforward, chaotic attractors are often characterised by a complex geometry, with structures on an arbitrarily fine scale. It is therefore important to define a dimension able to provide a quantitative characterisation of such complicated objects.

Box Counting Dimension

Let us consider a set M in an N-dimensional Cartesian space [35]. We cover the space by a grid of N-dimensional cubes of size length ε. Let $\tilde{N}(\varepsilon)$ be the number of cubes needed to cover M. The box-counting dimension is given by

$$D_0 = \lim_{\varepsilon \to 0} \frac{\ln \tilde{N}(\varepsilon)}{\ln(1/\varepsilon)}. \tag{2.3}$$

2.3 reproduces the common intuition of dimension. In fact, it attributes dimension 0 to a point (it is covered by one cube independently on the size length ε), dimension 1 to a segment (it can be covered by $\tilde{N}(\varepsilon) \approx l/\varepsilon$ with l being the length of the curve), dimension 2 to an area A ($\tilde{N}(\varepsilon) \approx A/\varepsilon^2$), etc... A fractal set is instead characterised by a dimension D_0 ranging between 0 and 1 (see for example the case of the middle third Cantor set, for which $D_0 = \ln 2 / \ln 3$ [36]).

Reny Dimension

A fundamental problem with the box-counting dimension is that it consider all cubes to have the same weight, without taking into account the fact that the system might spend more time in some rather than others. While the box-counting dimension describes the geometry of the set, we would like to introduce a notion of dimension that also takes into account the dynamics of the system.

The concept outlined above can be captured by the definition of *natural measure*. If one looks at the frequencies with which the trajectories visit the different cubes covering the attractor when the length of the trajectory goes to infinity, in the assumption that such frequency do not change when considering a different initial condition for the trajectory except that for a set of measure zero, then, given x_0 in the basin of attraction of Ω, it is possible to define the natural measure of the cube C_i as

$$\mu_i = \lim_{T\to\infty} \frac{\nu(C_i, x_0, T)}{T}, \tag{2.4}$$

where $\nu(C_i, x_0, T)$ is the fraction of time that the trajectory originating from x_0 spends in the cube C_i in the time interval $0 < t < T$.

We now wish to introduce a notion of dimension that takes into account the frequency at which cubes are visited in the limit of an infinite trajectory. Such concept was first introduced by Grassberger [37, 38] and Henstshel and Procaccia [39].

We define [35] the *Reny dimension* D_q as

$$D_q = \frac{1}{1-q} \lim_{\varepsilon\to 0} \frac{\log I(q,\varepsilon)}{\ln(1/\varepsilon)}, \tag{2.5}$$

where

$$I(q,\varepsilon) = \sum_{i=1}^{\tilde{N}(\varepsilon)} \mu_i^q, \tag{2.6}$$

q is continuous index, and the sum is over all the $\tilde{N}(\varepsilon)$ cubes in a grid of unit size ε that covers

the attractor. We can see that for positive values of q, cubes with bigger μ_i weights more in the determination of the dimension D_q. It is interesting to note that when we consider either $q = 0$ or when all the cubes have equal natural measure (independently on q) we retreive 2.3.

Another interesting property is that

$$D_{q_1} \leq D_{q_2} \quad if \quad q_1 > q_2. \tag{2.7}$$

A special meaning has been attributed to D_1, called the *information dimension*, that can be obatined considering the limit $q \to 1$ and applying L'Hopital's rule [35, 40]

$$D_1 = \lim_{\varepsilon \to 0} \frac{\sum_i^{\tilde{N}(\varepsilon)} \mu_i \log \mu_i}{\ln \varepsilon} \tag{2.8}$$

We will see later in section 2.1.6 an important conjecture regarding this quantity.

2.1.4 Defining a physical measure

It appeared clear from previous discussions that one of the possible approaches to overcome the difficulties in the study of chaotic systems is obtained by assuming a statistical perspective on the properties of the system. In particular, from a physical standpoint, we are specifically interested in time averages. In fact, when we look at physical phenomena, we are usually interested in the behaviour of the system over a certain period of time, which can be described through time averages. Ergodic theory offers the appropriate mathematical framework to assume the necessary statistical perspective on chaotic systems, providing practical tools to measure dynamical quantities of interest. Roughly speaking, ergodic theory states that in a certain class of systems, phase space averages equal time averages, and the weights used for such space averages are invariant measures. Selecting the appropriate invariant measure is thus a fundamental matter. A few criteria guide the selection process.

- the chosen measure should be *ergodic*, in order to reproduce well defined time averages;

- the chosen measure should be *physically relevant*, in order to be able to represent experimental time averages (which are affected by a certain level of noise).

In this section we will show that for a certain class of systems, this measure exists and can be defined uniquely.

Invariant Measure If $\rho(A)$ represents the proportion of mass contained in the set A, the invariant measure ρ can be thought as a measure that conserves mass, that is preserved under the action of f. More precisely, we say that ρ is an invariant measure [34] if it satisfies the equation

$$\rho(S^{-t}(A)) = \rho(A) \tag{2.9}$$

where $A \in \mathbb{R}^m$. In general, a system might admit more than one invariant measure, but not all of them are physically relevant. If we consider for instance an unstable fixed point of the system $\bar{x}$, then the δ-measure at $\bar{x}$ is invariant, but it cannot be observed.

If the system admits an ergodic measure ρ, ρ can be uniquely specified in terms of time averages, which turns to be the *natural measure* introduced earlier in a general case. In fact, by a corollary of Birkhoff theorem applicable to natural measures [41, 42, 43, 34] a set of randomly chosen initial conditions will generate trajectories that would distribute according to the natural measure for ρ-almost all initial conditions. Namely, we have that ρ is defined for ρ-almost all initial conditions x_0 by

$$\rho = \lim_{T\to\infty} \frac{1}{T} \int_0^T dt \delta_{(S^t x_0)}, \tag{2.10}$$

where $\delta(x)$ is the Dirac delta at the point x or, similarly, given $\varphi : M \to \mathbb{R}$, by

$$\langle \varphi \rangle = \int \rho(dx)\varphi(x) = \lim_{T\to\infty} \frac{1}{T} \int_0^T \varphi(S^t x_0) dt. \tag{2.11}$$

Physical Measure

Usually an attractor contains uncountably many ergodic measures. Among this set of invariant ergodic measures, one would like to select a measure which is of physical relevance. A physical

system usually produces well defined time averages, so it is reasonable to pose this question. A possible option, firstly presented by Kolmogorov, is based on the idea that if a system admits a certain level of noise, then it is possible to define uniquely a physical measure that the system selects in the weak limit of zero noise. More precisely, if we add to the deterministic system 2.1 a noise term ω modulated by $\varepsilon > 0$ parameter as follows:

$$\dot{x}(t) = f(x(t)) + \varepsilon\omega(t), \tag{2.12}$$

according to this idea the physical measure can be obtained

$$\rho = \lim_{\varepsilon \to 0} \rho_\varepsilon. \tag{2.13}$$

Such definition of physical measure is however problematic for at least two reasons:

- in a chaotic system, even a small level of noise could have a large impact, and it might be difficult to study under which condition and for which type of noise (2.13) holds;
- if the system in exam presents multiple attractors, the noise could force the system to travel around the different attractor basins.

There exist another possibility to select a physical measure, by requiring that condition (2.11) holds for almost all initial conditions $x(0) \in S$, with $S \subset \mathcal{M}$ subset with positive Lebsesgue measure. This definition is more natural than (2.11), since it corresponds to a more natural notion of sampling (ρ could often be singular and concentrated on a fractal set.).

We will see that for a special class of measures, the SRB measures, the above two definition coincides.

SRB measures

The ergodic theory of Axiom A attractor was developed by Sinai, Ruelle and Bowen in the '70s [34, 33]. One of the most important results was the construction of the so-called Sinai-Ruelle-

Bowen (SRB) measures. We will leave the technical definition of the SRB measures to the interested reader who could refer to [34] for more details, but roughly speaking, SRB measures are defined as measures which are smooth along the unstable directions of the system.

SRB measures are particularly relevant since in the case of Axiom A systems it is possible to show that they coincides with the physical measure, ergodic and invariant, satisfying (2.13). Morover, in the case of Axiom A system we have that the ergodic average

$$\lim_{T\to\infty} \frac{1}{T} \int_0^T dt \delta_{(S^t x_0)} \tag{2.14}$$

tend to the SRB measure ρ for $x(0)$ in a set of positive Lebesgue measure, and not just for ρ-almost x.

In the next chapters we will assume that a physical measure, ergodic and able to represent experimental time averages, exists and it can be defined as in (2.11).

2.1.5 Evolution of densities

In the previous section we saw that the behaviour of individual trajectories in nonlinear dynamical systems is very hard to characterise and predict. The solution is offered by focusing on the characterisation of the evolution of densities of sets instead. When the interest shifts from individual trajectories to densities, one no longer seeks a description in terms of the evolution operator S^t presented in equation (2.2) describing the future position in time of an initial point. Instead, one defines the *Perron-Frobenius* or *transfer operator*, that describes the time evolution (push forward) of densities. In this paragraph we introduce the Perron-Frobenius operator. This tool is wildly used in the applications, where a numerical discretisation is needed. The discretisation of the transfer operator is an example of extraction of a Markov chain process from the dynamics of a continuous system. We will review this and other examples. In order for this section to be self contained we will also introduce background information on Markov chain process.

Transfer Operator

The transfer operator is a global linear propagator for the flow that describes how densities and measures globally evolve with time.

Let us consider a dynamical system $(\mathcal{M}, \phi)$. We define [44] the Perron-Frobenius operator or transfer operator as the linear operator $\mathcal{P}_\phi : L^1(m) :\to L^1(M)$ given by

$$\int_E \mathcal{P}_\phi(h)dm = \int_{\phi^{-1}(E)} hdm, \tag{2.15}$$

for any integrable function h and measurable set E, where m is the Lebesgue measure. $\mathcal{P}_\phi$ is the pull-back of ϕ on $h \cdot m$. This definition can be rewritten for the special case of smooth flows with an attractor Ω as:

$$\mathcal{P}^t\rho(x) = \int_\Omega \rho(y)\delta(x - S^t(y))dy = \rho(S^{-t}(x))|det(DS^{-t}(x))|, \tag{2.16}$$

where D indicates the Jacobian of the flow.
$\mathcal{P}^t$ evolves probabilities densities ρ under the dynamics of the system, meaning that if ρ is the density of an absolutely continuous probability measure ν, then $\mathcal{P}^t\rho$ is the density of the probability measure $\nu \circ S^{-t}$.

From its spectral properties we can gather information about the statistical features of the system, such as ergodicity and mixing properties [45] and rates of decay of correlations and invariant densities [44, 46].

Extracting Dynamical Behaviour through Markov chains: discretised transfer operator

The transfer operator machinery has been applied to investigate problems in the most diverse fields, among which geoscience [47, 48, 49]. For such applications, particularly those that require a high-dimensional model, it is necessary to consider a discretisation of the phase space in order to set up a numerical approach. A classical technique is to divide the phase space

into a finite collection of regions and mass moves from one region to the other as prescribed by an appropriate numerical estimate of the transfer operator that provides the probability of transition between different regions. As a result, a coarse grained dynamics is obtained, and one is interested only in transitions between regions. It is worth noticing that the numerical effort of such approach is mainly due to the complexity of the underlying dynamics rather than the dimensionality of the system itself.

It is thus necessary to specify what it is meant exactly with *appropriate numerical estimate* of $\mathcal{P}^t$. One of the most common framework to define such estimate is known as Ulam's method [50]. This process yields a discretisation of the dynamics in terms of a finite state Markov chain. Even though this reduced setting contains less information than the original system, it is possible to retain its essential properties [51].

Let us consider a partition of the phase space $\mathcal{M}$ into N connected sets $\{B_i\}_{i=1}^N$ (usually a grid of boxes). We define the projection $\pi_N : L^1 \to span\{\chi_{B_i}\}_{i=1}^N$ as

$$\pi_N \rho = \sum_{i=1}^{N} \frac{\chi_{B_i}}{\upsilon(B_i)} \int_{B_i} \rho \chi_{B_i} \upsilon(dx), \tag{2.17}$$

where χ_{B_i} is the characteristic function of the set B_i and υ can be chosen depending on the nature of the problem to express some notion of volume. The so called discretised transfer operator $\pi_N \mathcal{P}^t : span\{\chi_{B_i}\}_{i=1}^N \to span\{\chi_{B_i}\}_{i=1}^N$ admits a matrix representation

$$M_{n,t,ij} := \left(\pi_N \mathcal{P}^t\right)_{i,j} = \frac{1}{\upsilon(B_i)} \int_{B_i} \mathcal{P}^t \chi_{B_j} \upsilon(dx). \tag{2.18}$$

We can see from (2.18) that the practical construction of $M_{n,t,ij}$ depends on the measure υ. In general, if the interest is on the asymptotic properties of the system, υ will be chosen as the invariant measure of the system. If instead one wants to look at the effect of the flow on the entire phase space and the correlation properties, the most appropriate choice for υ is the Lebesgue measure m. In this latter case we have

$$M_{n,t,ij} = \frac{m(B_i \cap S^{-t}(B_j))}{m(B_i)}. \tag{2.19}$$

The matrix $M_{n,t}$ is stochastic, thus having a spectral radius of one. Each B_i can in fact be considered as a state of the system and the entry $M_{n,t,ij}$ corresponds to the probability that a typical point in B_i moves into B_j after time t. See [52, 46] for classical results on the use of the Ulam's method for approximating the properties of chaotic dynamical systems.

Correlation properties

From the spectrum of the transfer operator it is possible to extract significant information about the mixing properties of the system.

As we mentioned earlier, mixing is a necessary condition for deterministic chaos that indicates that if we consider two events $x \in A$ and $S^N(x) \in B$ for any pair of measurable subsets $A, B \in \Omega$ for large N the two events become statistically indipendent. We can further quantify their loss of correlation through the formula

$$\mathcal{C}_{f,g}(N) := \left| \int (f \circ S^N x) g(x) \rho(dx) - \int f(x)\rho(dx) \int g(x)\rho(dx) \right| \tag{2.20}$$

where f and g are smooth observables. Specifically, $C_{f,g}(N)$ quantifies the correlations between observing g at time t and f at time $t+N$, measuring how quickly physical observables become uncorrelated. Within this context the physical measure can be thought as a reference measure for the "equilibrium" of the system.

The transfer operator is strongly connected with the decorrelation properties of the system. In particular, it is possible to prove that the eigenfunctions of P^t corresponding to the largest eigenvalues indicates the mass distributions that approach the equilibrium distribution given by the physical measure at the slowest possible rates [46].

Stochastic Matrix

In section 2.1.5 we mentioned the concept of stochastic matrix. We now wish to discuss some of its properties that will be useful in later sections.

We consider a stochastic variable $x(t)$ that takes values at each instant of time t over a set of N states $S = s_1, ..., s_N$. We call $p_i(t) := p(x(t) = s_i)$ the probability that at time t the variable is in state s_i. When the state of the process at time t only depends on the state at time $t-1$, we say that $x(t)$ defines a *Markov process*. We will consider *stationary* processes, meaning that the transition probability from the state s_i to the state s_j

$$W_{ji} = \Omega(x(t) = s_j | x(t-1) = s_i) \tag{2.21}$$

does not depend on time.

We require that the aformentioned quantities satisfy the followings [53]:

$$\begin{aligned} p_i(t) \geq 0, \quad \forall i, t, \\ \sum_i p_i(t) = 1, \quad \forall t, \\ W_{ij} \geq 0, \quad \forall i, j, \\ \sum_i W_{ij} = 1 \quad \forall j. \end{aligned}$$

If we call $\mathbf{p}(t) = (p_1(t), ..., p_N(t))$ the column vector containing the probabilities and W the $N \times N$ matrix with entries W_{ji}, called *stochastic matrix*, then we can define the stochastic dynamical rule as

$$\mathbf{p}(t+1) = W\mathbf{p}(t). \tag{2.22}$$

It is easy to prove by induction that

$$\mathbf{p}(t+n) = W^n\mathbf{p}(t), \tag{2.23}$$

and W^n is also a stochastic matrix.

Another important relation is the *Chapman-Kolmogorov* equation, according to which

$$\mathbf{p}(t+n) = W^n\mathbf{p}(t) = W^nW^t\mathbf{p}(0) = W^{t+n}, \tag{2.24}$$

that represent the analogous for stochastic processes of the semigoup property of the evolution operator S^t of deterministic dynamical systems.

Properties of the stochastic Matrix It is possible to prove interesting properties from the spectrum of the stochastic matrix W. Let us consider the right eigenvectors $\mathbf{w}^\lambda$, so that

$$W\mathbf{w}^{(\lambda)} = \lambda\mathbf{w}^{(\lambda)}. \tag{2.25}$$

Its leading eigenvalue is $\lambda = 1$, and its corresponding eigenvector $\mathbf{w}^{(1)}$. The other eigenvalues, which can be proven to be inside the unit circle, fulfill the condition $\sum_j w_j^{(\lambda)} = 0$, where $w_j^{(\lambda)}$ indicates the j^{th} component of the eigenvector $w^{(\lambda)}$ [53].

Ergodic Markov chains We now introduce a special case of stochastic matrix. Let us first introduce some definitions and some particular cases of Markov chain. We say that a state s_j is

- *accessible* from state s_i if there is a finite value of time t such that $(W^t)_{ji} > 0$;
- *persistent* if the probability of returning to s_j after some finite time t is 1;
- *transient* if there is a finite probability of never returning to s_j for any finite time t.

We say that a Markov chain is

- *irreducible* if all the states are accessible from any other state;
- *periodic* if the return times T_j on a state s_j are all integer multiples of a period T.

A Markov chain with a finite phase space is *ergodic*, if it is irreducible, nonperiodic and all states are persistent.

Ergodic Markov chains determine a unique invariant measure, which can be calculated as the eigenvector $\mathbf{w}^{(1)}$ associated to the maximal eigenvalue $\lambda = 1$ and it is attained exponentially

fast on a timescale τ independently on the initial condition as

$$\mathbf{p}(t) = \mathbf{w}^{(1)} + Ae^{-t/\tau}. \tag{2.26}$$

The subdominant eigenvalues of a stochastic ergodic Markov chain, ordered accordingly to $1 > \Re(\lambda_2) \geq \Re(\lambda_3) \geq ... \geq \Re(\lambda_M)$ (where $\Re$ indicates the real part) can be thought of as modes of decay, as they determine the time scale of convergence to the stationary probability measure. We can quantify these time scales by defining the corresponding decay rate as $\tau_k = -\frac{1}{log(\Re(\lambda_k))}$. In particular, τ_2 identifies the mixing time scale [54].

2.1.6 Characterising the chaoticity of a system: Lyapunov analysis

A chaotic system is characterised by sensitive dependence on the initial conditions on the attractor. Following Pesin's theory [18], such characterisation can be most easily accomplished by using Lyapunov analysis [54], that provides very powerful tools for studying rates of expansion or decay (and corresponding modes) of perturbations with respect to a background chaotic trajectory by analysing the properties of the tangent linear operator.

Let's start by considering any two chaotic trajectories $x(t) = S^t(x_0)$ and $x(t) + \delta x(t) = S^t(x_0 + \delta x_0)$. If the system in exam is chaotic, they will separate exponentially with time and in a finite time their separation will grow to the size of the attractor.

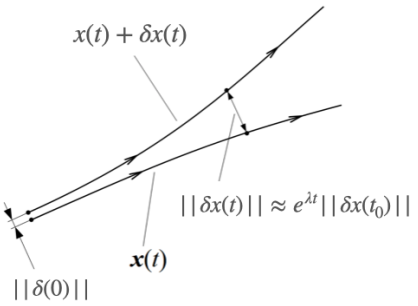

Figure 2.2: Exponential separation of trajectories

Such exponential separation in time of neighbouring trajectories can be quantified as

$$||\delta x(t)|| \approx e^{\lambda t}||\delta x_0||, \tag{2.27}$$

where λ is called leading Lyapunov exponent and it is a global measure of the rate at which nearby trajectories diverge, averaged over the attractor of the system.

We can formalise these observations in the following manner. Let us consider the dynamical system given in (2.1), with $x(t)$ being the state of the system at time t. In systems of practical applications, this initial state cannot be specified with infinite accuracy, since its measurement is affected by noise. We can describe the evolution of such infinitesimal perturbation $\delta x(t)$ in the tangent space by linearising the dynamics around the trajectory as:

$$\delta \dot{x}(t) = J(x,t)\delta x(t), \tag{2.28}$$

where

$$J(x,t) = \frac{\partial f(x(t))}{\partial x(t)} \tag{2.29}$$

is the Jacobian matrix of the flow.

We can write the solution of this equation as:

$$\delta x(t) = M(t, x(t_0))\delta x(t_0), \tag{2.30}$$

where M is the fundamental matrix [55]. Oseledec multiplicative ergodic theorem [56] states that, for an appropriate type of systems, there exists a matrix $\Lambda_{x(t_0)}$ such that

$$\Lambda_{x(t_0)} = \lim_{t_0 \to \infty} (M^T(t, x(t_0))M(t, x(t_0)))^{1/2(t-t_0)} \tag{2.31}$$

It is also possible to prove that its eigenvalues Λ_i are constant almost everywhere with respect to the invariant measure of the system. Roughly speaking, the theorem states that for a measure-preserving dynamical system, there exists a splitting of the tangent bundle into invariant subspaces, such that the Lyapunov exponents associated with each subspace are well-defined

and have certain asymptotic properties. The Oseledec assumption is fundamental because it ensures that the splitting of the tangent bundle into invariant subspaces is well-defined.

We call Lyapunov exponents (LE) of the systems the objects defined as $\lambda_i = \log(\Lambda_i)$. Usually they are ordered by size in descending order $\lambda_1 \geq \lambda_2 \geq ... \geq \lambda_N$ and they are dynamically invariant, since they are independent on both metric and choice of variables. The Lyapunov exponents provide an exhaustive description of the behaviour of all possible perturbations, meaning that reproducing a perturbation such that its exponential growth rate differs from any of the Lyapunov exponents of the systems has probability zero with respect to the measure. In particular, the largest LE is responsible of the description of the asymptotic linear stability of a given trajectory. A positive first LE indicates that the system is chaotic (exponential instability), whereas a negative first LE implies that the system is linearly stable.
It is also interesting to note that in a chaotic system the largest LE λ_1 provides a way to measure the predictability time (or characteristic time) of the system as the inverse of λ_1. More precisely, if a point in the phase space undergoes a perturbation of size δ, such perturbation grows exponentially in time as $\exp(\lambda_1 t)$. The time that it takes for the perturbation to reach to a size Δ can be calculated as:

$$T_{PR} \approx \frac{1}{\lambda_1} \log\left(\frac{\Delta}{\delta}\right) \tag{2.32}$$

Since λ_1 quantifies the average growth rate it is not necessary valid in all the different regions of the attractor, but it can be rather interpreted as an average quantity (see later discussion in the following section).

Finite Time Lyapunov Exponents

Lyapunov exponents are asymptotic quantities and refer to average properties over the attractor. This notion can be extended via their local correspondents, constructed by considering finite time horizon (finite-time LEs - FTLEs) [57], and by considering finite scale, rather than infinitesimal perturbations with respect to the background trajectory (finite size LEs - FSLEs)

[5].

In this thesis we will in particular take into account FTLEs. These quantify the amount of stretching about the trajectory with initial condition $x(t)$ over a finite time interval $[t, t+t_0]$. They are local objects since their value depends on x and t_0. They can be computed as the logarithm of the eigenvalues of the matrix

$$L_{x(t_0)} = (M^T(t, x(t_0))M(t, x(t_0)))^{1/2(t-t_0)}. \tag{2.33}$$

The long time average along the trajectory of each $\lambda_j(x,t)$ corresponds to the global Lyapunov exponent λ_j.

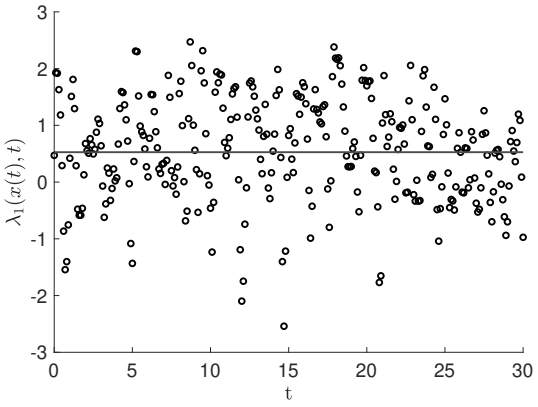

Figure 2.3: First finite-time Lyapunov exponent for the Lorenz-96 model with parameters $N = 20$, $F = 5$ [58]. Each dot represents the first FTLE computed over time with a time step of $\tau = 0.1$. The solid line is the asymptotic average value of the first global Lyapunov exponent.

In fig. 2.3 we can observe the dependence of the first FTLE of the Lorenz-96 model [58] from the initial condition $x(t_0)$ (the reader can refer to chapter 4 for a more detailed discussion). We can see that, even though the average value λ_1 is positive for the considered parameters of the model, negative contributions are not rare. In fact, since FTLEs are computed as averages over a finite time they can be subject to large fluctuations. We will discuss later in chapter 4 that for a certain type of systems, these fluctuations can be observed even for large values of τ (even though their are less likely to be observed) and are a symptom of a strong violation of hyperbolicity.

Roughly speaking, if a FTLE fluctuates between positive and negative values along the trajec-

tory, there exist a direction whose behaviour is oscillating between contractive and expansive, thus ruling out hyperbolicity. This behaviour originates from the the so-called Unstable Dimension Variability [11], namely the presence of unstable periodic orbit embedded in the attractor that present a different number of unstable dimension.

Applications of Lyapunov analysis Lyapunov analysis plays a pivotal role in modern dynamical system theory, as a result of new mathematical theory being developed and growing progress in computer capabilities [59]. Lyapunov vectors and exponents have found applications in the most different research communities, from mathematics, to physics to atmospheric sciences [54].

A prominent application of such theory is the investigation of the predictability properties of the atmosphere and the climate. In fact, as we previously mentioned, atmospheric and climate systems exhibit sensitive dependence on the initial conditions [60]. Such sensitivity not only affects the propagation of errors on the initial conditions, but also emerges in the model parametrisation and boundary conditions [61, 62]. Quantifying such sensitivity is thus of the most relevant importance in order to improve forecasts at short, medium and long term [63]. Initially Lyapunov exponents have been computed in low dimensional systems, but the scope was soon expanded to spatially distributed system with a high number of degrees of freedom. Lyapunov exponents have been computed in intermediate order atmospheric quasi-geostrophic models [64, 65, 66], showing that when considering realistic boundary conditions and forcing, the number of positive LE is high, resulting in an high-dimensional attractor and indicating the impossibility of reducing such models to a lower order system. Another important issue is quantifying the prediction horizon of weather forecast.

Dynamical indicators

Kaplan-Yorke dimension The full Lyapunov spectrum allows to define the Kaplan-Yorke dimension of the system [67] as:

$$D_{KY} = m + \frac{\sum_{i=1}^{m} \lambda_i}{|\lambda_{m+1}| \leq N} \tag{2.34}$$

with m being the highest index for which the sum of the largest m Lyapunov exponents is strictly positive.

The Kaplan-Yorke conjecture states that

$$D_1 = D_{KY} \tag{2.35}$$

where D_1 is defined as in 2.8.

This quantity provides an estimate for the fractal dimension of the attractor and it can be thought as an approximate value of the number of excited degrees of freedom acting in the system [68].

Kolmogorov-Sinai entropy The degree of chaoticity of a dynamical system can also be quantified via the Kolmogorov-Sinai entropy (approximated via Pesin's theorem in the case the invariant measure is of the Sinai-Ruelle-Bowen type) [34] as:

$$h_{KS} = \sum_{i=1}^{N} \lambda_i \tag{2.36}$$

that describes the production of information due to the chaoticity of the system.

2.2 Periodic orbit theory

Since the birth of calculus, differential equations were used with the scope of modelling natural phenomena. However, the approach to such problems was very different than the current one. The default method involved extracting individual solutions, either approximated with a time series or using a transformation to reduce the equation to a known function. A breakthrough in the understanding of nonlinear and in particular chaotic dynamics was offered by a shift in

the perspective in the way of looking at the problem. From this perspective, as noticed early on by Poincaré [69], the dynamics can seen as a walk through repeating patterns. More precisely, these repeating patterns are unstable periodic orbits (UPOs), true nonlinear modes of the flow, that provide a rigid structure hidden in the chaos of the dynamics [70]. When dense in the attractor [34], they can approximate any chaotic trajectory with an arbitrary accuracy [71, 72]. We can think of the chaotic trajectory as being continuously scattered from one neighbourhood of an UPO to another, because of their instability. Within this context, for lower dimensional systems that present strong chaoticity, it is possible to develop a theory that allows dynamical averages to be written as weighted sums over the full set of UPOs. For higher dimensional systems a direct extension of this theory is not yet formalised, but promising results are present in the literature [2].

In this section I will review the main results of periodic orbits theory for Axiom A systems and their applications. I will present some extensions for higher dimensional systems and applications in the geophysical context.

2.2.1 Averages

One of the main results of periodic orbit theory is the development of a "cycle expansion formula" [1] that allows to express averages over chaotic phase space regions in terms of unstable periodic orbits. This result could be achieved starting from the observation that the motion in dynamical system with a low number of degrees of freedom can be organised around some of its "relevant" periodic orbits [73]. Such orbits are skeletal for the dynamics in the sense that even though they are determined in a finite period of time, they remain there forever. The phase space is tiled by periodic orbits that can provide an approximation of the chaotic trajectory at any instant of time, since these are closures of the set of the UPOs [34]. UPO theory has fast developed into a consolidated dynamical tool for the calculation of ergodic averages, providing a machinery that allows to use the knowledge coming from individual solutions to make predictions about statistics.

Historically, Gutzwiller [74] was the first to demonstrate that UPOs are the essential building blocks of chaotic dynamics. Cvitanović [3] argued that UPOs are the optimal practical tool for measuring the invariant properties of a dynamical system. Ruelle later derived the dynamical ζ function [75], that allows one to write averages over the invariant measure of the system as a weighted sum over the infinite set of UPOs. Trace formulas [1] became a standard instrument in the toolkit of the dynamicist, allowing to reconstruct the invariant measure of the system by considering the following expression for the average of any measurable observable φ:

$$\langle\varphi\rangle = \lim_{t\to\infty} \frac{\sum_{U^p, p\leq t} w^{U^p} \bar{\varphi}^{U^p}}{\sum_{U^p, p\leq t} w^{U^p}} \tag{2.37}$$

where U^p is a UPO of prime period p, w^{U^p} is its weight and $\bar{\varphi}^{U^p}$ is the average in time of the observable along the orbit. For the particular case of uniformly hyperbolic dynamical systems (2.37) is exact and the weight can be obtained, to a first approximation, by $w^{U^p} \propto \exp(-ph_{ks}^{U^p})$ [71] , with h_{ks} being the Kolmogorov-Sinai entropy of the system.
More generally, these results are proven to be valid for dynamical systems exhibiting strong chaoticity [76, 77], such as uniformly hyperbolic and Axiom A systems [23, 78].

2.2.2 Applications of UPOs theory

The significance of periodic orbits for the experimental study of chaotic dynamical systems has been demonstrated in a broad range of applications.
A first application of periodic orbit expansion was performed by Auerbach et al. [79] where they proved that UPOs are experimentally accessible and capable of unfolding the structure of chaotic trajectories. In fact, by extracting the complete set of UPOs of symbolic length up to period n and calculating their instability, they approximated the fractal dimension and topological entropy of the strange attractor of the paradigmadic Hénon map with very high accuracy. Cvitanović [3] argued that UPOs are the optimal practical tool for measuring the invariant properties of a dynamical system and provided a solid ground for the applications of periodic orbit theory (POT). Artuso et al. tested this procedure through a series of applications [80, 73] and demonstrated that cycle expansion of the dynamical ζ function is instrumental for

the analysis of deterministic chaos, even in more generic settings than the ones required by [3], i.e. when the system is not uniformly hyperbolic nor the results depend on the assumption of the existence of invariant measures or structural stability of the dynamics. Eckhardt and Ott [81] presented one of the first numerical applications of the periodic orbit formalism for studying the statistical and the dynamical properties of the Lorenz 1963 (L63) system [25]. A subsequent analysis of the linear and nonlinear response of the L63 to perturbations show that specific UPOs are responsible for resonance mechanisms leading to an amplified response [82].

Applications to (geophysical) fluid dynamics

Later on, periodic orbit theory found fruitful applications also within the context of higher dimensional NESSs, and specifically in the case of (geophysical) fluid dynamics. UPOs can be considered as a mean to simplify and interpret qualitative behaviour of a complex system [14], allowing to extract information and distill its dynamical structure. This observation, together with the study of the stability and thus predictability properties of the tangent space, allows to associate relevant dynamical features of the flow to specific UPOs or classes of UPOs. UPOs, true nonlinear modes of flow, can be interpreted as a generalisation of the normal modes observed in a network of coupled linear oscillators, that allow for a study of the system in its complexity, without the necessity of considering a heavily truncated model. Even though a complete UPOs-based analysis of turbulent flows is still a far reaching goal, many steps have been made in this direction [2]. Kawahara and Kida [7], who found a UPO embedded in the attractor of a numerical simulation of plane Couette flow, showed that one UPO only manages to capture in a surprisingly accurate way the turbulence statistics. At a moderate Reynolds number, Chandler and Kerswell [10] identified 50 UPOs of a turbulent fluid and used them to reproduce the energy and dissipation probability density functions of the system as dynamical averages over the orbit. These encouraging results suggested that periodic orbit theory could represent a valid investigation tool also in the realm of climate systems. In the geophysical context, Gritsun [83, 84] proposed using an expansion over UPOs to reconstruct the statistics of a simple atmospheric model based on the barotropic vorticity equation of the

sphere. Gritsun and Lucarini [85] used the UPOs for interpreting non trivial resonant responses to forcing that underlined the violation of the standard fluctuation-dissipation relation for NESS for deterministic chaotic systems. Lucarini and Gritsun [14] used UPOs for clarifying the nature of blocking events in a baroclinic model of the atmosphere. Specifically, they found that blocked states are associated with conditions of higher instability of the atmosphere, in agreement with a separate line of evidence [86].In fig. 2.4 we can in fact see that the statistical distributions describing the stability properties of blocked states (first finite-time Lyapunov exponent, local estimate of the Kolmogorov-Sinai entropy and number of unstable dimensions) are biased substantially high compared to the distribution of all UPOs. This results in a bimodal distribution of the stability indicators of the UPOs of the system, where more the more unstable peak (right peak) corresponds to the UPOs associated to blockings, and the more stable peak (left peak) is associated to the UPOs in a non-blocked state. Additionally, the analysis of UPOs was instrumental in proving that the atmospheric model was characterised by variability in the number of unstable dimensions, hence being not uniformly hyperbolic [12].

The analysis by Lucarini and Gristun [14] proposed the idea that the observed blocked states of the atmospheric flow should be interpreted as conditions where there is not only proximity of the trajectory to special classes of UPOs, but also co-evolution, at least locally in time (the so-called *shadowing*). This implies that blocking can be associated with actual nonlinear modes of the atmosphere. This calls for looking at both the proximity and the co-evolution of chaotic trajectories with approximating UPOs. Recent investigations have been carried out exactly in this direction, yet in a different context. Both Yalnız and Budanur [8] and Krygier et al. [87] investigated the process of shadowing of time-periodic solutions in three-dimensional fluids, although using different shadowing metrics, providing a numerical evidence of the shadowing of a trajectory in terms of UPOs. (A more complete review of the shadowing process can be found in section 3.1.4).

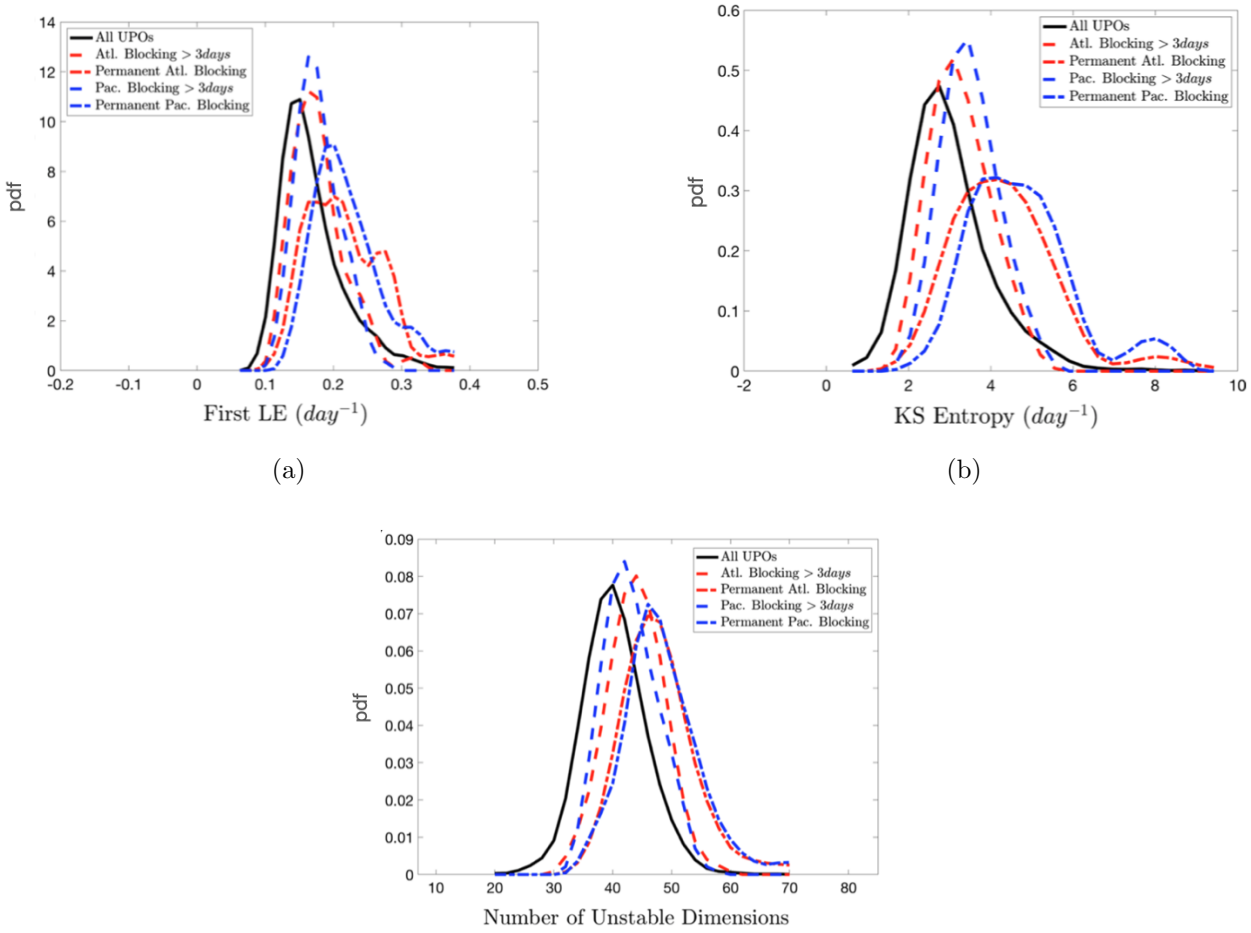

(a) (b)

(c)

Figure 2.4: Statistics of UPOs: first finite-time Lyapunov exponent (panel (a)); local estimate of the Kolmogorov-Sinai entropy (panel (b)); number of local unstable dimensions (panel (c). Black lines: all UPOs. Red dashed lines: UPO with Atlantic blocking patterns with duration longer than 3 days. Red dash-dotted line: UPO with perpetual Atlantic blocking. Blue dashed lines: UPO with Pacific blocking patterns with duration longer than 3 days. Blue dash-dotted line: UPO with perpetual Pacific blocking. Orbits including short-lived blocking events (duration equal or less than 2 days) are barely distinguishable from the statistics of all UPOs. When looking at UPOs featuring blockings whose lifetime is equal to or longer than 3 days, we find confirmation that blocked states are anomalously unstable, and that the lifetime of a blocking event correlates positively with its average instability. The estimates of their KS entropy are biased substantially high compared to the statistics of all UPOs. The special nature of instability during blocking events is better understood when looking at the properties of UPOs that are in perennially blocked state. For these UPOs the mean and the standard deviation of the first FTLE, of the local values of the KS entropy, of the KY dimension, and of the number of unstable dimensions are much higher than for the other UPOs. Figures and caption are (with permission) from [14].

2.3 Numerical Methods

In this section we introduce the numerical methods used to reproduce the results of this thesis. The numerical choices and parameters in the case of the Lorenz-63 and Lorenz-96 are presented in a separate section of the Appendix.

2.3.1 Numerical methods for finding Lyapunov spectra

Lyapunov exponents play a crucial role as diagnostic tool of chaotic dynamics. In fact, as we mentioned in the previous section, any system that presents at least one positive Lyapunov exponent is deemed as chaotic, with an horizon of predictability specified in terms of the value of the largest Lyapunov exponent. A major breakthrough in the study of chaotic dynamical system happened in the '80s when Benettin and collaborators [28] and separately Shimada and Nagashima [88] developed an algorithm for the numerical extraction of the full Lyapunov spectrum, motivated by the interest in numerically computing the metric entropy of nonlinear dynamical systems [89]. Before that time, only a technique for computing the maximal exponent was known [90, 91, 57]. This had great impact from the perspective of the applications since it enabled to extend the study of chaotic dynamics to systems that were inaccessible from a theoretical perspective. Wolf at al. successively developed an algorithm that allowed to determine Lyapunov exponents from an experimental time series without necessarily knowing the the equation of motion, tested first on models with both a known Lyapunov spectrum and then applied to experimental data for chemical [92] and hydrodynamical data [93].

We review here the algorithm for the extraction of the Lyapunov spectrum presented in [54].

Lyapunov exponents and evolution of volumes

From the knowledge of the full Lyapunov spectrum it is possible to measure the contraction rate of volumes in the phase space as $C_N = \sum_{k=1}^{N} \lambda_k$ where N is the dimension of the system [54]. In particular, if we consider a finite volume spanned by two generic inital vectors $\mathbf{u}(0)$

and $\mathbf{v}(0)$, that typically has components along all directions $\mathbf{E}^k(0)$ with $k = 1, ..., N$. We now let the system evolve forward in time. After a certain time t, the area spanned by their iterates is given by $\mathbf{u}(t) \times \mathbf{v}(t)$. If we assume Oseledets splitting [56], meaning that the Lyapunov exponents associated with each subspace are well-defined, each of the components will expand or contract multiplied by a factor $exp(t\lambda_k)$. This expansion has an effect over the volume: if we denote with V_2 the area spanned by the two generic initial vectors the rate of growth can be calculated as

$$\lambda_1 + \lambda_2 = \lim_{n\to\infty} \frac{1}{t} \frac{V_2(t)}{V_2(0)} \tag{2.38}$$

in fact, the leading component is given by the cross term $\mathbf{E}^1(t) \times \mathbf{E}^2(t)$ since the term $\mathbf{E}^1(t) \times \mathbf{E}^1(t)$ vanishes in the cross product. In a similar manner we can deduce that the volume spanned by M generic different inital vectors V_M can be obtained as

$$\sum_{k=1}^{M} \lambda_k = \lim_{n\to\infty} \frac{1}{t} \frac{V_M(t)}{V_M(0)}. \tag{2.39}$$

Algorithm

The idea behind the algorithm is to take advantage of the relationship between the evolution of a volume in phase space and the Lyapunov exponents (2.38). Namely, we consider a set of m vectors in the phase space, denoted with a $N \times m$ orthogonal matrix Q_0. At time t, the matrix Q_0 evolves into a volume $P = M(t)Q_0$, where M is the matrix describing the tangent linear evolution operator. The matrix P, as an effect of the time evolution, will not necessary be orthogonal, and most likely some of the vectors that represent its columns will align along the most expanding direction. However, there exist a unique decomposition [94] that allows to write P as

$$P(t) = QR, \tag{2.40}$$

where Q is an orthogonal $N \times m$ matrix and R is an upper triangular $m \times m$ matrix with positive diagonal elements. The crucial information is that since Q only involves rotations and reflections without affecting the volume, the determinant of R is equal to the volume V_m of a

generic m-dimensional parallelepiped as

$$V_m = \prod_{i=1}^{m} R_{i,i}. \tag{2.41}$$

We recall that the rate of growth of such volume can be estimate as

$$\lim_{t\to\infty} \frac{\ln V_m}{t} = \sum_{i=1}^{m} \lambda_i. \tag{2.42}$$

If we now substitute (2.41) in (2.42) and apply such relation consecutively for $m = 1, 2, ...$ we finally find an expression for the Lyapunov exponents as

$$\lambda_j = \lim_{t\to\infty} \frac{\ln R_{jj}}{t}. \tag{2.43}$$

A great advantage of such procedure is that it possible to decompose the matrix R as a product of different subterms, allowing to periodically re-normalise the matrix, in order to avoid the different directions (represented by the columns of the matrix) to align along the greatest as time evolves, and preventing from a corrected estimation of the full spectrum.

We consider L intervals of equal size τ in $[0, t]$. We have that

$$P = \prod_{k=1}^{L} M_k Q_0 \tag{2.44}$$

where M_k is the operator considered between time $(k-1)\tau$ and $k\tau$. We define $P_K = M_k Q_{k-1}$ and apply the QR decomposition on each P_k as $P_k = Q_k R_k$. We have that

$$P = Q_k \prod_{k=1}^{L} R_k \tag{2.45}$$

by recursive iteration. The computation of the jth Lyapunov exponent can be obtained as a sum of the L $R_{j,j}$ contributions over the interval $[0, t]$. In fact, the product of upper triangular matrices is still upper triangular and the same holds true for orthogonal matrices.

The interested reader can find different implementation of the algorithm in [95, 96, 97].

Numerical Errors

Different type of errors arise in the computation of the Lyapunov spectrum. The main source is linked to the integration of the evolution equation in the tangent space. In fact, the time-scale on the tangent space might be very different than the time-scale of the nonlinear equation, and in the case of the calculations of very negative Lyapunov exponents this problem might be even more accentuated due to the fact that such timescale is typically smaller. In order to account for this type of error it is crucial to choose an appropriate numerical integration scheme. See for instance (Arnes 1992, Quarteroni and Valli 1994, Morton and Mayers 2005).

When considering numerical errors purely specific to Lyapunov exponents, the two major sources are imputable to the finite orthogonalisation time and statistical fluctuations.

The first is due to the non-normality of the matrix R. In fact, some directions might be very close one to the other, making difficult to estimate the diagonal terms of the matrix. Such problem grows with the orthogonalisation time τ, as the directions tend to align towards the direction given by λ_1. Choosing a sufficiently small τ will limit this source of errors.

The most important source of error is due to statistical errors. In fact, different regions of the phase space might present very different stability properties, that generates unavoidable source of fluctuations. A possible way to determine the effect of such fluctuations on the estimates of the LEs is by introducing appropriate observables as a tool to estimate the error on the LW, such as a diffusion coefficient quantifying the time evolution of the expansion factor, which can be seen as a diffusive process with a drift (see [54] for more details).

2.3.2 Numerical methods for finding UPOs

Detecting UPOs from chaotic system still represents open challenge [10]. In fact, the computational cost of the extraction is extremely high, and the difficulty grows with the period T of the orbit [98]. In a limited number of cases, the special structure of the system allows to apply

efficient methods that lead to a complete knowledge of the full set of orbits up period T. This is the case for instance of lower dimensional systems that admits a symbolic dynamics [99], where it is possible to develop a technique that allows to extract UPOs given that the their symbolic value is known. An example is offered by Biham and Wenzel in [100, 101], where the authors present the case of the Hénon map, developing a method that, given the symbolic dynamics description of a UPO, converges to that orbit. Such techniques are not directly extendable to generic systems, for which iterative algorithms represent the favorable choice. One of the most popular is the Newton-Raphson method [102] applied on the periodicity condition. Another possibility takes advantage of the technology of chaos control [103] to stabilise the periodic orbit. Kazantsev instead, proposed a method requiring techniques similar to the one used in data assimilation [104], whereas Land and Cvitanovic presented an algorithm based on a variational method [105].

The algorithms introduced above have been successfully used to detect UPOs in chaotic systems in very different fields. Kazantsev [104, 106] extracted UPOs in a barotropic ocean model and used those UPOs to analyse the sensitivity of the attractor to external perturbations. Gritsun [83] compared the performance of different methods of extractions of UPOs for a barotropic model of the atmosphere and subsequently used those UPOs to provide an estimate for the system PDF [84]. Kawahara and Kida [7], Kato and Yamada [107], Van Veen et al. [108] and Crowley at all [109], detected UPOs in fluidynamics model and used them to characterise dynamical properties of the system.

We will review here the classic Newton algorithm [102] for detecting UPOs of the ordinary differential equation

$$\dot{x} = f(x), \quad x \in \mathcal{M}, \tag{2.46}$$

where $\mathcal{M} \subset \mathbb{R}^n$ is a compact manifold. This method is particularly appropriate for finding periodic solutions even in high-dimensional systems.

The problem of numerically finding UPOs can be reduced to the solution of the periodicity

condition, which corresponds to a system of nonlinear equations with respect to the initial condition of the UPO and its period:

$$S^T(x_{in}) = x_{in}. \tag{2.47}$$

where x_{in} is the initial condition and T is the period of the UPO. Even for simple nonlinear systems this represents a difficult numerical problem. Hence, the choice of the algorithm and initial guess represent an important aspect to be considered.

There exist several techniques of choosing initial conditions. The first one is represented by a random choice, where the seed of initial conditions is chosen randomly on the attractor and the initial guess for the period is extracted from a given range of values. Another method consists in choosing as initial guess quasi-recurrent orbits. Namely, we integrate the system for a long time T_{max} starting from a random initial state; the result is a numerical trajectory consisting of the set of ordered points $\{x\}_{j=1}^{T_{max}}$. We then calculate the quantity $d_{ij} = |x_j - x_i|$ $\forall i, j \in \{1, ...T_{max}\}$ and take the minimum, obtained at say x_m, x_n. We have a pair of points for which the trajectory starting from x_m passes again near the starting point x_m in time $n - m$. We can then consider the pairs $(x_m, m - n)$ as initial condition for determining the UPO with the Newton method. At last, another option would be to consider as initial conditions the data obtained from already detected periodic orbit, with the purpose of constructing longer orbits. In [83] the author compares the efficiency of these different methods for a barotropic model of the atmosphere, concluding that by using a random selection of initial condition one might find a greater number of periodic solution. Choosing quasi-recurrences would instead lead to finding more stable orbits with higher probability, but with the drawback of struggling to obtain highly unstable orbits. It is important to stress that the choice of initial guesses reflects on the rate of convergence and efficiency of the iterative method.

We now present the standard implementation of Newton algorithm for periodic search. Let us

rewrite the periodicity condition 2.47 as follows:

$$S^T(x_{in}) - x_{in} = 0 \tag{2.48}$$

This is a system of n nonlinear equations (n is the dimension of the phase space) in $n+1$ unknowns (the vector x_{in} and the orbit period T). We start with an initial condition (x_0, T). As we mentioned before, a way to choose it is by calculating a long trajectory and selecting a quasi-recurrence occurring over a period T such that $|S^T(x_{in}) - x_{in}| < \varepsilon$ with ε decided a priori. Let then be x^i and T^i the ith approximations for initial condition and period. The aim of the algorithm is to calculate a correction $(\Delta x_i, \Delta T_i)$ so that we can improve the initial guess in such a way that

$$||S^{T^i+\Delta T_i}(x^i + \Delta x_i) - (x^i + \Delta x_i)|| < ||S^{T^i}(x^i) - x^i||, \tag{2.49}$$

We obtain the approximate corrections $(\Delta x_i, \Delta T_i)$ by expanding

$$S^{T_{i+1}}(x^{i+1}) - x_{i+1} = S^{T_i+\Delta T_i}(x^i + \Delta x_i) - (x^i + \Delta x_i) = 0 \tag{2.50}$$

into a Taylor series with respect to Δx_i and ΔT_i

$$S^{T^i+\Delta T_i}(x^i+\Delta x_i) - (x^i+\Delta x_i) \approx S^{T^i}(x^i) - x^i + \Big(\frac{\partial S^{T^i}(y)}{\partial y}\Big|_{y=x^i} - I\Big)\Delta x_i + \frac{\partial S^T(x^i)}{\partial T}\Big|_{T=T^i}\Delta T_i = 0 \tag{2.51}$$

where I is the identity matrix of order n, $\frac{\partial S^{T_i}(y)}{\partial y}$ is the tangent linear operator and it is an approximation M_i of the monodromy matrix M [1]. $\frac{\partial S^T(x_i)}{\partial T}\Big|_{T=T^i}$ is the derivative of the solution with respect to time $\dot{x} = f(x)$ evaluated at the final condition $f(S^{T_i}(x_i))$. In order to remove the excess in degrees of freedom, we impose the *phase condition* by requiring the orthogonality of the correction vector to the orbit

$$(f(S^{T_i}(x_i))) \cdot \Delta x_i = 0. \tag{2.52}$$

We thus reduced the problem of finding the corrections at step i to the solution of a linear system of $n+1$ equations in $n+1$ unknowns

$$\begin{pmatrix} M_i - I & f(S^{T_i}(x_i)) \\ (f(S^{T_i}(x_i)))^T & 0 \end{pmatrix} \begin{pmatrix} \Delta x_i \\ \Delta T_i \end{pmatrix} = \begin{pmatrix} x_i - S^{T_i}(x_i) \\ 0 \end{pmatrix} \tag{2.53}$$

We define two errors associated to the numerical algorithm, them being at iteration i:

$$err_i^{in} := |S^{T_i}(x_i) - x_i| \tag{2.54}$$

$$err_i^{corr} := |(\Delta x_i, \Delta T_i)| \tag{2.55}$$

We consider the UPO to be numerically detected when both (2.54) and (2.55) are sufficiently small.

The solution of (2.53) gives the next approximations for the UPO initial condition and period.

It is important to notice that in some cases the standard Newton method may not give convergence (or the convergence could be very slow). This happens for instance when the initial guess is far from the solution, so that the linear Taylor expansion is not valid or the linear system is degenerate. In this case, one can use a nonlinear expansion in Eq. 2.51 as well as other techniques known as step relaxation together with line search procedure (see [83] for more details). Another drawback is represented by computational difficulties for large systems, since the implementation of this method requires the integration of n linearised systems. This can be improved by considering an approximation [110, 111] for the inverse of the matrix of the system (2.53).

Chapter 3

Averages, transitions and quasi-invariant sets

In Chapter 2 we saw that the attractor of a chaotic system is densely populated by an infinite number of unstable periodic orbits, which are exact periodic solutions of the evolution equations. In section 2.2 we explained that UPOs can be used to decompose the complex phenomenology of a chaotic flow into elementary components and have shown great potential for the understanding of macroscopic features in turbulent fluid flows.

In this chapter we aim at contributing to the understanding of how UPOs can be used for distilling the dynamical and statistical properties of chaotic systems of a three-dimensional model. In particular, we will investigate how a long forward trajectory of the celebrated Lorenz 1963 model featuring the classical parameters' value can be seen as a scattering process where the scatterers are the UPOs (*ranked shadowing process*).

Namely, at each point in time we rank in different ranks the UPOs of our database based on their distance with respect to the trajectory (the first rank containing the closest orbits, the Kth rank containing the K closest orbits, etc. See fig. 3.1) and we study the persistence of the ranking. Our goal is twofold. On the one hand, we aim to numerically understand how chaotic trajectories are approximated in terms of UPOs. We anticipate that it emerges that longer period UPOs play a major role in reproducing the invariant measure of the system,

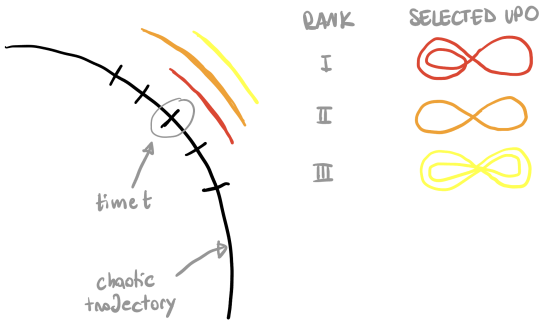

Figure 3.1: Ranked shadowing process. The UPOs of the database are ranked in terms of distance from at each point in time t along the discretised chaotic trajectory (in black).

meaning that they are the most representative of the chaotic trajectory. On the other hand, we study the statistics of the scattering of the orbit between the various UPOs. This study of scattering uses a partition of the phase space of the L63 model that is different than the classical Ulam's partition [50],according to which the phase space is discretised in a regular grid of cubes of equal side. Each UPO (and its immediate neighbourhood) is instead interpreted as a building block of the system, a spatially extended state, and the scattering can be seen as subsequent transitions between different states (see also the recent study of a turbulent flow performed along these lines [112]). In such approximation process, the chaotic trajectory jumps from a UPO to another, as a result of their instability. We will show that this viewpoint allows for a different interpretation of quasi-invariant sets [113]. Namely, by studying the spectral properties of the discretised transfer operator, we obtain a partition of the phase space in different bundles of UPOs, namely UPOs grouped together accordingly to a common behaviour (see later discussion), each one identifying a quasi-invariant region. We prove that UPOs represent a valid tool to investigate diffusion properties of the system, in fact, being exact solutions, they retain a memory of the geometrical structure of the attractor and the dynamics.

The structure of the rest of the chapter is as follows. In section 3.1.4 we present the UPOs database we consider and describe our analysis of the shadowing and discuss its statistical properties. We prove the robustness of the results independent of the shadowing criteria. In section 3.2 we construct the discretised transfer operator in terms of a finite-state stochastic

matrix and use it to describe the scattering of the chaotic trajectory by the various UPOs. We identify quasi-invariant sets through the study of the spectrum of the transition matrix and investigate the decay of correlations associated with the relaxation process of arbitrary ensemble to the invariant measure. In section 3.3 we outline our conclusions and perspectives for future works.

3.1 Shadowing of the Model Trajectory by Unstable Periodic Orbits

3.1.1 Mathematical Framework

With reference to the notation introduced in Section 2, we consider a continuous-time autonomous dynamical system $\dot{x} = f(x)$ on a compact manifold $\mathcal{M} \subset \mathbb{R}^n$. We have that $x(t) = S^t x_0$, where $x_0 = x(0)$ is the initial condition and S^t is the evolution operator defined for $t \in \mathbb{R}_{t>0}$. We define $\Omega \subset M$ as the compact attracting invariant set of the dynamical system that supports a unique invariant physical measure ρ. Hence, for any sufficiently regular function (observable) $\varphi : M \to \mathbb{R}$, we have that:

$$\langle \varphi \rangle = \int \rho(dx)\varphi(x) = \lim_{T\to\infty} \frac{1}{T} \int_0^T \varphi(S^t x_0)dt \tag{3.1}$$

for almost all initial conditions x_0 belonging to the basin of attraction of Ω. Another key concept we already mentioned is the one of periodic orbit. A periodic orbit of period T is defined as

$$S^T(x) = x. \tag{3.2}$$

This representation is not unique. In fact, if equation 3.2 is satisfied, $S^{nT}(x) = x$ is verified as well $\forall n \in \mathbb{N}$. By the semigroup property of the evolution operator, we also have that $S^T(y) = y$ if $y = S^s(x)$ for any choice of s. From now onward we will considered a periodic orbit to be identified by its prime period $T > 0$ (we do not consider equilibria) and an initial condition

x_0. As discussed above, the attractor of a chaotic system is densely populated by UPOs, which provide key information on the system despite being non-chaotic themselves. Indeed, a forward trajectory on the attractor can alternatively be seen as undergoing a process of scattering between the neighbourhood of the various UPOs. For a while, the trajectory shadows with a certain persistence - see later discussion - a nearby UPO before being repelled. The UPOs act as scattering centers exactly as a result of their instability. An interesting alternative tool to measure persistence is provided by the extremal index [114], a concept first introduced in extreme value theory [115] that measures the presence of clusters of exceedances. Within the dynamical systems framework, such quantity can provide information on the local and global properties of the attractor of the system and in particular it can be used to estimate the average cluster size of the trajectories within the neighbourood of a given point [116, 117].

3.1.2 The Model

Our analysis is performed on the L63 model, which arguably is the most paradigmatic continuous-time chaotic systems. The evolution equations of the L63 model are:

$$\dot{x} = -\sigma(x + y)$$
$$\dot{y} = Rx - y - zx$$
$$\dot{z} = -\beta z + xy$$

where the three parameters σ, R, β are positive numbers respectively proportional to the Prandtl number, Rayleigh number and geometry of the considered region. For specific choices of the parameters' value the attractor is a strange set, the dynamics is characterised by sensitive dependence on initial conditions [118] and the system is dissipative ($\nabla \cdot f < 0$). Additionally, the attractor is densely populated by an infinite number of UPOs [119].

We consider the standard parameters value $\sigma = 10$, $R = 28$ and $\beta = 8/3$. For such values, the dynamics of the system is characterised by a chaotic behaviour on a singularly hyperbolic attractor (see fig 3.2a) that supports an SRB measure [120]. In particular, the maximal Lya-

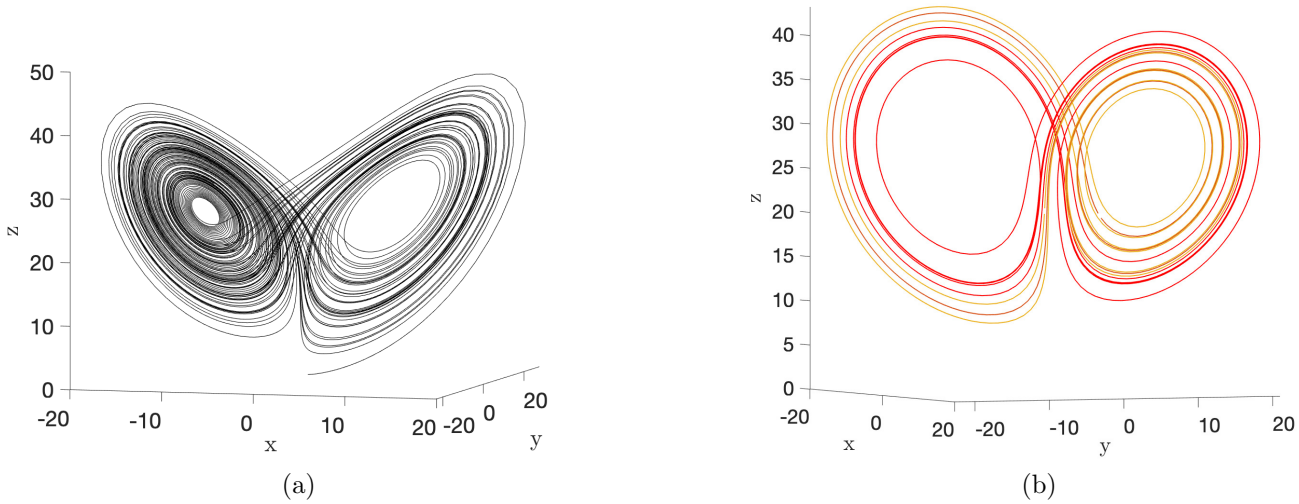

(a) (b)

Figure 3.2: Panel (a): Lorenz attractor. Panel (b): four periodic orbits of the L-63 system

punov exponent of the system is $\lambda_1 \approx 0.91$, corresponding to a characteristic time of the system $\tau_1 \approx 1.1$.

Many studies on UPOs of the Lorenz system have been carried out. Eckhardt and Ott [81] presented one of the first numerical applications of the periodic orbit formalism by considering an approximate symbolic coding [3] (UPOs with period up to 9) to calculate Hausdorff dimensions and Lyapunov exponents. Franceschini, Giberti and Zheng [121] calculated a number of UPOs of the Lorenz attractor at both standard and non standard parameter values and used them to approximate the topological entropy and Hausdorff dimension. Zoldi [6] investigated to what extent trace formulas can can predict the structure of the histogram of chaotic time series data extracted from the run of the L63 model with different parameter values. The use of a correct weighting in the trace formula has been extensively investigated[122, 123, 4].

3.1.3 The Database

In this section we describe some general characteristics of the collected set of UPOs. Many numerical algorithms for the extraction of UPOs in the Lorenz-63 model have been proposed so far. Saiki [124] reviewed the Newton-Raphson-Mees method, proposing a value for the damping coefficient related to the stability exponent of the orbit, while Barrio et al. [125] carried out an extensive high-precision numerical simulation in order to gather a benchmark database of

UPOs for L63.

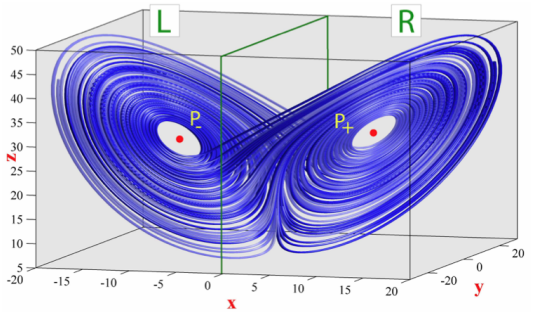

Figure 3.3: Lorenz attractor and its symbolic notation. The phase space is divided into the two region R and L that originates the symbolic dynamics. Figure from [125].

It is possible to construct a symbolic dynamics that characterises uniquely the UPOs of the L63 model [126]. Namely, we can attribute symbol sequences to trajectories of the Lorenz attractor by following them in time. Every time a trajectory passes through the right lobe of the attractor we attribute the symbol R, and we attribute the symbol L when it passes through the left lobe. In this manner every trajectory is assigned a bi-infinite label, and periodic orbits repeat indefinitely the finite sequence of symbols of its period, thus being characterised by their finite period sequence only. For example, if a trajectory does one loop on the left and one of the right, it will be defined by the sequence LR. If a trajectory does a loop on the left and three on the right and another one on the left, it will be characterised by the sequence LRRRL.

Motivated by the work of Galias and Tucker [127], who computed all $M = 2536$ UPOs of symbolic sequence period up to 14, we decide to use this set of UPOs as a benchmark for the rest of our analysis. In particular, A. Gristun and myself computed the UPOs using Newton's method (see section 2.3.2) and as a sanity check compared the obtained period and stability properties of the UPOs with the results presented in [127]. The database can be found as supplemental material of [128] and it contains all initial conditions, periods and first Lyapunov exponents of the computed UPOs. More details on the numerical calculations are presented in the appendix. The statistics of prime periods is shown in Fig. 3.4. The periods span from $T_{min} = 1.5587$ to $T_{max} = 10.8701$, and our sample presents the characteristic exponential growth with the period [129]. The values of Λ_1 ranges from 0.756 to 0.994 and agree within an error of 1% with the values of Λ_1 obtained in [126] (See fig. 3.5). No UPO has a vanishing or

negative value of Λ_1 (which would go against the chaotic nature of the flow).

Note that, as well known, the local instability of the L63 model varies wildly within its attractor, where regions with very high instability alternate with regions where one observes return-of-skill for finite-time forecast [130]. Hence in this case, as opposed to what observed in [14], the heterogeneity of the attractor in terms of instability cannot be explained using the properties of the individual UPOs, possibly because we are considering here a very low-dimensional flow, whereas a higher level of detail at spatial level would be needed.

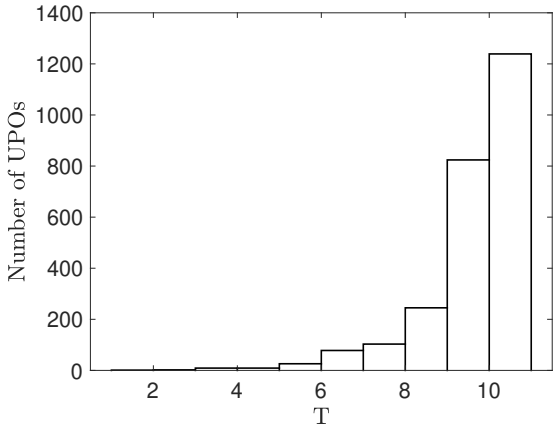

Figure 3.4: Number of UPOs in our database vs their prime period. We have considered symbolic sequences of period up to 14.

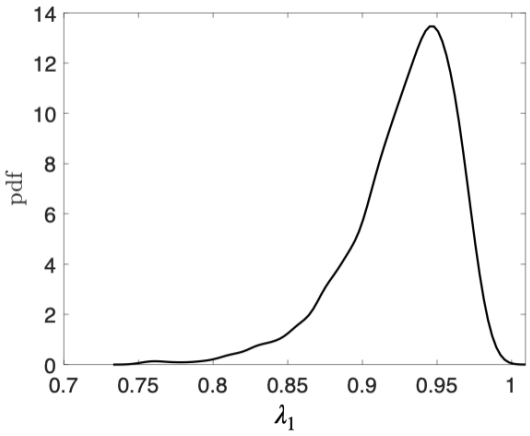

Figure 3.5: Distribution of the maximal Lyapunov exponent

3.1.4 Shadowing

A very appropriate tool to explore the geometry of the attractor under the lens of its UPOs is called "shadowing", namely the process of approximation of a chaotic trajectory in terms of unstable periodic orbits. For uniformly hyperbolic systems without continuous symmetries, UPOs are dense in the attractor [131]. This implies that it is always possible to find a periodic orbit arbitrarily near to a chaotic trajectory, allowing for a reconstruction of the trajectory up to any arbitrary accuracy. In general, even though the shadowing property has not yet been formalised for more general system, it is widely assumed to be valid. Evidence of turbulent trajectories being shadowed by unstable equilibria and UPOs are present in forced two-dimensional flows [104, 10, 132], isotropic turbulence [108], plane Couette flow ([133, 134, 135]), Kolmogorov flow in two [9] and three dimensions [8]. We say that a UPO is shadowing a chaotic trajectory if the UPO is "close" to the chaotic trajectory and co-evolve with the trajectory for "some period of time". It is important to note that when considering non-hyperbolic systems, closeness to a periodic solution is not a sufficient condition for shadowing, even though the two terms are often used as synonym in the literature. For infinitesimally small distances the two requirements becomes equivalent, but if the distance is not negligible it is important to verify one as well as the other. Both "closeness" and "period of time" required for the shadowing are not universal and will be determined based on the situation, assessing respectively both distance and co-evolution time (see later discussion). As one could expect, the length of the co-evolution period depends on the instability of the solution that is being shadowed.

In our numerical investigation we choose to consider the so-called "rank shadowing" [128]. Given a chaotic trajectory, at each point in time we rank in different ranks the UPOs of our database according to their distance to the chaotic trajectory, and we study the persistence of the ranking. By having a ranking we have the possibility to control both distance and persistence of the shadowing simultaneously, in order to assess the quality of the shadowing. As we mentioned before, we are not only interested in the distance with the trajectory, but in the combination of distance and co-evolution, since closeness only implies that the distance is small

regardless of having the two trajectories co-evolving. In fact, even though an orbit might not be the closest to the trajectory, it could persist in the shadowing in further ranks. It is also possible that multiple UPOs might be shadowing the trajectory at the same time (simultaneous shadowing) [87, 136]. Finally, the existence of a ranking allows us to test the robustness of our results when relaxing the shadowing condition.

3.1.5 Ranked Shadowing of the Chaotic Trajectory

We present here our results on how the UPOs rank shadow a long chaotic trajectory. The data reported below refer to a chaotic trajectory $\mathcal{X}_{chaotic}$ of duration $T_{max} = 10^5$ where the output is given every $dt = 0.01$. This leads to considering the set of points $\mathcal{X}_{chaotic} = \{x_t\}_{t=1}^{N_{max}}$ where N_{max} is $T_{max}/dt = 10^7$. Since the system is ergodic and we consider a long trajectory compared to the timescale of the system, the statistics presented here are extremely insensitive to the chosen initial condition. In fact, we have repeated the same procedure for a total of five different chaotic trajectories of duration $T_{max} = 10^5$ and all the numbers reported below change of at most 1%, while in most cases the difference is only of order 0.1%.

Let us denote the set of UPOs of the database as $\mathcal{U} = \{U_k\}_{k=1}^{M}$ where the UPO U_k is intended as a set of points in the system phase space $U_k = \{u_k(s)\}_{s=1}^{dt*T_k}$, with T_k being its period and dt the time step. the number of points of the chaotic trajectory. We define a metric of proximity that allows us to select and rank the closest UPOs to the trajectory at each point in time. More precisely, we say that the UPO $U_{\bar{k}}$ has the closest pass to the chaotic trajectory $\mathcal{X}_{chaotic}$ at time t if

$$\min_s |u_{\bar{k}}(s) - x(t)| = \min_k (\min_s |u_k(s) - x(t)|) \tag{3.3}$$

It is important to notice that closeness and shadowing become equivalent when (3.3) becomes

infinitesimal. The minimal distance between a UPO and the chaotic trajectory decreases as we consider complete sets of UPOs with larger and larger maximum symbolic length. The statistics of such distance for the case studied here is shown in Fig. 3.7a and discussed below. We can then define the *ranked shadowing*, where for each point x_t along the chaotic trajectory $\mathcal{X}_t$ we rank the UPOs according to their distance from x_t. Note that after a time step the distance between a given UPO and the chaotic trajectory will change, while its rank UPO might stay the same or also change.

This calculation was carried out using all available periodic orbits, using an output time-step $dt = 0.01$ (In particular, the trajectories were calculated using the mid-point scheme with an integration time-step of 10^{-3}). Such choice of output time-step allows to observe both persistence and co-evolution of the trajectory with the shadowing UPOs. Had we chosen a larger time-step we would not have observed the right time-scale of the process, and had we chosen a finer time-step the computation of the rank shadowing would have been computationally too expensive. Clearly, it is important to test whether all the UPOs of our database rank shadow at least once the chaotic trajectory.

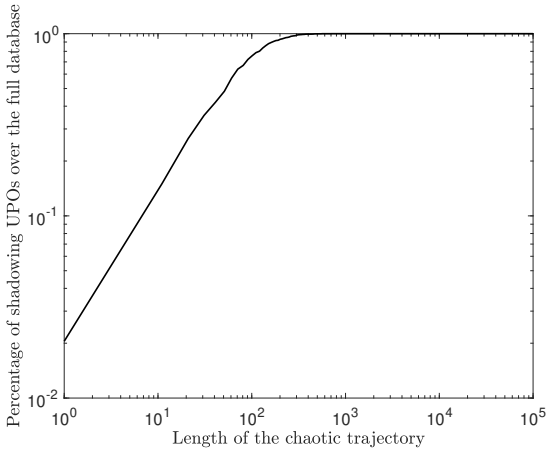

Figure 3.6: Percentage of shadowing UPOs over the full database as a function of the length of the shadowed chaotic trajectory

We can see in fact from Fig. 3.6 that the number of UPOs $N_U(t)$ that perform rank shadowing at least once grows very rapidly with the length of the trajectory t. We find an approximate power law $N_U(t) \propto t^\alpha$ with $\alpha \approx 0.78$ for moderate values of t up to ≈ 100. A chaotic trajectory having a duration of 10^3 time units already saturates the database, so that when considering

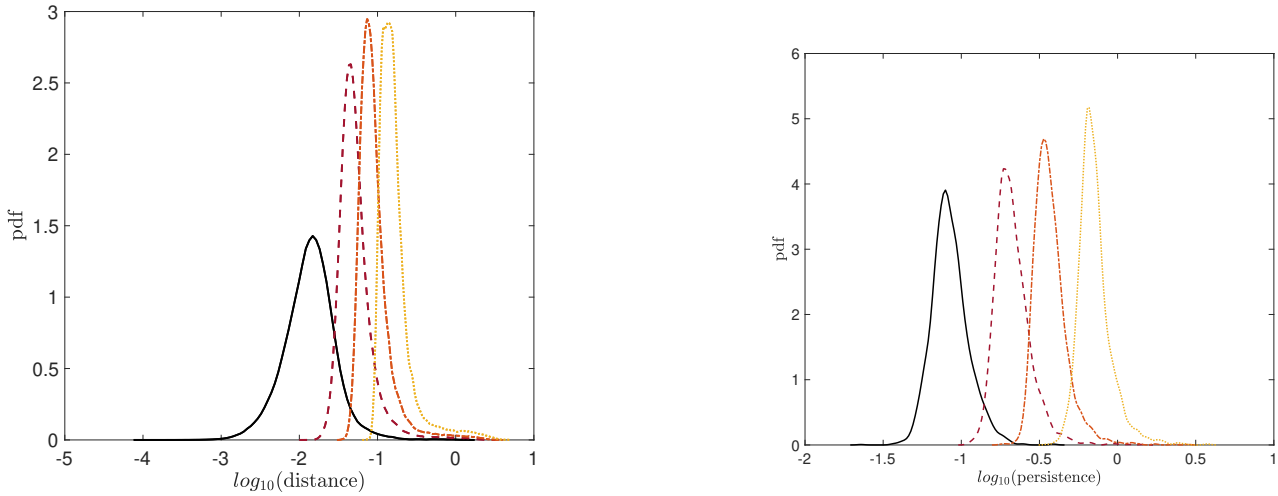

(a) (b)

Figure 3.7: Panel (a): Probability distribution function for the log_{10}-distance distribution of the first rank orbits (solid black line; mean distance 0.0189), rank $K = 10$ orbits (dashed red line; mean distance 0.0649 dashed red), rank $K = 30$ orbits (dashed and dotted orange line; mean distance 0.1130), and rank $K = 100$ orbits (dotted yellow line; mean distance 0.2106). Panel (b): Probability distribution function of log_{10}-persistence of the rank 1 orbits (solid black line; mean persistence 0.0880), and of the shadowing orbits with modified definition allowing for fluctuations withing the first $K = 10$ ranks (dashed red line; mean persistence 0.2218), $K = 30$ ranks (dashed and dotted orange line; mean persistence 0.3846), and $K = 100$ ranks (dotted yellow line; mean persistence 0.7371). See the main text for further details.

a trajectory of duration $T_{max} = 10^5$ all UPOs in the dataset shadow the trajectory multiple times.

The reader might think that the definition of shadowing proposed in Equation 3.3 could be unreasonably strict. In fact, at each time step we are only selecting the nearest UPO, thus possibly discarding many other UPOs that are also extremely close to the trajectory. Hence, we also propose a looser definition of shadowing that allows to take into account the fact that a UPO might still be nearby the trajectory even if it is not anymore the nearest one. In particular, if U_t is the closest UPOs to the trajectory at time t, we say that U_t persists in shadowing at time $t + 1$ if by then U_t is one of the K closest UPOs, or, in other terms, it belongs to one of first K ranks. In this fashion we are rewarding the quality of the shadowing of the UPOs within the first K ranks. When the UPOs exits the first K ranks of shadowing, the closest UPO to the trajectory is selected as shadowing UPO. In this chapter we will consider various values of K ($K = 1$ corresponding to the original, strictest definition of shadowing) in order to

	$P(d > 1)$	$P(d > 10^{-1})$	$P(d > 10^{-2})$
rank 1	0.0001	0.0096	0.6891
rank 10	0.0026	0.0816	1
rank 30	0.0076	0.2997	1
rank 100	0.0230	0.9551	1

Table 3.1: Probability that the distance between the chaotic trajectory and the shadowing UPO exceeds the indicated thresholds.

assess the robustness of our results.

In general, the shadowing UPOs are characterised by two properties. First, by definition, they have a close proximity with the chaotic trajectory. Additionally, since the flow is smooth, we expect a certain degree of persistence in the shadowing: if a UPO is near the chaotic trajectory, the velocity fields will also be similar, and one expects that the UPO will persist its shadowing property for a certain time. The persistence, namely the mean time duration of the shadowing process, quantifies the temporal co-evolution of the chaotic trajectory with the approximating UPOs. In the present discrete numerical implementation of the ranked shadowing process it is possible that the closest UPO might not be the orbits that has the higher persistence. However, even in the case of existence of another orbit with higher persistence, the bounds on the velocity field and, more importantly, on the norm of the Jacobian of such field, guarantee that the selected orbit, chosen solely based on the proximity criteria, would stays close to the trajectory for a certain period of time. We could quantify this information by noticing that the mean speed over the attractor is about 26 with stdev 9. This results on an average displacement of about 0.26 for the considered numerical discretisation $dt = 0.01$.

Fig. 3.7a presents the probability distribution functions (pdfs) of the distance of the shadowing UPOs for ranks $K \in \{1, 10, 30, 100\}$. By definition, as we look at successive ranks, the average distance of the shadowing UPOs with the chaotic trajectory increases, going from $\mathcal{O}(10^{-2})$ for $K = 1$ up to $\mathcal{O}(10^{-1})$ for $K = 100$. More precisely, the mean distance is respectively 0.0189, 0.0649, 0.1130 and 0.2106 for the orbits in rank 1, 10, 30 an 100. One should keep in mind that the rank $K = 100$ includes the top 4% of the UPOs. Note that substantial overlaps exist between the various pdfs, thus indicating that, in absolute terms, the quality of the shadowing

varies throughout the attractor. As we could further quantify in Table 3.1, the quality of the shadowing is in general very high: even considering the weakest definition of shadowing, only about 2% of the recorded distances are above 1. Choosing the strictest definition of shadowing, only 0.1% of the recorded distances are above 0.1. This can be better appreciated also by considering that the attractor of the L63 model is contained in the Cartesian product $\mathcal{P} = [-20, 20] \times [-27.5, 27, 5] \times [1, 48]$ [137]. One can cover this region with 103400×10^{3l} cubes of equal size 10^{-l}. We will use such a partition (for $l = 0$) later in this chapter.

Figure 3.7b shows the distribution of the mean persistence of the shadowing UPOs when we consider the strict as well as looser definitions of shadowing, with $K \in \{1, 10, 30, 100\}$. By construction, the mean persistence increases with K as we are using looser and looser criteria for defining it. Note that in all cases the time persistence is strictly larger than four time steps, meaning that our procedure captures in all cases at least some co-evolution of the chaotic trajectory and of the approximating UPOs. This also suggests that the adopted temporal resolution for our chaotic trajectory and UPOs is sufficient: had we chosen a longer time step, we would have lost the property of co-evolution. Specifically, the mean persistence is 0.0880, 0.2218, 0.3846, 0.7371 (corresponding to approximately 9, 22, 38, and 74 time steps) when allowing for fluctuations respectively in the first and first 10, 30, and 100 ranks. In the latter, case, persistence is of the same order as the Lyapunov time (Λ_1^{-1}). These average temporal durations translate into average rectified distances of co-evolution of about 2, 5, 10 and 19. These figures are larger by a factor $\mathcal{O}(10^2)$ than the corresponding average distances between the chaotic trajectory and the shadowing UPOs, thus reinforcing our claim that the shadowing is accurate and persistent.

3.1.6 Longer Period UPOs Shadow the Trajectory for a Longer Time

We define the *shadowing time* of a UPO as the total amount of time that the UPO spends shadowing the chaotic trajectory. More precisely, if the UPO U_k is selected as shadowing orbit t_k times, its shadowing time will be $r_k = t_k * dt$. This quantity is a good indicator

for the absolute shadowing time, but it does not take into account the length of the UPO. Longer period UPOs correspond to a longer trajectory in phase space. We then introduce the *occupancy ratio* for the UPO U_k, defined as $o_k = \frac{t_k}{T_k/dt}$ with T_k being the period of the UPO. In this way we are able to measure the shadowing time normalised over the period of the UPO. An occupancy ratio much larger than one indicates that it is likely that a large portion of the UPO has shadowed the trajectory at least once.

One could interpret the trace formula given in Eq. (2.37) as suggesting that on the average low period orbits should dominate in terms of shadowing a chaotic trajectory, because the statistical weight of long period orbits is exponentially suppressed. Instead, as shown in Fig. 3.8, the shadowing time increases with the period of the UPOs, while the occupancy ratio remains the same. This means that, by and large, all the UPOs are selected to shadow the chaotic trajectory with the same weighting, independently of their period. We thus found evidence that the occupancy is approximately independent of the UPO period and, since the number of periodic orbits grows exponentially with the period (see Fig. 3.4), longer orbits overall dominate, as shown in Fig. 3.9. In order to assess the robustness of our results, we have studied the shadowing orbits in the first K ranks, with the goal of testing whether even allowing for a looser definition of shadowing UPOs, the role of longer orbits remains consistently dominant. In this context, we are interested in average quantities over all ranks. Namely, we define the *average occupancy ratio* at time t as

$$\bar{o}_t = \frac{1}{K}\sum_{k=1}^{K} o_k \tag{3.4}$$

where o_k is the occupancy ratio of the UPO that shadows the trajectory at time t in rank k. Similarly we define the *average period* and *average shadowing time* at time t. As mentioned above, a given UPO might appear in different ranks at different times.

The robustness of the analysis is confirmed when reproducing the statistics presented in Fig. 3.8 with K shadowing UPOs. Allowing for more shadowing UPOs does not affect the correlation

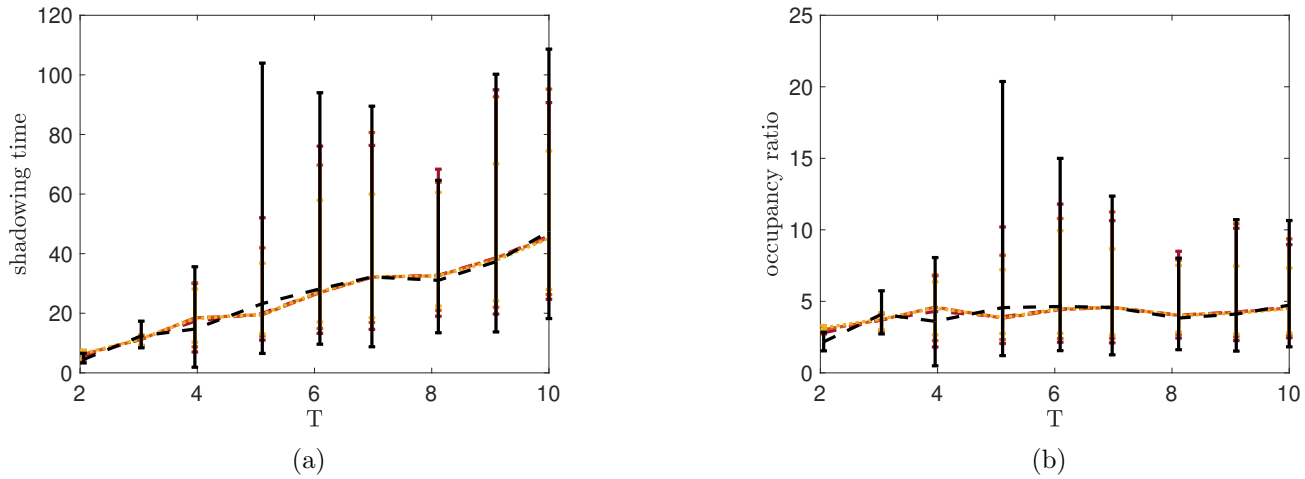

(a) (b)

Figure 3.8: Average shadowing time (panel (a)) and occupancy ratio (panel (b)) of the first rank (dashed black line) and averaged over first 10 (dashed red), 30 (dashed and dotted orange line) and 100 (dotted yellow line) ranks for UPOs of period T. The bars indicate the range between the percentiles 2.5 and 97.5 for each value of T.

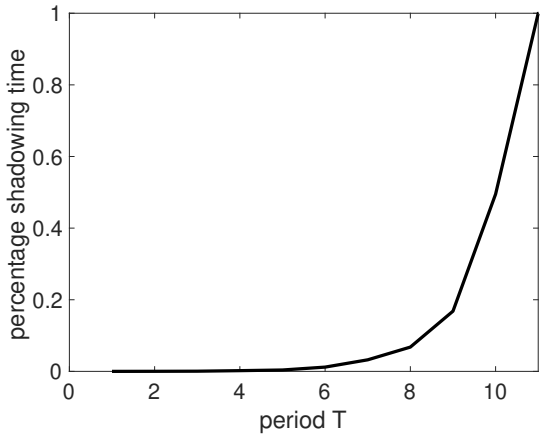

Figure 3.9: Cumulative fraction of the shadowing time performed by UPOs having larger and larger period.

found in the previous section when considering average quantities. Note that the numbers reported in Figs. 3.8a,b scale proportionally to T_{max}.

These findings, which seem at odds with what the trace formula seems to indicate, support the idea that long period orbits play an important role for computing ensemble averages [138, 139, 140].

3.2 Transitions

In this section we use UPOs as a tool to investigate the mixing properties of the system. The *ranked shadowing* will be used to define the Markov process that describes the sequence of transitions between neighbourhoods of UPOs that defines the time evolution of the chaotic trajectory.

3.2.1 Extracting a Markov Chain from the Dynamics

In section 2.1.5 we defined the transfer operator and presented a classical method to consider a discretised version. (See [141, **?**] for recent applications on the L63 model.)

We propose here a different way to discretise the dynamics of the system. Similarly to what done in [112], we select M numerical UPOs $U_1, ..., U_M$ and we associate the states $A_1, ..., A_M$ obtained by considering the UPOs together with their neighbourhoods. Each A_i represents one of the possible discrete states of the system. We implement the shadowing algorithm: at each time step t the UPO U_k that minimises the distance with the chaotic trajectory is selected (See section 3.1.5 for more details on the algorithm). Hence we say that the system is in the state A_k at time t. The stochastic variable $s : \{1, ..., N_{max}\} \subset \mathbb{N} \to \mathcal{A}$ describes the shadowing process just outlined as follows:

$$s(t) = A_k \tag{3.5}$$

with A_k being the shadowing UPO at time t and corresponding neighbourhood. We then construct the stochastic matrix as

$$P_{i,j}^{dt} \approx \frac{\#\{k : (s(k) = A_j) \wedge (s(k + dt) = A_i)\}}{N_{chaotic}} \tag{3.6}$$

where # defines the cardinality of the set and $\wedge$ is logical *and*. The element $P^{dt}_{i,j}$ so defined represents the probability of transitioning from state j to state i, calculated by counting the number of transitions happening from state j to state i and normalising over the total number of transitions (in this case such number is given by number of points of the discretised chaotic trajectory).

We now numerically derive the matrix P^{dt} following the procedure outlined above, by considering the shadowing of a chaotic trajectory with length $T_{max} = 10^5$ with the full set of $M = 2536$ UPOs. We use the spectrum of the stochastic matrix P^{dt} to study the mixing properties of the system. P^{dt} is a stochastic matrix by construction, its first eigenvalues are $\lambda_1 = 1, \lambda_2 = 0.9841, \lambda_3 = 0.9806, \lambda_4 = 0.9706$ and the corresponding decay rates are $\tau_2 = 0.6239, \tau_3 = 0.5104, \tau_4 = 0.3351$. We also verified that there exists a value $\hat{N}$ so that $P^{\hat{N}}_{i,j} \neq 0 \ \forall \ i, j$, implying that the process is ergodic. Additionally, we tested the markovianity of the process by verifying that the stocastic matrix P^{ndt} defining the scattering sampled every $n > 1$ time steps of the chaotic trajectory between the neighbourhoods of the various UPOs has very similar dominant eigenvectors as those of P^{dt}, while the corresponding eigenvalues scale, with a good approximation, with the n^{th} power, as expected.

3.2.2 Quasi invariant sets

We here introduce some key ideas regarding the macroscopic structures and large scale dynamics of the system. When the behaviour of individual trajectory is hard to predict, as it is the case in chaotic systems, the study of the global evolution of densities represents a powerful tool to gain insight into the dynamics. In fact, even if it is not possible to characterise the evolution of a single initial condition, it often happens that we can group the phase space in sets characterised by predictable behaviour. Despite chaotic systems are often transitive, this property can be very weak and it is often the case that the phase space can be decomposed in macroscopic dynamical structure such that the probability of individual trajectories beginning in the subset would leave it in short time is very little. Trajectories tend to stay for a very long time in

one of those regions before entering another region. We call these subsets quasi-invariant sets. More precisely, [142] let $\mathbf{F} : \Omega \in \mathbb{R}^d :\to \mathbb{R}^d$ be a smooth vector field, generating the dynamical system or flow $\{\Phi^t\}_{t\in\mathbb{R}}$, $\Phi^t : \Omega \to \Omega$ be the flow of the autonomous system, μ preserved by Φ. We say that a subset $A \subset \Omega$ is *almost-invariant* over the interval $[0, \tau]$ if

$$\rho_{\mu,\tau} := \frac{\mu(A \cap \Phi_{-\tau}(A))}{\mu(A)} \approx 1 \tag{3.7}$$

in fact $\rho_{\mu,\tau}$ measures the percentage of mass that does not escape the set A within the time interval $[0, \tau]$ ($\mu(A \cap \Phi_{-\tau}(A))$ is the amount of mass still in A after having considered a time evolution within $[0, \tau]$).

Quasi-invariant sets can also be regarded as a valuable tool to study transport and mixing properties of the flow [143], by evolving with minimal dispersion.

Quasi-Invariant Sets and UPOs

We wish to attempt an interpretation of the eigenvectors of P^{dt} corresponding to the subdominant eigenvalues. Let $\mathbf{w}^{(k)}$ be the eigenvector associated with λ_k, $k \geq 2$. This allows us to define two sets B_1 and B_2:

$$B_1 = \bigcup_{i\in\mathcal{I}_1} A_i \quad where \quad \mathcal{I}_1 = \{i : \varsigma(w_i^{(k)}) = 1\} \tag{3.8}$$

$$B_2 = \bigcup_{i\in\mathcal{I}_2} A_i \quad where \quad \mathcal{I}_2 = \{i : \varsigma(w_i^{(k)}) = -1\} \tag{3.9}$$

where $\varsigma(w_i^{(k)}) = sign(w_i^{(k)})$. The sets B_1 and B_2 corresponding to the eigenvectors $w^{(k)}$, $k = 2, 3, 4$ are presented in Figure 3.10. We propose that regions characterised by the same colour (red and blue in our figures) are associated with separate groups, bundles of UPOs. As we will see below, for each eigenvector, the red (blue) regions describe parts of the attractors

with positive (negative) anomalies of the density with respect to the invariant one. Such regions correspond to the distributions that will converge onto the invariant one at a time-scale given by τ_k. We can think of the forward trajectory undergoing transitions between the neighbourhood of the UPOs belonging to a bundle, and being repelled with low probability towards the neighbourhood of an UPO belong to the other bundle. The closer to one the real part of an eigenvalue, the less efficient is the exchange between regions of different colours in the corresponding mode. More precisely, the subdominant eigenvectors $w^{(k)}$ provide an ordering of the quasi-invariant structures in terms of "leakiness".

Keeping in mind that each individual UPO is an actual invariant set and provides an exact solution of the evolution equations, we propose that our method defines structures that are closely related to the so-called quasi-invariant sets [144, 145, 113, 146, 51]. In particular, the red and blue regions in Figs. 3.10a, 3.10b, and 3.10c closely resemble the structures defined by the first three Fiedler vectors defining the connectivity of the graph describing the mass transport of the L63 model (Figs. 5a,b and 6 in [46]).

3.2.3 Relaxation Modes

The red-and-blue representation of the subdominant modes given in Figs. 3.10a-3.10c is essentially qualitative because we distinguish the various UPOs only in terms of the sign of their projection on the eigenvectors. We want now to portray the eigenmodes in $\mathbb{R}^3$, in such a way that it is possible to retain quantitative information associated to the evolution of ensembles of trajectories. We proceed as follows. We partition the compact subset of $\mathbb{R}^3$ given by the Cartesian product $\mathcal{P} = [-20, 20] \times [-27.5, 27, 5] \times [1, 48]$. As mentioned before, this set includes the attractor of the L63 model. We cover this region with 103400 cubes $\mathcal{D} = \{D_i\}_{i=1}^{103400}$ with sides having unitary length. The cubes are built having adjacent sides, so that $\mathcal{D}$ constitutes a partition of $\mathcal{P}$. Each UPO and corresponding neighbourhood intersects a certain number of cubes and each cube might contain contributions from different orbits. We now define a quantity (mass) that weights the contribution given by UPOs of different types within each cube. We set a fixed number of points $\bar{N}$ to be represented in the phase space a priori and assign

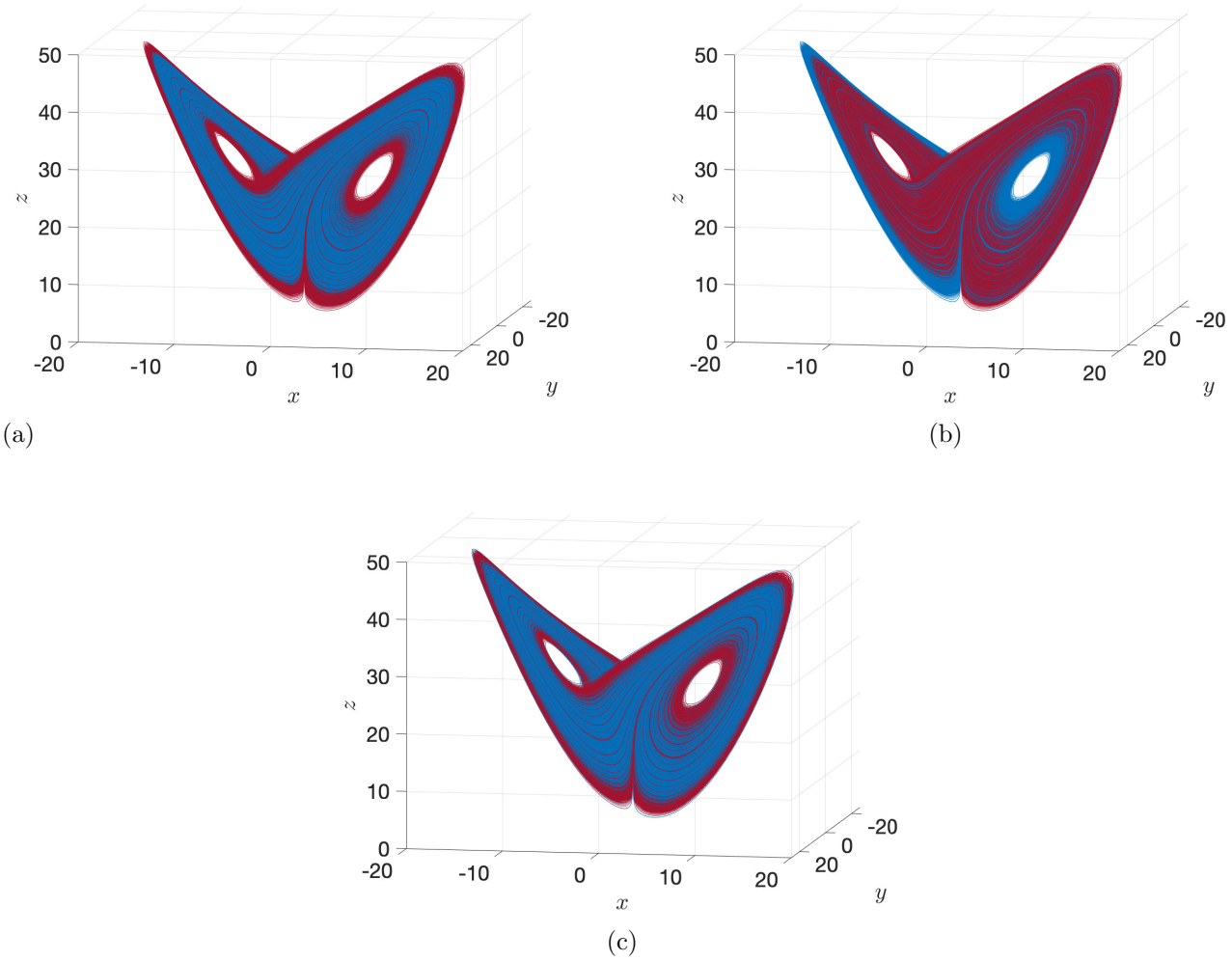

(a) (b)

(c)

Figure 3.10: Quasi-invariant bundles of UPOs obtained with the method outlined in Section 3.2.2. (a): $\lambda_2 = 0.9841$, $\tau_2 = 0.6239$; (b): $\lambda_3 = 0.9806$, $\tau_3 = 0.5104$; (c): $\lambda_4 = 0.9706$, $\tau_4 = 0.3351$.

the points to the different UPOs and relative neighbourhood depending on the weight given by the corresponding component of the eigenvector $w^{(k)}$. These points are chosen along the orbits equally spaced in time. We also distinguish between negative and positive contributions, depending on the sign of the component $w_i^{(k)}$. We finally quantify the mass contained in each cube D_i of the partition by calculating the algebric sum of the points contained in it.

Correspondingly, Fig. 3.11a describes the invariant measure, while Figs. 3.11b, 3.11c, and 3.11d describe the eigenvectors corresponding to the subdominant eigenvalues λ_2, λ_3, and λ_4, respectively. The eigenvectors $w^{(2)}$, $w^{(3)}$, and $w^{(4)}$ are the three slowest modes responsible for the relaxation of an initial probability measure towards the invariant one, the rate of convergence being given by the corresponding eigenvalues. By construction, one can see a good correspondence between the red and blue regions in the panels of Figs. 3.10 and 3.11 associated with the same eigenvalue. Indeed, the physical process responsible for the slow decay of anomalies of an ensemble with respect to the invariant measure described in Fig. 3.11 is indeed the slow mixing occurring in phase space between the regions described by the quasi-invariant sets associated with different bundles of UPOs depicted in Fig. 3.10.

3.2.4 Robustness of quasi-invariant sets

The reader might wonder how robust the results presented in Figs. 3.10a-3.10c and Figs. 3.11a-3.11d with respect to the shadowing criteria defined in Eq. 3.3, which takes into consideration only rank 1 shadowing UPOs. To assess the robustness of the method, we have repeated our analysis using the looser definition of shadowing described in Sect. 3.1.5 that leads to increased persistence of the co-evolution of the chaotic trajectory and of the shadowing UPOs described in Fig. 3.7b. The results are presented in the appendix. The subdominant eigenvectors change very little as larger values of K are considered, whereas, as expected the value of the corresponding eigenvalues get closer and closer to 1, so that slower decay of correlation is found. Clearly, this is the probabilistic counterpart of the results shown in Fig. 3.7b and supports the idea expected, since allowing for more persistence in the shadowing of the chaotic trajectory results in less frequent transitions and thus slower decay rates.

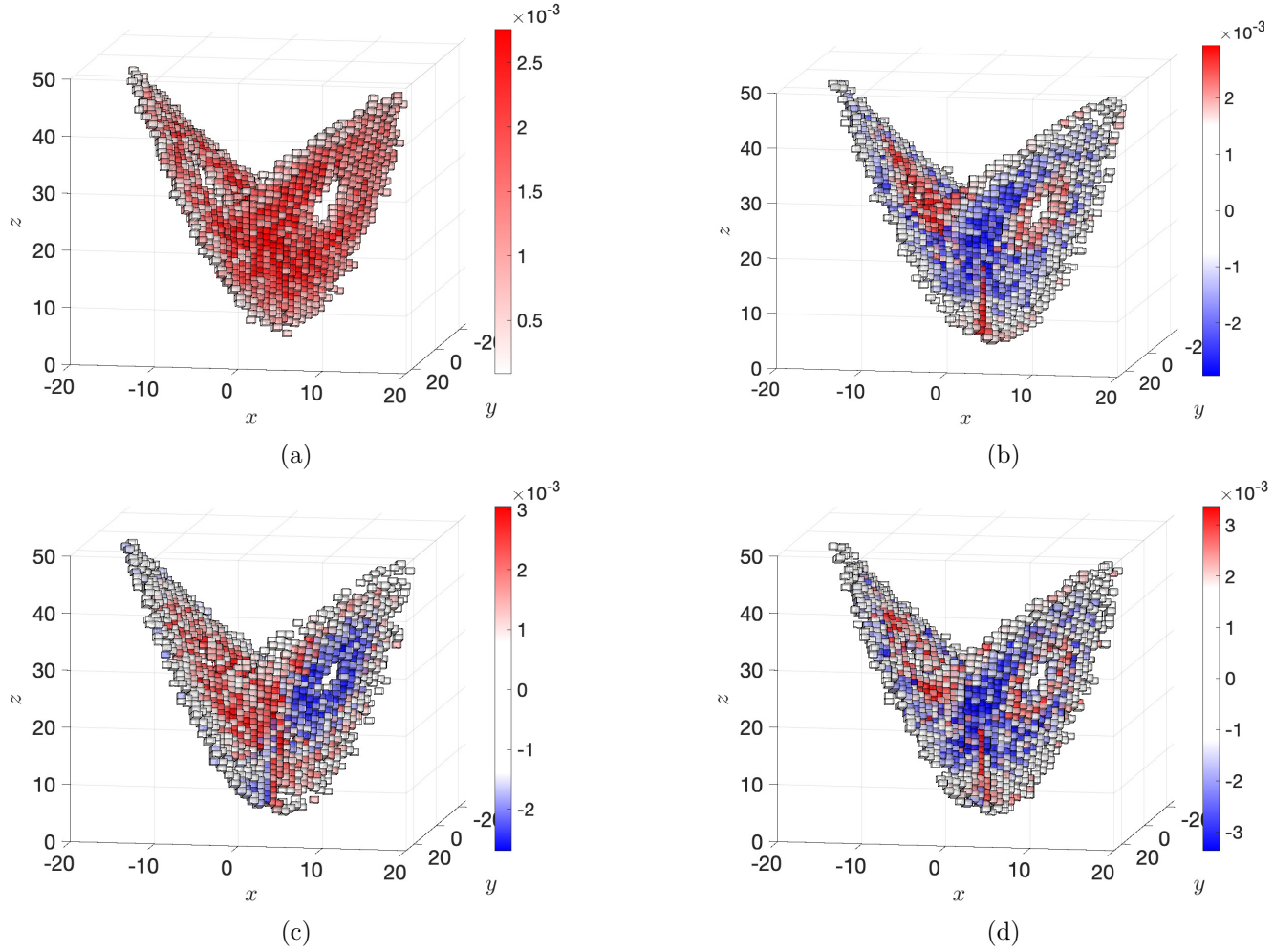

Figure 3.11: Invariant Measure of the system obtained by projection of $w^{(1)}$ (a). Projection in the phase space of (b): $w^{(2)}$ ($\lambda_2 = 0.9841$), (c): $w^{(3)}$ ($\lambda_3 = 0.9806$), (d): $w^{(4)}$ ($\lambda_4 = 0.9706$).

3.3 Summary

The theory of UPOs has found extensive applications in the study of low-dimensional chaotic systems, in particular as a mean to calculate dynamical averages through the use of trace formulas [81, 121, 6]. In recent times promising developments have been made regarding its use for understanding the behaviour of higher dimension dynamical systems [7, 83, 84, 14, 2, 10]. Very recently, efforts has been dedicated to better understanding the similarity of chaotic trajectory segments and of locally approximating UPOs in fluid flows [8, 87]. It usually assumed that the low-period UPOs are the most relevant ones for achieving an accurate representation of statistical properties of the system [81, 147, 80, 148, 149]. Nonetheless, even if the trace formulas [3] seem to suggest the opposite, it is sometimes found that long-period UPOs can be of great importance for computing statistical averages [138, 139, 140]. Additionally, UPOs have been used as a way to perform coarse-graining: it has been shown that it is possible to approximate accurately the evolution of a fluid flow using a finite-state Markov chain where each state corresponds to the neighborhood of a UPOs [112]. Finally, specific UPOs have been shown to key to separating quasi-invariant sets for the L63 model [142].

In this chapter we have attempted to bring together these research lines by performing an accurate analysis of how a long chaotic trajectory of the L63 model with the standard parameter values can be approximated using the complete set of UPOs having symbolic dynamics with period up to 14, numbering 2536 UPOs. The chaotic trajectory can be seen as a continuous process of scattering between the neighbourhood of the various UPOs. At each time step, we rank the UPOs in terms of their distance to reference point, and investigate how the distances and the ranking changes in time. The shadowing of the trajectory involves both proximity and the fact that, as a result of the smoothness of the flow, the reference point of the trajectory and of the considered UPOs co-evolve; indeed we can say that the rectified distance of the co-evolving UPO with the trajectory is of order of magnitude larger than the initial distance between the two. We find that longer UPOs, as a result of their higher number and longer spatial extent, are the most effective in shadowing the orbit of the system. This holds true if we consider a relaxed version of our algorithm, which allow for the rank of the shadowing UPO

to fluctuate up to a certain threshold (*very good* vs. *optimal* shadowing).

We then investigated a finite-state representation of the dynamics where each state is given by an UPO and its neighbourhood, and the stochastic matrix is defined in a frequentist way by studying the transitions defining the time-dependent shadowing of the chaotic trajectory. Since we are implementing a discretized representation of the transfer operator, the eigenvectors corresponding to the subdominant eigenvalues describe the process of relaxation of ensembles towards the invariant measure. In particular, they are instrumental in defining sets corresponding to positive and negative anomalies with respect to the invariant measure that describe how mass decays to the invariant measure at different decay rates. While a similar UPOs-based Markov chain model has been recently proposed by [112] with the goal of computing averages, to the best of our knowledge, this is the first time this specific discretization is performed with the purpose of analysing the mixing properties of the system. In addiction, building on the fact that UPOs are invariant sets that transport mass across the attractor, the regions of the eigenvectors having the same sign can be thought as approximately defining quasi-invariant sets. Indeed, the patterns defined in this way exhibit qualitative agreement with the structures found in the L63 model by Froyland and Froyland and Padberg in [46] and [142] using the discretization of the transfer operator based on the classical Ulam's partition. We interpret our findings as follows. The forward trajectory typically undergoes scattering between UPOs belonging to a bundle of UPOs associated with a quasi-invariant set, while, rarely, the scattering process bring the trajectory with close proximity of an UPO belonging to the other bundle, associated with a competing quasi-invariant set. Such process is qualitatively depicted in fig. 3.12: the forward trajectory (not represented) jumps with a high frequency between UPOs of the red type (each segment in red is the shadowing segment of a different UPO) and it is repelled with a very low probability to UPOs belonging to the competing blue bundle.

Clearly, further research is needed in this direction in order to assess differences and similarities between these approaches. Our procedure seems to have a good degree of robustness. It is encouraging to see that if we construct the stochastic matrix using the relaxed definition of the shadowing mentioned above, the eigenvectors corresponding to the subdominant eigenvalues are virtually unchanged, whereas the decay rates become slower, as persistence is enhanced by

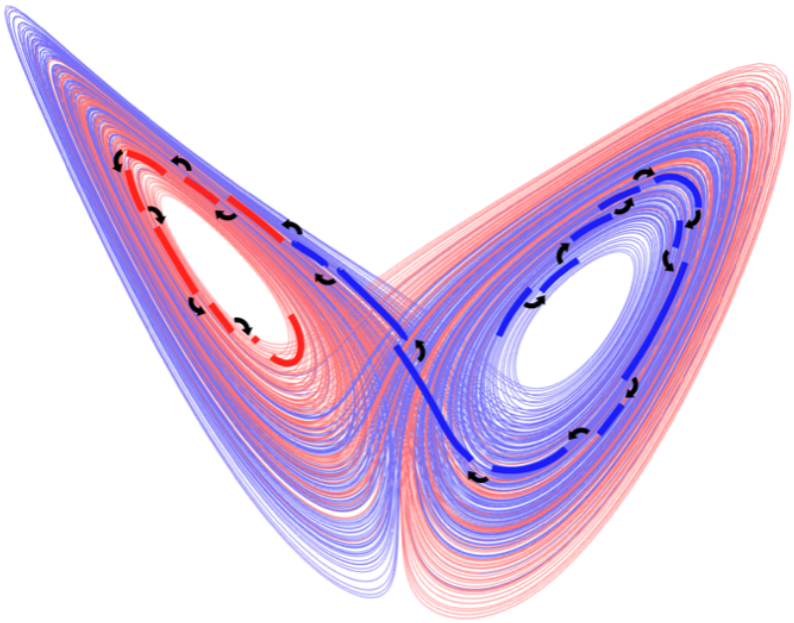

Figure 3.12: Qualitative figure representing the interpretation of our results: regions with the same colours are associated with separate bundles of UPO, each one identifying a quasi-invariant set (light red and blue region). The forward trajectory (not represented) scatters with a high frequency between UPOs of the same bundles and it is repelled with very low probability to UPOs belonging to the other bundle (solid blue and red lines are different segments of UPOs).

slowing down the transitions between the competing neighbourhoods.

Chapter 4

Explaining the heterogeneity of the attractor in terms of UPOs

In chapter 3 we have studied the classical version of the 3-dimensional (3D) Lorenz 1963 model [25] using a rather extensive set of UPOs, following [125], and covering up to period 14 in symbolic dynamics. We have been able to accurately investigate the process of shadowing and elucidate how the statistics of occupation of individual UPOs and of their respective neighbourhood and the transitions between them can be used to construct a finite-state Markov chain representing the statistical and dynamical properties of the system, including its almost-invariant sets [143]. The attractor of the L63 model is extremely heterogeneous in terms of predictability, and features specific regions where return of skill is observed [150]. We have seen that the detected UPOs do differ in terms of their dynamical characteristics, and specifically in the value of the first LE (see Fig. 3.5), thus providing a global counterpart of the heterogeneity of the properties of the tangent space. Nonetheless, considering a 3D chaotic flow imposes that all UPOs feature one positive, one negative, and one vanishing LE. Hence, if we want to investigate the heterogeneity of the attractor of a chaotic flow and possibly relate it to the presence of variability in the number of unstable directions, one needs to consider a higher dimensional system.

In this chapter we would like to characterise and explain the heterogeneity of the attractor of

the Lorenz '96 (L96) [58] model by combining the information derived from the analysis of an extensive set of UPOs and from Lyapunov analysis. As we will discuss below, the L96 model exhibits a rather rich dynamics: depending on the level of forcing, the model features regular, quasi-periodic, or chaotic dynamics, up to the case for extensive chaos. Our goal is to:

- explore whether we can detect the property of variability in the number of unstable dimensions, which, in turn, allows us to rule out hyperbolicity. In fact, very interestingly, the investigation of the UPOs of a chaotic system allows one also to identify violations of hyperbolicity in a relatively simple manner. Indeed, if one detects e.g. two UPOs immersed in the attractor of the system that feature a different number of positive LEs, hyperbolicity is broken through the mechanism of so-called unstable dimensions variability (UDV), which establishes the presence of a fundamental heterogeneity in the attractor of the system and hinders the shadowing property, *i.e.* the existence of an actual trajectory of the systems that stays uniformly close to a numerical one for long time intervals [12]. UDV is typically associated with the presence of large fluctuations of certain FTLEs between positive and negative values [13, 151, 11] and more will be discussed in later sections.

- bridge the gap between global and local properties of the system. We will investigate whether anomalously unstable UPOs preferentially populate regions of the attractor where, applying Lyapunov analysis to the tangent space, one gets, anomalously high instability indicators.

Heterogeneity of the Attractor in Geophysical Fluids The study of the tangent space is a key aspect of the science and technology related to geophysical fluids [152, 153]. In this context, it is well known that the predictability of a system, far from being in any sense uniform, is dramatically state-dependent: certain regions of the attractor feature larger instability than others [154, 155], and this has great impact on data assimilation strategies [156, 157], since it is very hard to define an estimate for the growth of the error along the unstable manifold. In turn, the skill of data assimilation exercises can be used to infer the instability of the underlying

system [158]. The state-dependent predictability results into substantial fluctuations in the value of the FTLEs and in the number of positive FTLEs [159], which is clearly indicative of a violation of the condition hyperbolicity and is associated with the UDV mentioned above [14]. The UDV can be particularly problematic for the efficiency of otherwise very powerful data assimilation schemes [158]. A separate yet extremely important issue that hinders framing the dynamics of geophysical flows in the context of uniform hyperbolicty emerges when one takes into account the whole coupled atmosphere-ocean system. In this case, the large time scale separation between the two geophysical fluids leads to the presence of a non-trivial central manifold, so that the previously mentioned notion of nonuniform partial hyperbolicity becomes relevant [160]. The presence of multiple near-neutral directions, has important consequences for the production of reliable forecasts [161] and for the construction of data assimilation systems for the whole climate [162, 163].

The chapter is structured as follows. Section 4.1 provides a description of the L96 model and of some of its basic properties in the configuration chosen for this study. In Section 4.2 we present the database of detected UPOs and discuss their accuracy in reproducing the dynamics of the system. In Section 4.3 we supplement the UPOs-based analysis with the Lyapunov analysis. In Section 4.4 we discuss the main results of our study and present perspectives of future investigations.

4.1 The Lorenz '96 Model

The L96 model, while not corresponding to a truncated version of any known fluid dynamical system, was developed as a prototype for the midlatitude atmosphere, with the scope of investigating problems of predictability in weather forecasting [58, 164].

Each variable of the model corresponds to an atmospheric quantity of interest at a discrete location on a periodic lattice (Fig. 4.1), representing a latitude circle on the sphere. The variables are spatially coupled, and their equation of motion include nonlinear (quadratic) terms to simulate advection, linear terms representing dissipation and constant terms representing ex-

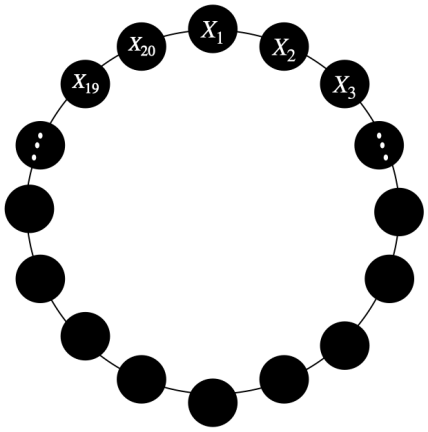

Figure 4.1: Variables of the Lorenz-96 model distributed on a periodic lattice.

ternal forcing. While the model only shares only such basic characteristics with more complete geophysical fluid dynamical models, it has emerged as an important testbed for different applications, including the study of bifurcations [165, 166], of parametrizations [167, 168, 169], of data-driven and machine learning techniques, [170, 171, 172], of extreme events [173, 174, 175], of data assimilation schemes [176, 177], and of ensemble forecasting techniques [178, 179], to develop new tools for investigating predictability [180, 181], and for addressing basic issues in mechanics and statistical mechanics [182, 183, 184, 185, 186]. The evolution equations of the model are:

$$\dot{X}_j = (X_{j+1} - X_{j-2})X_{j-1} - X_j + F, \tag{4.1}$$

where

$$X_{-1} = X_{M-1}, \quad X_0 = X_M, \quad X_{M+1} = X_1. \tag{4.2}$$

impose the periodicity conditions and $F \in \mathbb{R}^+$ is a constant forcing. The two free parameters of the model are M and F. For large values of F and M the model exhibits extensive chaos [185]. We have considered $M = 20$ and $F = 5$ (More details on this choice can be found in the Appendix). In all the simulations the model is integrated with a Runge-Kutta second order scheme with fixed time step $dt = 0.01$. The choice of this (suboptimal but sufficiently accurate) integrator is motivated by the UPOs detecting algorithm used. For such choice of the parameters the model is well within the chaotic regime. It features four positive LEs with the leading one being $\lambda_1 \approx 0.54$ (Fig. 4.2). The characteristic Lyapunov time of the system is

then $\tau_1 = 1/\lambda_1 \approx 1.85$, the Kolmogorov-Sinai entropy can be approximated as $\sum_{i\geq 0} \lambda_i \approx 1.23$ and the Kaplan-Yorke dimension of the attractor is 9.25. The diameter of the attractor is

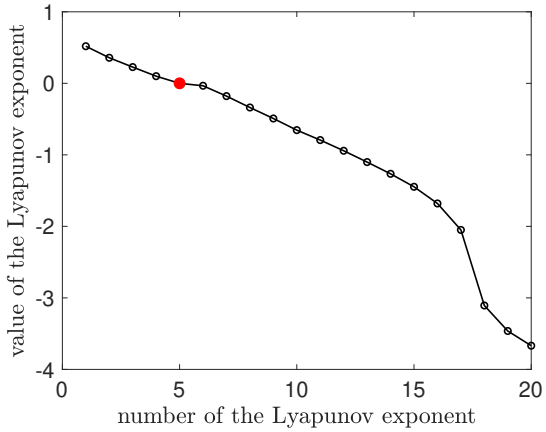

Figure 4.2: Global Lyapunov exponents of the system. The red dot indicates the LE with value zero corresponding to the direction of the flow. There are 4 positive LE and 15 negative LE.

approximately 25, with point-to-point distances distributed as shown in Fig 4.3. The relatively high dimensionality of the attractor is apparent from the very low prevalence of nearby points [187]. The mean speed over the attractor is ≈ 38, meaning that on average the trajectory spans a distance of 0.38 for a time-step of $dt = 0.01$.

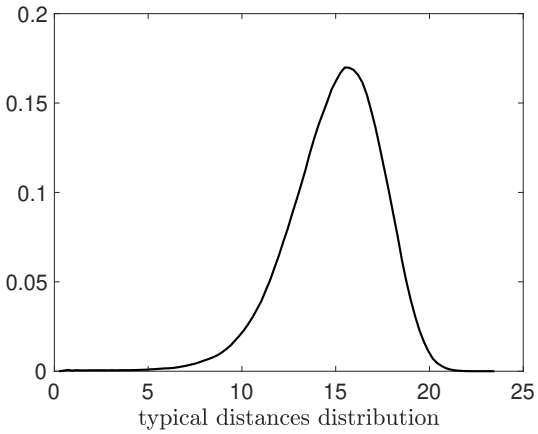

Figure 4.3: Distribution of the typical distances over the attractor

4.2 Unstable Periodic Orbits Analysis

4.2.1 Database of Unstable Periodic Orbits

We mentioned in Section 2.3.2 that the numerical extraction of UPOs from a chaotic model represents one of the greatest challenges in the application of periodic orbit theory [124, 188, 83]. For the Lorenz 96 model it is worth noticing that the equations are symmetric with respect to a cyclic permutation of the variables, so that each time an orbit is detected, the other 19 can be automatically obtained by simply considering all the possible cyclic permutations of variables. Andrey Gritsun constructed a database of 15019 fundamental UPOs (i.e. none of these orbits can be obtained from another orbit of the database through cyclic symmetry) immersed in the attractor with period ranging from a minimum of ≈ 1.5 ($\approx 0.8/\lambda_1$) to a maximum of ≈ 22.8 ($\approx 12.3/\lambda_1$), and lengths ranging from ≈ 2 to ≈ 35 diameters of the attractor (Fig. 4.4).

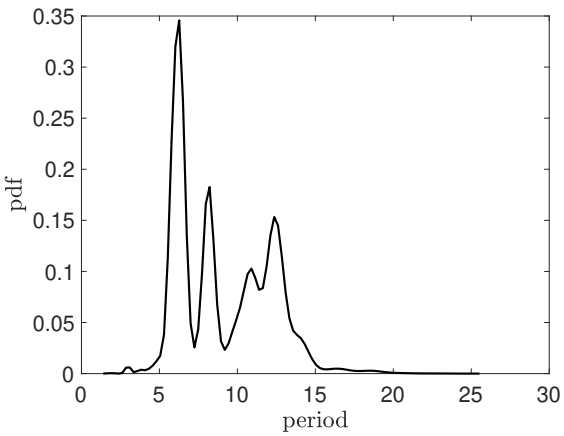

Figure 4.4: Distribution of the periods of the UPOs of the complete database.

In a chaotic system one expects to find that the number of UPOs with prime period smaller or equal than T grows as $\propto \exp(h_{top}T)$, where h_{top} is the topological entropy [1]. As opposed to the study presented in chapter 3, it is clear that our set of UPOs is far from being complete, as longer-period orbits are clearly underrepresented. The difficulty in computing long-period UPOs has been widely discussed in the literature [98, 1, 83]. Nonetheless, we will see that such a set can still provide valuable information on the properties on the L96 model.

Figure 4.5 shows that the UPOs of the database are characterised by vastly different instabilities

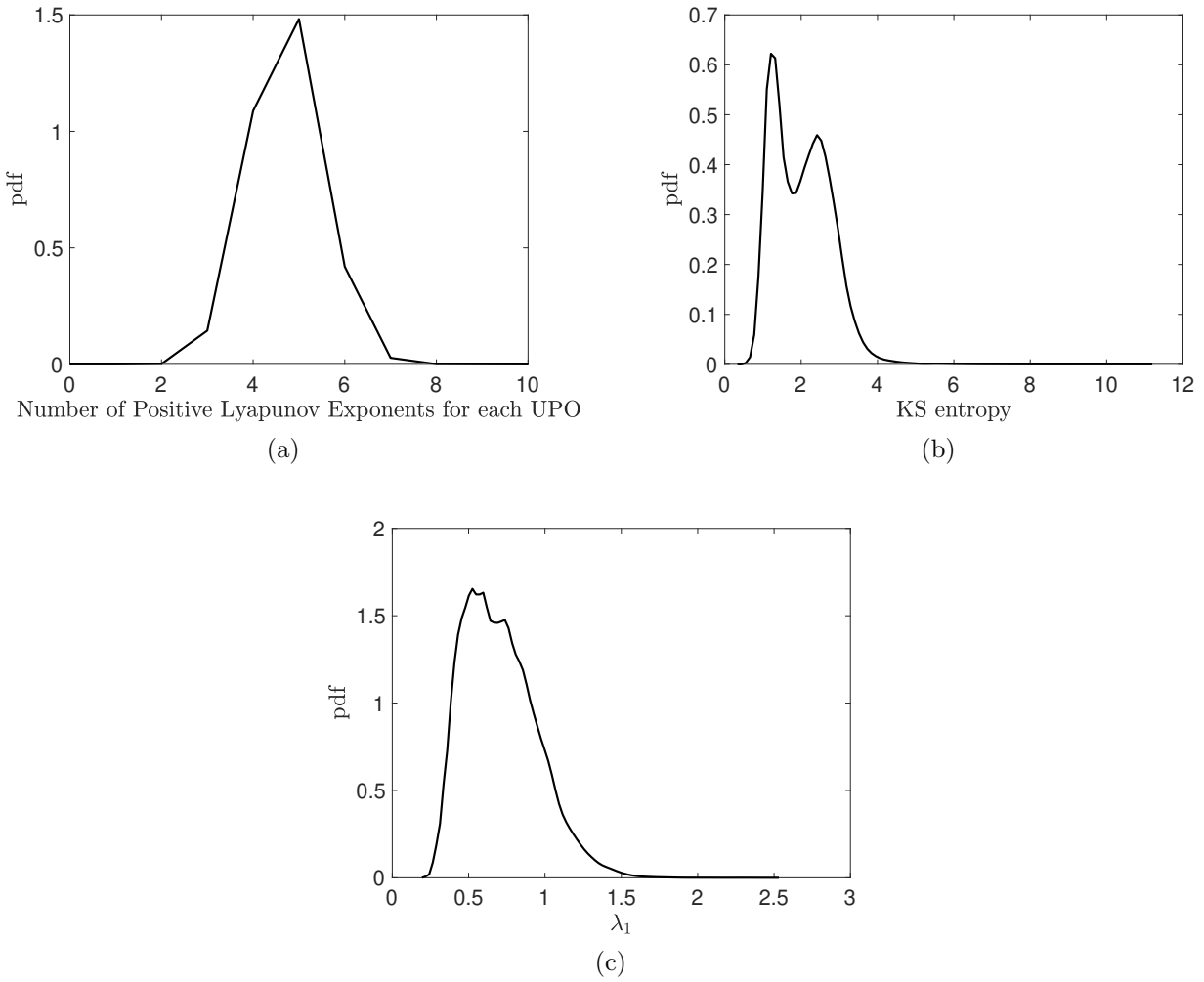

Figure 4.5: Heterogeneity of the instability properties of the UPOs of the database. Panel (a): Distribution of the number of positive Lyapunov exponents of the UPOs. Panel (b): Distribution of the KS entropy of the UPOs. Panel (c): Distribution of λ_1 across the UPOs of the database.

properties, which provide a clear evidence of the heterogeneity of the attractor of the L96 model. The number of unstable dimensions, given by the number of positive LEs of each UPOs, varies from 2 to 9 across all the UPOs: this indicates a very serious violation of hyperbolicity via UDV [12, 13, 151, 11, 14]. The Kolmogorov-Sinai entropy varies between ≈ 0.5 and ≈ 10.0 and the first LE varies between ≈ 0.3 and ≈ 1.8. In the following sections we will provide an interpretation of such behaviour in terms of the behaviour of specific FTLEs of the system.

4.2.2 Ranked shadowing of the chaotic trajectory

In section 3.1.4 we introduced the mechanism of shadowing and discussed its relevance as a tool to explore the geometry of the attractor in terms of UPOs. We mentioned the importance of testing both co-evolution and proximity and verified for the L63 model that our database of UPOs did a very good job in shadowing the trajectory. In this numerical investigation we again consider the so-called "rank shadowing" as defined in 3.1.5. We will refer to both the stricter definition of ranked shadowing given in (3.3), and the looser definition, that prioritises persistence over distance, by allowing for fluctuations in the first $K = 10, 100, 1000$ ranks, in the selection process (See 3.1.4 for more details).

We present here the results on how the UPOs of the database rank shadow a long chaotic trajectory. The data refers to a chaotic trajectory of length $T_{max} = 10^4$ and an output time-step $dt = 0.01$, motivated by the fact that such time-scale is the maximal that allows to observe persistence in the shadowing, realising a trade-off between computational cost and necessity of observing the phenomena. In the implementation of the algorithm we considered all available periodic orbits, but only around 26% was selected in the shadowing of the chaotic trajectory for the first rank, with many instances of orbits shadowing in more than one point the trajectory.

When we instead considered the UPOs that shadows the trajectory at least once in the first $M = 10, 100, 1000$ ranks, the cardinality of such set naturally increased to $79\%, 99.6\%$ and 99.9% respectively of the complete database. The distribution of periods and stability properties of the shadowing orbits are presented in Fig. 4.6 and Fig. 4.7 respectively. In the following paragraph we will show that the quality of the shadowing is almost indistinguishable with respect to the

choice of M, proving the robustness of the shadowing process with the chosen time-step and database of UPOs.

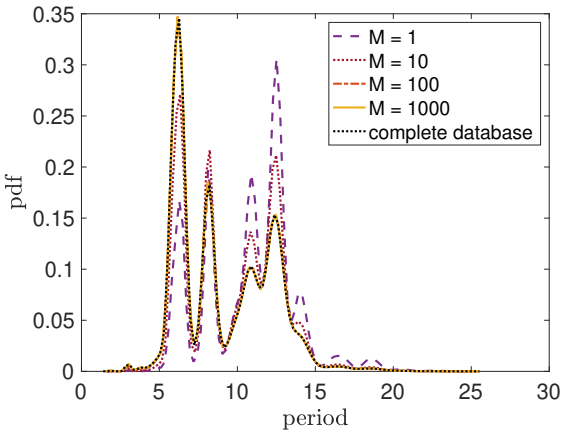

Figure 4.6: Distribution of the periods of the shadowing UPOs that shadows the trajectory at least once in the first M = 1, 10, 100, 1000 ranks.

Distances In order to assess the quality of the shadowing, we first look at the distribution of the distances of the shadowing UPOs from the chaotic trajectory. We can see that when selecting further ranks, by definition, the support of the distribution shifts to the right (Fig. 4.8a), since we are considering UPOs increasingly far from the chaotic trajectory. However, if we use the looser definition of ranked shadowing, all the orbits are significantly close to the chaotic trajectory (Fig. 4.8b), with distances ranging from 0.27 to 7.97. Regardless of the choice of K, the quality of the shadowing is rather good, see Table 4.1; One notices that the quality of the shadowing is extremely similar for $K = 1$ and $K = 10$: the 95% quantile of shadowing distances is approximately 2.99 and 3.21, which is well within the 0.5% quantile of the typical distances distribution over the attractor (See Fig. 4.3). The fact that such distances can be achieved with a very small probability means that if we consider the evolution of a generic chaotic trajectory we will have to wait a very long time before being able to observe the trajectory achieving such distances at time t with the initial condition.

Co-evolution We now investigate the co-evolution criteria. In fact, in order to assess the significance of the shadowing it is crucial to check whether the trajectory and the shadowing orbit co-evolve for a satisfactory period of time. Assessing co-evolution is instrumental for

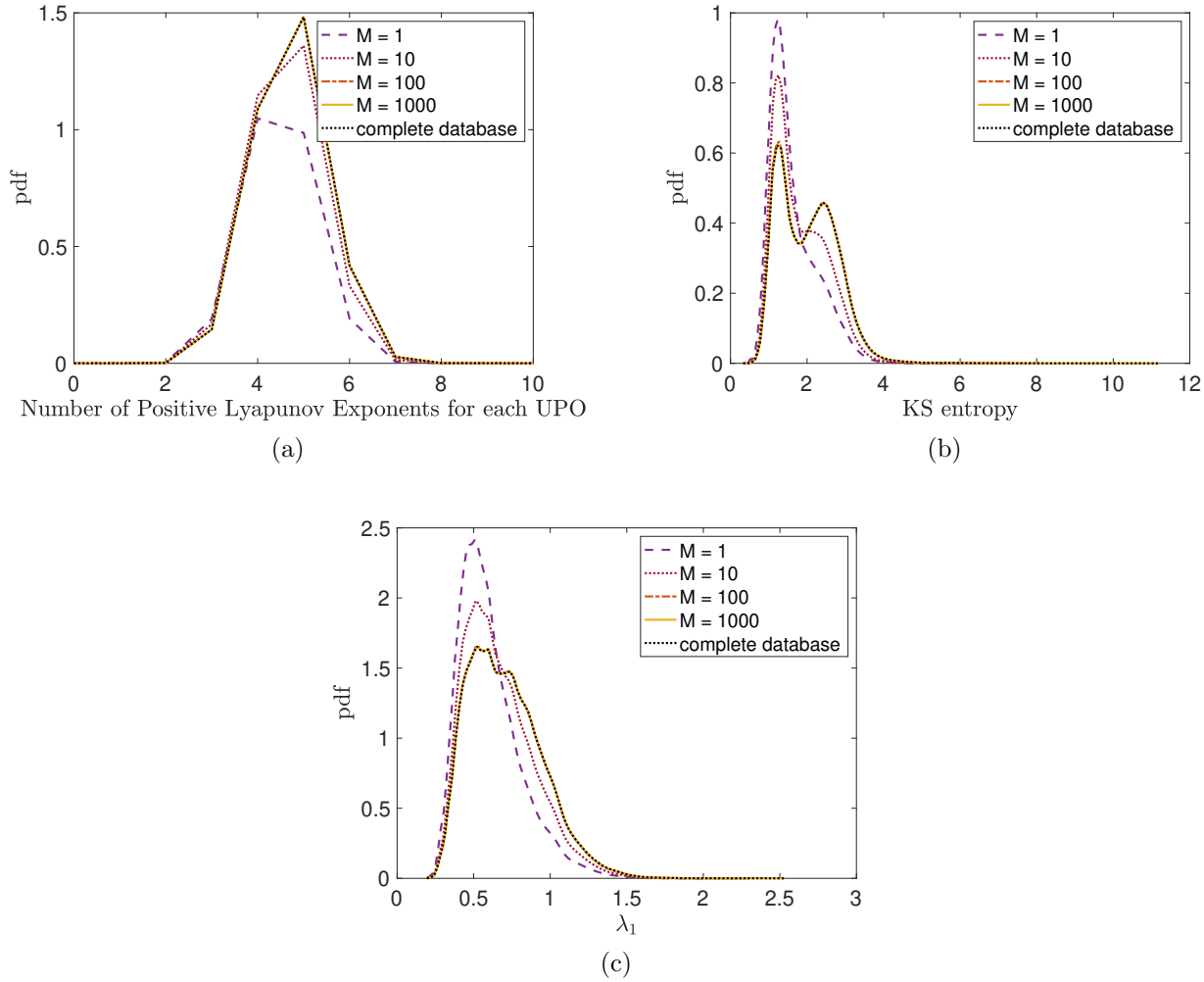

Figure 4.7: Heterogeneity of the instability properties of the shadowing UPOs. Each distribution represent the properties of the UPOs that shadows the trajectory at least once in the first M = 1, 10, 100, 1000 ranks and the complete database. Panel (a): Distribution of the number of positive Lyapunov exponents of the orbits. Panel (b): Distribution of the KS entropy of the UPOs. Panel (c): Distribution of λ_1 across the UPOs of the database.

K	1	10	100	1000
$95th$ percentile	2.99	3.21	3.76	4.64
$mean_{dist}$	1.81	1.96	2.26	2.70
$P_{\%}(d < mean_{dist})$	0.09	0.10	0.12	0.14
$5th$ percentile	0.87	0.95	1.05	1.17

Table 4.1: Distances of the shadowing orbits from the chaotic trajectory. We present data for both shadowing orbits of the first rank and for $K = 10, 100, 1000$.

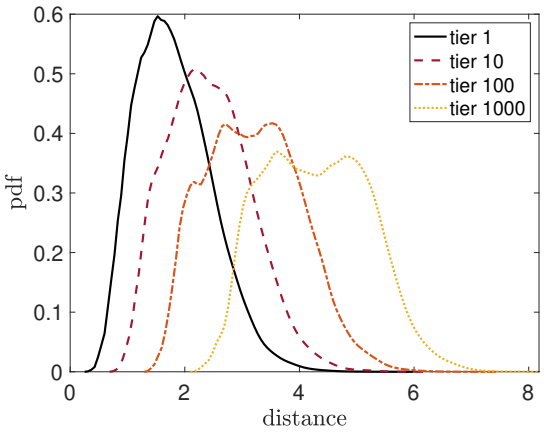

(a)

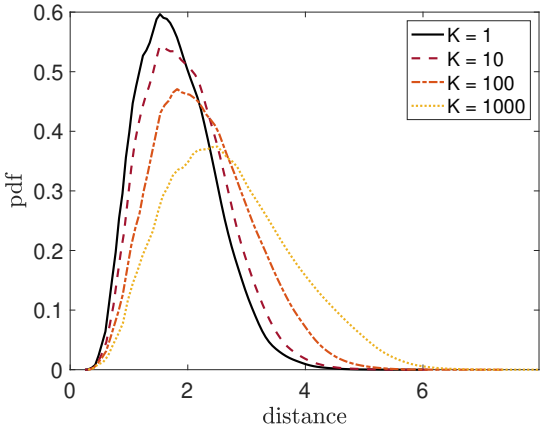

(b)

Figure 4.8: Panel (a): Probability distribution function for the distance of the first rank orbits (black solid line, mean distance 1.81), rank 10 orbits (red dashed line, mean distance 2.42), rank 100 orbits (dashed and dotted orange line, mean distance 3.20), rank 1000 orbits (dotted yellow line, mean distance 4.30). Panel (b): Distribution of the distances from the chaotic trajectory when considering the looser definition of shadowing orbits that allows for fluctuations within the first K=10 ranks (red dashed line, mean distance 1.96), rank 100 orbits (dashed and dotted orange line, mean distance 2.26), rank 1000 orbits (dotted yellow line, mean distance 2.7) and again first rank orbits (black solid line, mean distance 1.81).

constructing a framework that allows an accurate statistical and dynamical description of the chaotic flow [87]. In general, as one might expect, shadowing persistence is negatively correlated with the stability of the orbit. More unstable UPOs will shadow the chaotic trajectory for a shorter time (In particular the correlation between shadowing time and KS entropy of the shadowing UPO is -0.3 for $K = 1000$, -0.23 for $K = 100$, -0.26 for $K = 10$ and -0.13 for $K = 1$).

Figure 4.9 shows the distribution of the mean persistence of the shadowing UPOs when considering the strict (rank 1, in black) and the looser definition of shadowing, with $K \in \{10, 100, 1000\}$. The mean persistence, by definition, increases with K as we are using looser and looser criteria for defining it. In particular, the mean persistence is 0.22, 0.54, 1.04 and 1.69 ($22, 54, 100$ and 170 time steps), that corresponds to an average rectified distance of about $8, 20, 38$ and 63 which, compared to both the size and typical distances over the attractor (Fig. 4.3) and the average distance between the chaotic trajectory and the shadowing UPOs (Fig. 4.8) confirms that the shadowing is persistent and there is evidence of co-evolution.

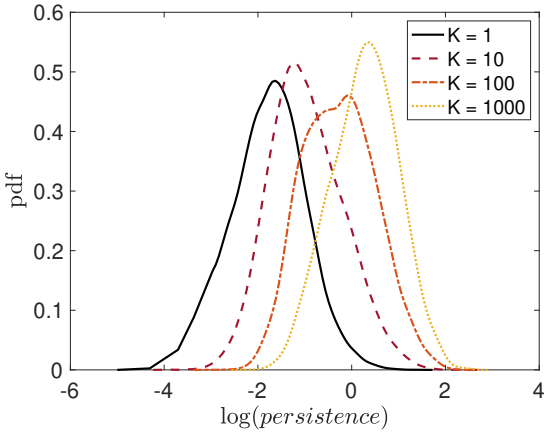

Figure 4.9: Probability distribution function of the log-persistence of the rank 1 orbits (solid black line; mean persistence = 0.22), and the shadowing orbits with the looser definition with $K = 10$ orbits (dashed red line, mean persistence 0.54), $K = 100$ (dashed and dotted orange line, mean persistence 1.04) and $K = 1000$ (dotted yellow line, mean persistence 1.69).

4.3 Local Properties of the Tangent Space

4.3.1 Lyapunov analysis to detect UDV

In [13, 151, 11] it was shown how the UDV could be explained in terms of the presence of fluctuations of one specific FTLE (the one corresponding to the LEs with smallest absolute value) computed over a time scale τ between positive and negative values also when considering very large values of τ. The presence of changeovers between the sign of the FTLE over such long time scales was proposed as evidence of the trajectory following closely UPOs having different number of unstable dimensions. As mentioned earlier, in the system of interest here the UDV involves fluctuations between 2 and 9 of the number of unstable dimensions, hence one could expect to find that several FTLEs feature large fluctuations between positive and negative values, because the UDV manifest itself as a large change in the number of unstable dimensions. This is indeed confirmed by our data.

Figure 4.10a portrays the dependence of the ratio between the value of the j^{th} LE and the the standard deviation of the distribution of the j^{th} FTLEs computed over a time-scale τ as a function of τ. We show results for the first 10 LEs, ordered from the largest to the smallest. Note that the 5^{th} LE is the vanishing one and corresponds to the direction of the flow. The presence of a vanishing LE is generally true for every continuous dynamical system with a bounded non-fixed point dynamics since the separations in the direction of time neither shrink nor grow on average, as a result of the flow being bounded. It is apparent that such ratio is smaller than 3 for all the 10 considered LEs for τ up to 5. Note that for sufficiently large values of τ, the distribution of all the FTLEs corresponding to nonzero LEs converges to a Gaussian with variance $\propto 1/\tau$, in agreement with previous studies [189, 190, 159]. A different scaling is found for the FTLE corresponding to the vanishing LE. Nonetheless, even considering very long averaging times, the support of the pdf of more than one FTLEs includes zero. Excluding the vanishing LE, this applies to 5 FTLEs for $\tau = 10\tau_1$, which is already much longer than the period of the longest detected UPO), see Fig. 4.10b. Clearly, the number of FTLEs fluctuating about zero decreases as one consider larger values for τ. Nonetheless one finds four of such

FTLEs when $\tau = 30\tau_1$ (Fig. 4.10c), and still two for the ultralong averaging time $\tau = 100\tau_1$ (Fig. 4.10d). The fluctuations about zero of the 6^{th} FTLE persist even for much longer averaging times.

Figure 4.11 provides further support regarding how heterogeneous the attractor is in terms of instability. Panel 4.11b shows that the sum of the FTLEs corresponding to the four largest LE - this provides the finite-time estimate of the Kolmogorov-Sinai entropy - have very large fluctuations, and the distribution has support extending to negative values up to averaging times of about $\tau = 3\tau_1$. We also see - Panel 4.11c - that the largest (ordered) FTLEs can have negative values for averaging times up to $\tau = 3\tau_1$. This implies that the system features (temporary) return of skill for a substantial amount of time, during which the largest singular value of the tangent linear operator is smaller than one. Note that the distribution of the largest FTLE differs from the one of the first FTLE - see Panel 4.11a. Finally, Panel 4.11d shows the distribution of the number of positive FTLEs. Note that we have removed from the count the direction of the flow, whose corresponding FTLE obviously fluctuates between small positive and small negative values. We observe that the number of positive FTLEs, in agreement with what shown in Fig.4.10 has very large fluctuations even for very long averaging times τ.

4.3.2 UDV explained in terms of UPOs

In this section we wish to provide an interpretation of the variability observed in the previous paragraph in terms of UPOs. Our intuition is that the local stability properties of the tangent space, measured in terms of the values of the FTLEs, are somehow encoded in neighbouring UPOs populating that same region of the attractor. In order to explore this correlation we will use the tool offered by the rank shadowing process, that provides an effective instrument to relate local properties of the chaotic trajectory with the shadowing UPOs. It is important to keep in mind that UPOs are large-scale structures in the phase space of the system and have a very long period compared to the typical shadowing times. Hence, we are comparing local and global properties of the system.

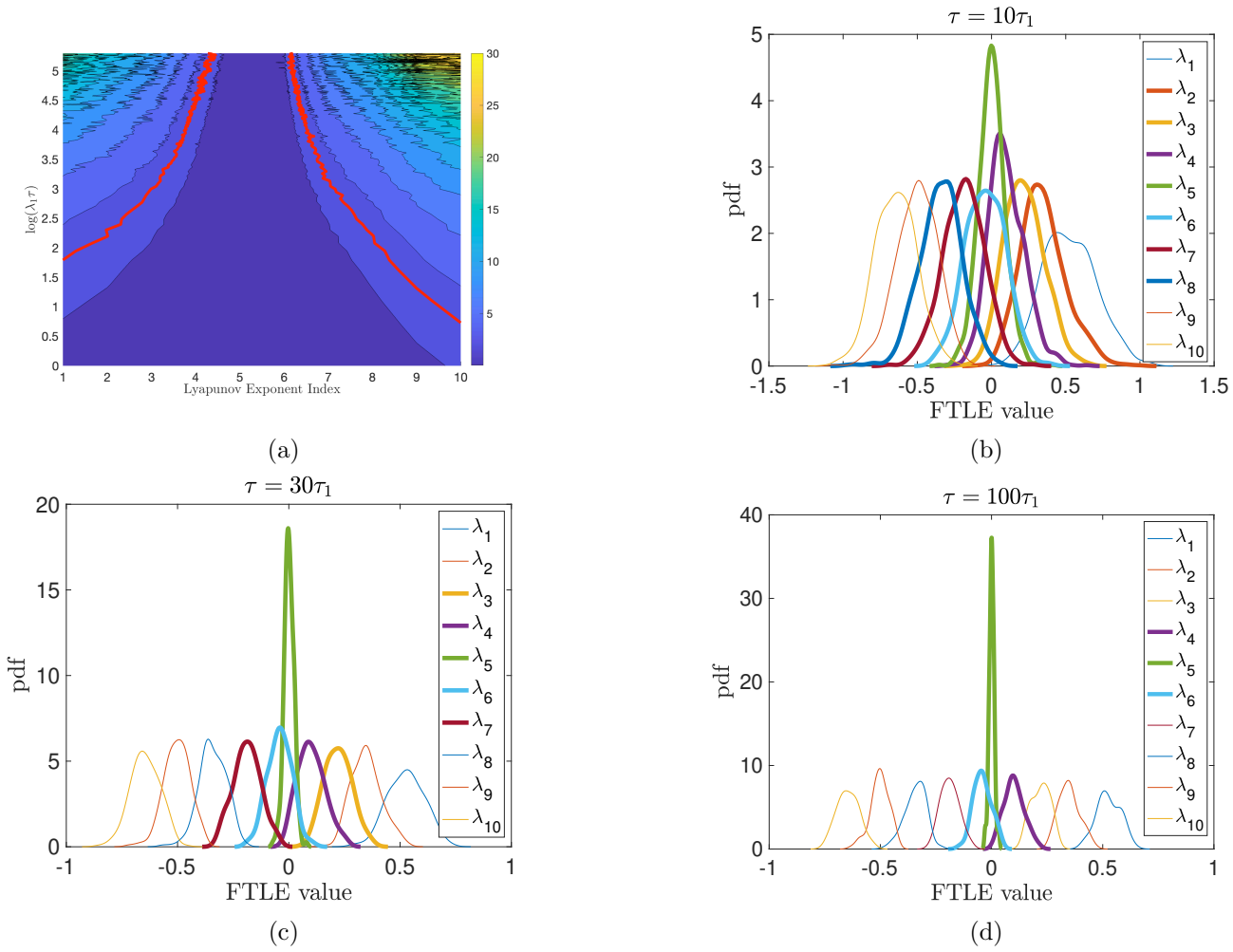

Figure 4.10: Evidence of large fluctuations about zero of several FTLEs. Panel (a): Ratio between the LEs and the standard deviation of the corresponding FTLEs computed over τ. The color level are separated in units of two. The red line indicates the isoline with value 3. Panel (b): Distribution of the first 10 FTLEs with averaging time $\tau = 10\tau_1$. Thick lines correspond to pdfs whose support include zero. Panel (c): Same as (b), with $\tau = 30\tau_1$. Panel (d): Same as (b), with $\tau = 100\tau_1$. The 5^{th} LE is the vanishing one and corresponds to the direction of the flow.

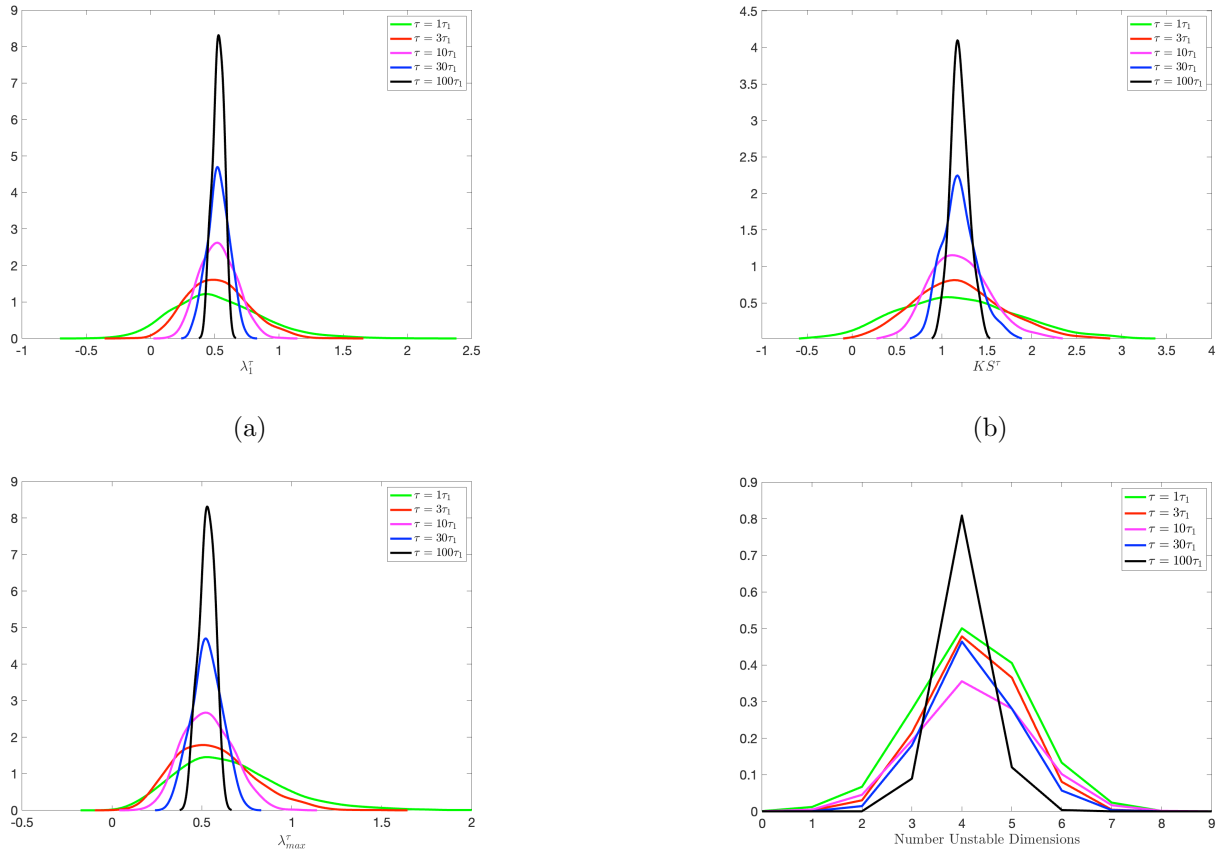

(a) (b)

(c) (d)

Figure 4.11: Evidence of heterogeneity of the tangent space. Panel (a): Distribution of the first FTLEs for different averaging times τ. Panel (b): Distribution of the sum of the first four FTLEs for different averaging times τ. Panel (c): Same as (a), for the largest FTLE. Panel (d): Distribution of the number of positive FTLEs for different averaging times τ.

K	1	10	100	1000
λ^{τ}_{max}	22	26	32	38
λ^{τ}_{1}	13	16	20	25
KS^{τ}_{+}	33	38	45	53
KS^{τ}	24	27	35	42

Table 4.2: Temporal correlation between the local properties of the chaotic trajectory and relative shadowing UPOs (expressed in %). We calculated such correlations for different values of K, between the local maximal Lyapunov exponent (and first lyapunov exponent respectively) and first Lyapunov exponent of the shadowing, local KS entropy (and sum of the positive local FTLE respectively) and KS entropy of the UPO.

We proceed as follows. With reference to the notation and framework defined in section 4.8, let's suppose that at time t_k the chaotic trajectory is being shadowed by the UPO U_k for a period of time τ_k, before being approximated by another UPO U_h at time $t_h = t_k + \tau_k$. We then have a sequence of shadowing orbits U_k, each one associated to a specify persistence time τ_k. For each U_k we calculate the spectrum of the FTLEs of the chaotic trajectory at time t_k for the shadowing interval τ_k, and investigate the correlation with the relative LEs and instability properties of the shadowing UPO U_K. Please note that each orbit might be considered more than once when looking at the correlations. Note also that the values of the time intervals τ_k can change substantially along the trajectory, hence the various considered FTLEs are fundamentally non homogeneous.

The results are presented in table 4.2. We can see that the correlation between the first LE λ_1 of the shadowing UPOs and the corresponding first FTLE λ^{τ}_1 is already satisfactory at the value of 14% when considering the orbits shadowing the trajectory in the first tier. We in fact compare such values to a baseline value of correlations between the same dynamical quantities when considering no particular ordering and find that they settle at around 0.5%.

We need to remember that we are comparing two very different objects: a local property with a global structure. The correlation becomes even stronger when we look at the value of the Kolmogorov-Sinai KS^{τ} entropy and its local correspondent KS^{τ}_{+}, that assume values 25% and 34% respectively for the orbits of the first tier. If we consider larger values of K this increases even more, arriving at 27% for λ^{τ}_1 and 44% and 53% for KS^{τ} and KS^{τ}_{+} in the case $K = 1000$. Such increase derives from the fact that higher values of K result in a

higher shadowing persistence of the UPOs (Fig. **??**), while maintaining good proximity to the trajectory (Fig. 4.8b). More details on the confidence level around the correlations values are presented in Fig. 4.12.

It is important to bear in mind that our database of UPOs is not exhaustive, since it does not cover all regions of the attractor in equal measure. We thus reproduce the correlation statistics of table 4.2 by selecting only those orbits with a persistence higher than a certain time G in order to assess how such correlation could change in correspondence of an ideal shadowing scenario.

By definition, the number of orbits considered for the statistics decreases as we demand more persistence (Fig. 4.13). We filtered up to around $G = 1.5$ in order to still have a satisfactory number of UPOs able to reproduce reliable statistics. Fig. 4.12 shows that the correlation between the local properties of the trajectory and the UPOs steadily increases as we consider more persistent orbits, arriving from 14% to around 35% for the first LE of the UPO λ_1 and the first FTLE λ_1^τ of the chaotic trajectory, and from 25% to around 50% for the correlation between KS^τ and the Kolmogorov-Sinai entropy of the corresponding shadowing UPO. This seems to confirm our guess that the local stability properties could indeed be explained in terms of UPOs.

4.4 Conclusions

The study of non-hyperbolic dynamics is very relevant for the understanding of high-dimensional dynamical systems of physical and biological interest. While it used to be believed that uniformly hyperbolic dynamics could represent a paradigma for chaos (see discussion in 2.1.2), it became later clear that many system of practical interest, while still featuring characteristics typical of chaotic motion, such as sensitive dependence on the initial condition, could not be bounded within the constraint imposed by the definition of uniform hyperbolicity. An example of generally non-hyperbolic system is offered by geophysical fluids, which are usually described by systems that are far from being uniformly hyperbolic and present very heterogenous prop-

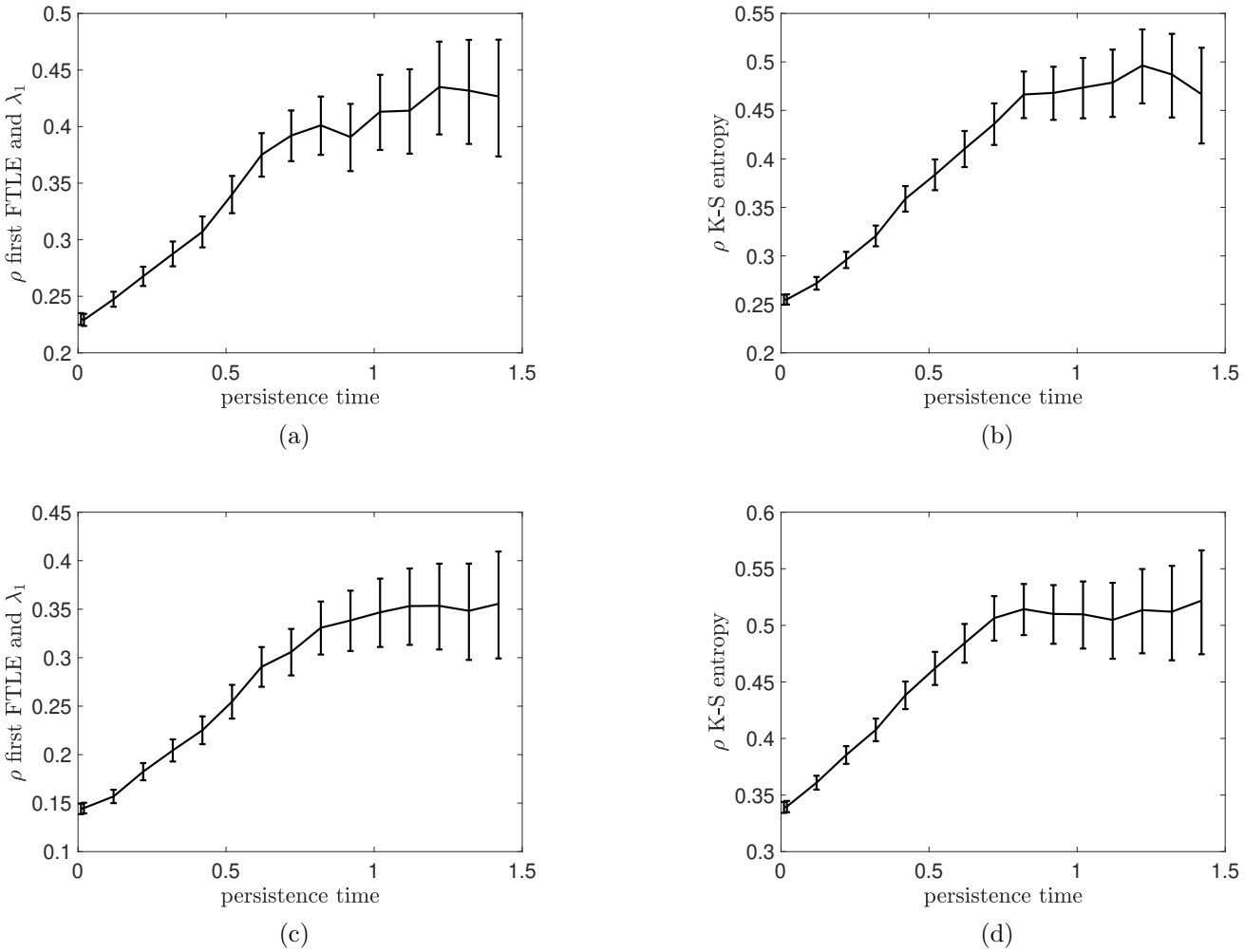

Figure 4.12: Correlation between the local stability properties of the trajectory and the relative shadowing orbits. Panel (a): correlation between the first FTLE λ_1^{tau} and the first LE of the corresponding shadowing UPO. Panel (b): correlation between KS^{τ} (sum of the first four FTLE) and the KS entropy of the corresponding shadowing UPO. Panel (c): Same than (a), for the largest FTLE $\lambda_{max}^{t}au$. Panel (b): Same than (b), for the Local Kolmogorov-Sinai entropy KS^{τ}(sum of the positive LE). The bars indicates the 95% confidence interval for each value of the persistence level.

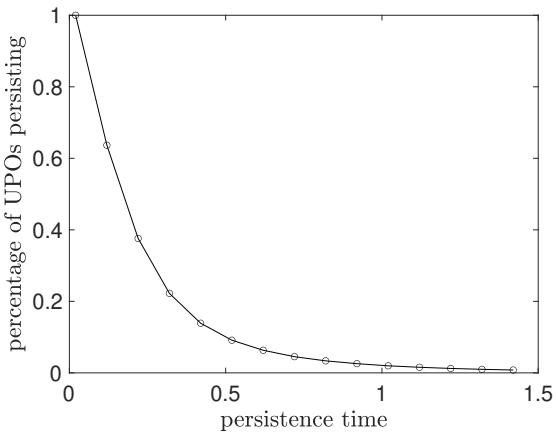

Figure 4.13: Number of orbits considered in the statistic as a function of the minimum persistence level required.

erties of their tangent space [154, 155]. Characterising the heterogeneity of the attractor is fundamental, since this can for instance impact negatively the performance of data assimilation techniques [156, 158, 157]. Within this context, understanding the global organisation of the phase space and interpreting the variability in the structure of its tangent space represent a very relevant problem. A very strong form of non-hyperbolicity is the so-called Unstable Dimension Variability (UDV), characterised by the presence of UPOs in the chaotic set with different number of unstable dimensions. While this phenomena was first described in [191], its evidence in chaotic systems of physical interest was only later found and studied [192, 193, 194]. Such form of non-hyperbolicity appears to be common in high dimensional dynamical systems. A "numerical fingerprint" [11] of this phenomenon, can be detected in the behaviour of the FTLEs of the system, whose value oscillates between positive and negative even for long averaging time. In fact, a FTLE that changes its sign along a chaotic trajectory, represents a signal that there is a direction which is oscillating between contraction and expansion, hindering the existence of an hyperbolic structure.

In this chapter we considered the Lorenz-96 model and we attempted to provide an interpretation of the heterogeneity of its attractor by combining the information provided by both Lyapunov and UPO analysis, bridging the gap between global and local properties of the systems. We first extracted a large database of UPOs from the system, which, although incomplete, allowed us to deduce that the hyperbolicity is not satisfied through the existence of UPOs with

different number of unstable dimensions, precisely ranging from 2 to 9 (see fig. 4.5). We found that the heterogeneity in the tangent space is indeed expresses at a local level by the existence of some FTLEs that fluctuates largely between negative and positive values and in section 4.3 we provided evidence of such behaviour; for instance, even for very large values of τ the sixth FTLEs present a distribution whose support is not strictly positive (See fig. 2.3). We then provided an interpretation of such local variability in terms of UPOs. Through the use of the mechanism of rank shadowing, we created a 1-1 correspondence between local properties of the attractor (FTLE) and global structure (UPOs). We found that the local instability properties of the chaotic trajectory are positively correlated with the ones of the shadowing UPOs, and such correlation is even stronger when looking at UPOs characterised by higher persistence (See fig. 4.12). Further research is needed. In particular we would like to study structural transitions between UPOs with the same dimension of the phase space and possibly investigate connections with quasi-invariant set using the method developed in [128].

Chapter 5

Conclusion

5.1 Summary of Thesis Achievements

In this thesis we provided a description of the geometrical and statistical properties of selected chaotic systems in terms of unstable periodic orbits. This work provides further support to the potential of developing a duality between the local and short time dynamically invariant compact sets (UPOs) and the global long-time evolution of densities of trajectories, in order to characterise and extend macroscopic features even for those systems for which periodic orbit theory has not been extended yet [7, 2, 8].

We considered two systems characterised by very different properties. We first looked at the Lorenz-63 model with standard parameters values, a three dimensional model that supports an SRB measure on a singularly hyperbolic attractor [120]. The UPO structure of this model is very well understood, in fact it is possible to prove that it admits a symbolic dynamics that allows to extract the complete set of UPO up to any given period T [120]. We then extended our analysis to the Lorenz-96 model in a 20-dimensional space with a forcing parameter for which the model exhibit extensive chaotic behaviour. This is a very interesting model to study, since it exhibits a very heterogenous structure of its tangent space.

The numerical implementation of the shadowing of a chaotic trajectory in terms of UPOs was

instrumental in our analysis and allowed us to understand and explore the geometry of the attractor under the lens of UPOs. Namely, at each point of time we ranked the UPOs of our database accordingly to their distance with the chaotic trajectory. Since the shadowing property is not proven to be valid for systems which are not Axiom-A, in both cases we had to assess both distance and co-evolution of the trajectory with the UPOs.

In the case of the Lorenz-63 model we extracted the full set of UPOs with symbolic dynamic period $T < 14$. We showed that the rectified distance of the UPO with the co-evolving trajectory is order of magnitudes larger than the initial distance between the two. We found that longer period orbits provide the best approximation of the chaotic trajectory, in virtue of both their quantity and spatial extent. This result, in agreement with other lines of research [139, 140, 6], seems at odd with what the trace formula suggest according to which short period UPOs should have more weight in the calculation of ergodic averages. We then extracted a finite state Markov chain process from the dynamics based on the process of scattering of the chaotic trajectory between the various UPOs. This study of scattering uses a partition where each UPO and its neighbourhood represent a state of the system and the stochastic matrix is defined in a frequentist way by studying the transitions defining the shadowing of the chaotic trajectory. It is known that eigenvectors corresponding to the subdominant eigenvalues determine the time scale of convergence to the invariant measure. Through this UPO based analysis, we find that eigenvectors associated to faster decay rates create finer structures in the phase space, in agreement with the intuition on how diffusion works. We then showed that each one of these resulting structures can be thought of as approximately defining a quasi-invariant set organised in bundle of orbits of the same type: the forward trajectory is scattered with high probability between orbits belonging to the same bundle, while with low probability it is scattered to orbits belonging to a different bundle that represent another quasi-invariant set.

In chapter 4 we consider the higher dimensional model Lorenz-96 that allowed us to extend the UPO-based investigation to the heterogeneity of the attractor of a chaotic flow. In fact, the dimensionality of the Lorenz-63 model does not allow for the presence of a region of the attractor presenting a different number of unstable dimension. We extracted a large database of UPOs with period ranging from a minimum of 1.5 to a maximum of 22.8.

We showed that the model is characterised by a strong violation of the hyperbolicity condition, called unstable dimension variability. Namely, we found UPOs with very different number of unstable dimensions, precisely ranging from 2 to 9. We analysed that the heterogeneity of the attractor is also manifested at a local level by large fluctuations between negative and positive values of some FTLEs, even for large averaging time. We proposed an explanation of such heterogeineity by providing evidence of correlation between local properties and UPOs, finding that anomalously unstable UPOs populate regions of the atrtactor characterised by analogous anomalous instability, bridging the gap between global and local properties of the system.

This thesis provides further support to the potential of using UPOs for reaching a comprehensive understanding of the properties - averages, correlations and tangent space - of chaotic dynamical systems. We would like to extend this analysis to higher dimensional system of practical relevance. In particular we would like to extend the work of Lucarini and Gritsun [14] on blocking events, investigating transitions between zonal flow and blocking by applying the methodology developed in this thesis. The investigation of this model is of interest both in terms of the physical process of interest - the low-frequency variability of the atmosphere is far from being a settled problem - and in terms of its mathematical properties, as it is characterised by high variability in the number of unstable dimension, thus featuring a serious violation of hyperbolicity.

Appendix A

Numerical Algorithms

A.1 Lorenz-63 model

The orbits have been calculated with Newton's iterative method by considering an integration time-step $dt = 0.001$. Such choice is a compromise between reaching enough accuracy to detect UPOs and achieving an acceptable computation time. An orbit was considered to be detected when $err_i^{in} := |S^{T_i}(x_i) - x_i| < 10^{-10}$ and such condition remains satisfied for at least two periods. Quasi-recurrences where considered as started condition for the algorithm. Namely, given a random initial condition x_c, we calculated a chaotic trajectory of length $T = 100$ and check whether the trajectory comes back very close to x_c ($|x_c - x_{t_c}| < 10^{-3}$) at any point in time $t_c < T$. If that happens we use the pair (x_c, t_c) as starting guesses for Newton's method. Newton's method is then iterated until either the orbit is detected or we reach a maximum number of allowed iterations ($I_{max} = 1000$). We also exit the algorithm in case the correction at step i $err_i^{corr} := |(\Delta x_i, \Delta T_i)|$ is greater than the correction at step $i - 1$, indicating that the algorithm is not converging. We verified that around 50% of such initial conditions resulted in UPOs being detected.

A.2 Lorenz-96 model

The choice of the parameters $M = 20$ and $F = 5$ rather than the standard parameters' values was motivated by the necessity of observing a sufficiently chaotic behaviour with evidence of UDV and numerical cost in the extraction of the orbits and shadowing ranking computations. We shortlisted the choices to $M = 20$ and $F = 8$, $M = 40$ and $F = 8$, $M = 20$ and $F = 6$, $M = 20$ and $F = 5$. For each of these model we run the rank shadowing algorithm and we found that in the latter case we could see that all the orbits of the extracted database resulted involved in the shadowing of a chaotic trajectory (shadowing and co-evolution), while in the other cases we either did not have a sufficient number of orbits or the computation was computationally too expensive.

Appendix B

Robustness of the UPO decomposition for the Lorenz-63 model

We present in this section the results of the UPO decomposition obtained in Section 3.2 when considering the looser definition of shadowing.

Fig. B.1 is the analogous of fig. 3.11 and represents the projection in the phase space of $w^{(2)}$, $w^{(3)}$, $w^{(4)}$ and invariant measure of the system obtained as a projection of $w^{(1)}$ 10 (respectively 30 - Fig. B.2) tiers persistence.

Fig. B.3 is the analogous of fig. 3.10 and represents the quasi-invariant bundles of UPOs obtained with the method outlined in section 3.2.2 considering the looser definition of shadowing with $K = 10$ (resp. $K = 30$ in Fig. B.4) tiers persistence.

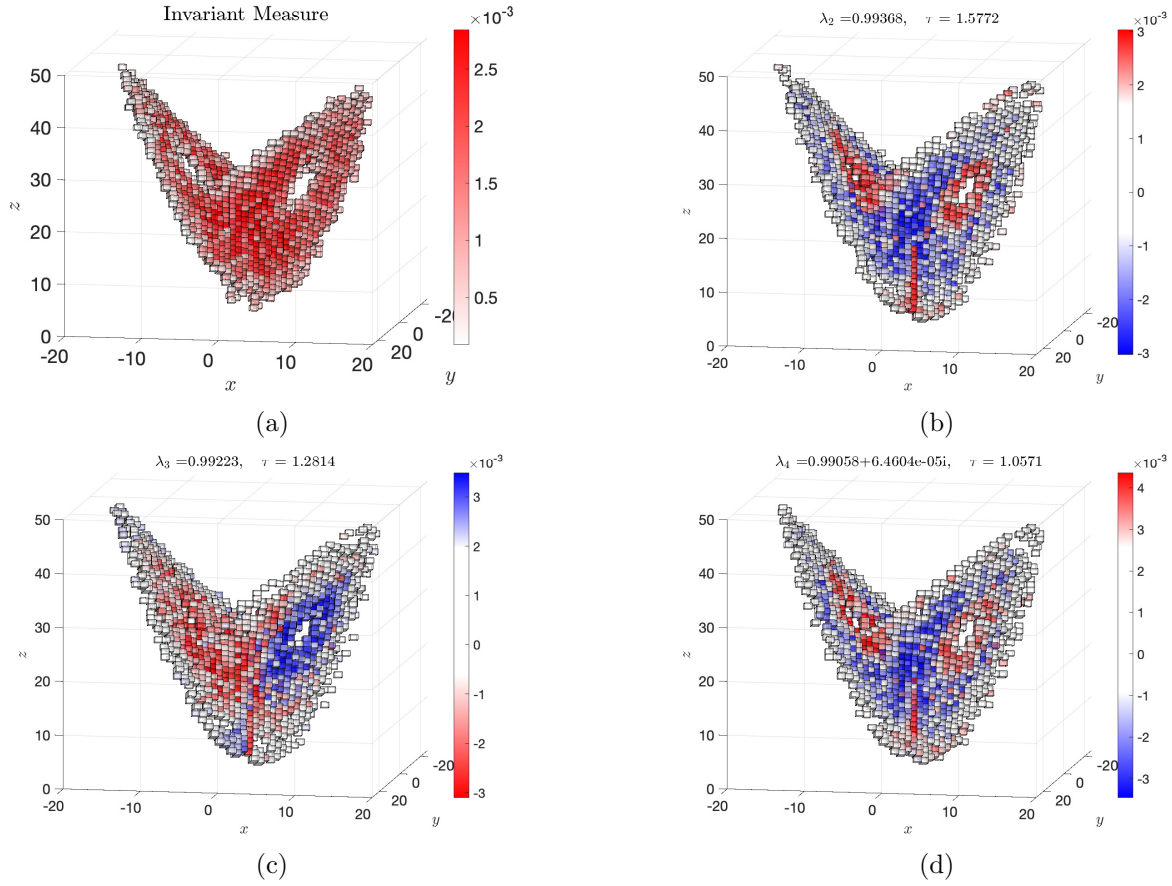

Figure B.1: Invariant Measure of the system obtained by projection of $w^{(1)}$ (a) considering a 10-states reduction of the dynamics. Projection in the phase space of (b): $w^{(2)}$ ($\lambda_2 = 0.99368$), (c): $w^{(3)}$ ($\lambda_3 = 0.99223$), (d): $w^{(4)}$ ($\lambda_4 = 0.99058$).

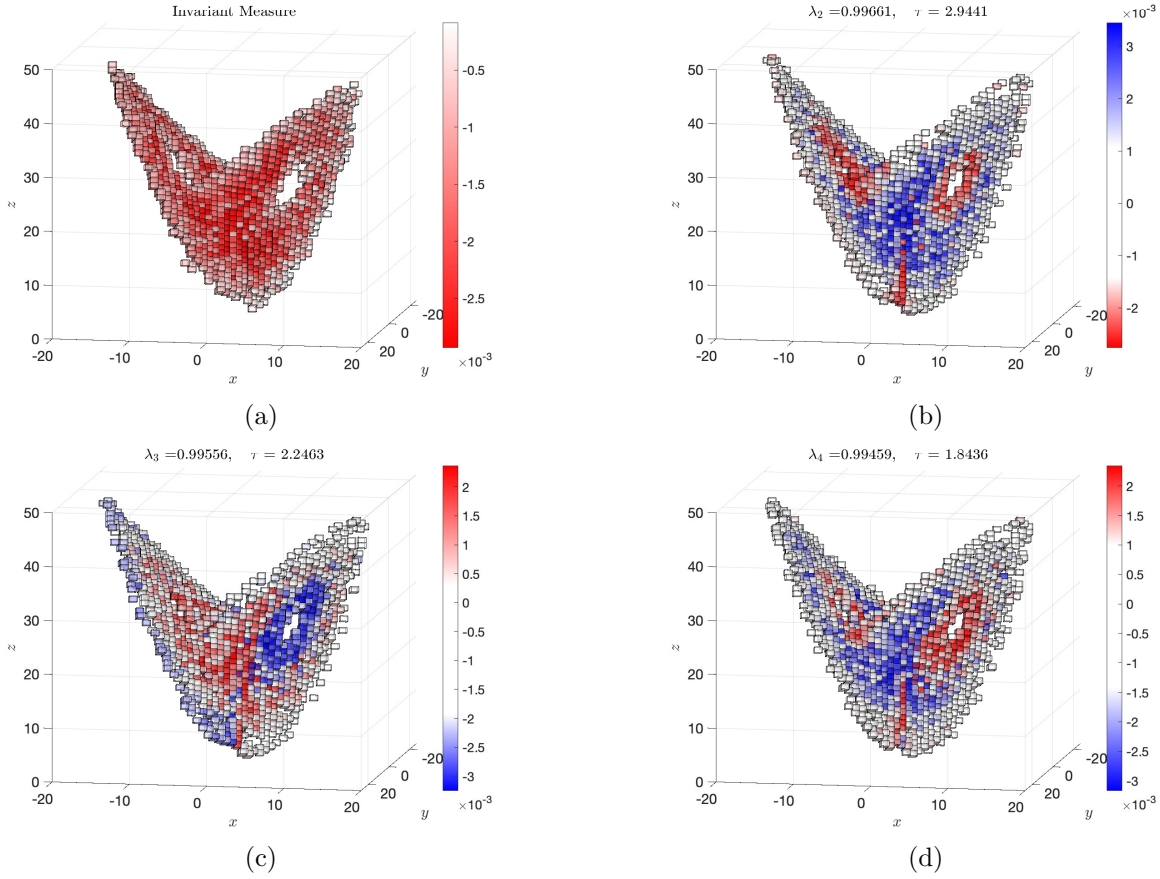

Figure B.2: Invariant Measure of the system obtained by projection of $w^{(1)}$ (a) considering a 30-states reduction of the dynamics. Projection in the phase space of (b): $w^{(2)}$ ($\lambda_2 = 0.99661$), (c): $w^{(3)}$ ($\lambda_3 = 0.99556$), (d): $w^{(4)}$ ($\lambda_4 = 0.99459$).

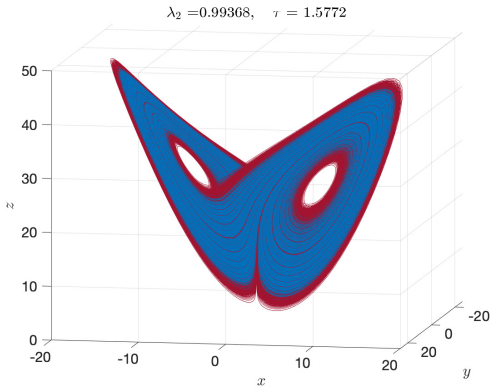

(a)

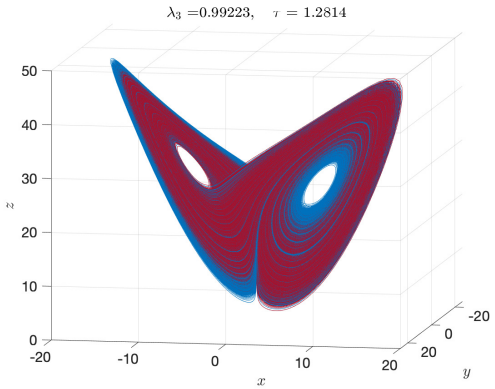

(b)

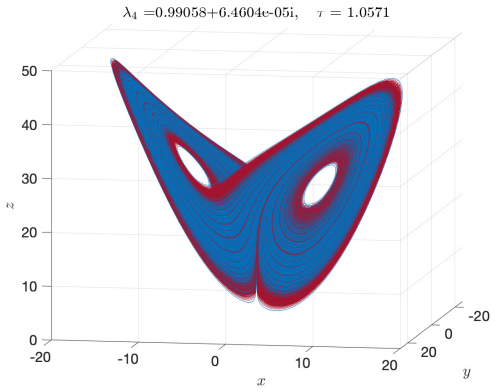

(c)

Figure B.3: Quasi-invariant bundles of UPOs obtained with the method outlined in Section 3.2.2 considering a 10-states reduction of the dynamics. (a): $\lambda_2 = 0.99368$, $\tau_2 = 1.5772$; (b): $\lambda_3 = 0.99223$, $\tau_3 = 1.2814$; (c): $\lambda_4 = 0.99058$, $\tau_4 = 1.0571$.

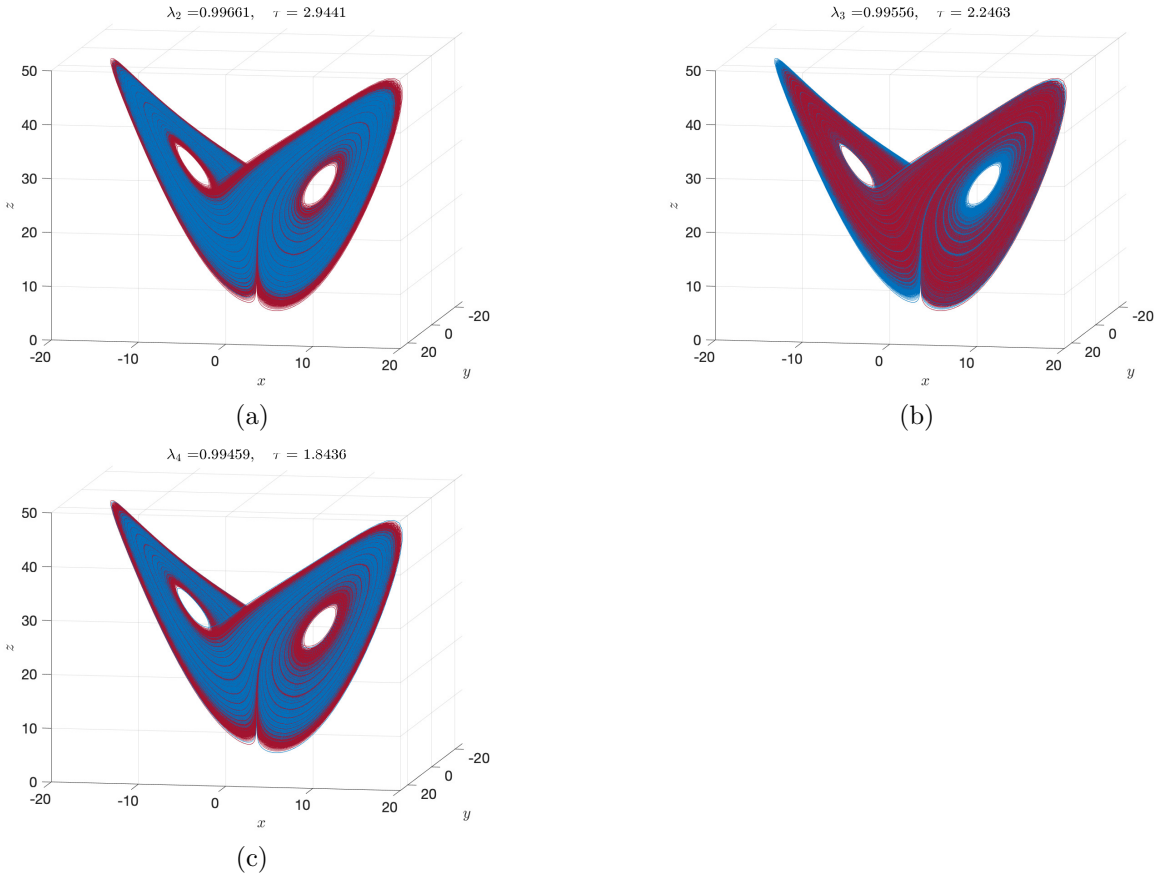

(a) (b) (c)

Figure B.4: Quasi-invariant bundles of UPOs obtained with the method outlined in Section 3.2.2 considering a 30-states reduction of the dynamics. (a): $\lambda_2 = 0.99661$, $\tau_2 = 2.9441$; (b): $\lambda_3 = 0.99556$, $\tau_3 = 2.2463$; (c): $\lambda_4 = 0.99459$, $\tau_4 = 1.8436$.

Bibliography

[1] P. Cvitanovic, R. Artuso, R. Mainieri, G. Tanner, G. Vattay, N. Whelan, and A. Wirzba, "Chaos: classical and quantum," *ChaosBook. org (Niels Bohr Institute, Copenhagen 2005)*, vol. 69, p. 25, 2005.

[2] P. Cvitanović, "Recurrent flows: the clockwork behind turbulence," *Journal of Fluid Mechanics*, vol. 726, pp. 1–4, 2013.

[3] P. Cvitanović, "Invariant measurement of strange sets in terms of cycles," *Physical Review Letters*, vol. 61, no. 24, p. 2729, 1988.

[4] M. A. Zaks and D. S. Goldobin, "Comment on "time-averaged properties of unstable periodic orbits and chaotic orbits in ordinary differential equation systems"," *Physical Review E*, vol. 81, no. 1, p. 018201, 2010.

[5] E. Aurell, G. Boffetta, A. Crisanti, G. Paladin, and A. Vulpiani, "Predictability in the large: an extension of the concept of lyapunov exponent," *Journal of Physics A: Mathematical and General*, vol. 30, pp. 1–26, jan 1997.

[6] S. M. Zoldi, "Unstable periodic orbit analysis of histograms of chaotic time series," *Physical review letters*, vol. 81, no. 16, p. 3375, 1998.

[7] G. Kawahara and S. Kida, "Periodic motion embedded in plane couette turbulence: regeneration cycle and burst," *Journal of Fluid Mechanics*, vol. 449, p. 291, 2001.

[8] G. Yalniz and N. B. Budanur, "Inferring symbolic dynamics of chaotic flows from persistence," *Chaos: An Interdisciplinary Journal of Nonlinear Science*, vol. 30, no. 3, p. 033109, 2020.

[9] B. Suri, L. Kageorge, R. O. Grigoriev, and M. F. Schatz, "Capturing turbulent dynamics and statistics in experiments with unstable periodic orbits," *Physical Review Letters*, vol. 125, no. 6, p. 064501, 2020.

[10] G. J. Chandler and R. R. Kerswell, "Invariant recurrent solutions embedded in a turbulent two-dimensional kolmogorov flow," *Journal of Fluid Mechanics*, vol. 722, pp. 554–595, 2013.

[11] R. F. Pereira, S. E. de S. Pinto, R. L. Viana, S. R. Lopes, and C. Grebogi, "Periodic orbit analysis at the onset of the unstable dimension variability and at the blowout bifurcation," *Chaos: An Interdisciplinary Journal of Nonlinear Science*, vol. 17, no. 2, p. 023131, 2007.

[12] Y.-C. Lai, Y. Nagai, and C. Grebogi, "Characterization of the natural measure by unstable periodic orbits in chaotic attractors," *Phys. Rev. Lett.*, vol. 79, pp. 649–652, Jul 1997.

[13] T. Sauer, C. Grebogi, and J. A. Yorke, "How long do numerical chaotic solutions remain valid?," *Phys. Rev. Lett.*, vol. 79, pp. 59–62, Jul 1997.

[14] V. Lucarini and A. Gritsun, "A new mathematical framework for atmospheric blocking events," *Climate Dynamics*, vol. 54, no. 1, pp. 575–598, 2020.

[15] H. Poincaré, *Science et Méthode*. Flammarion, Paris, 1908.

[16] D. Ruelle, "Henri poincaré's "science et méthode"," *Publications Mathématiques de l'IHÉS*, vol. S88, pp. 179–181, 1998.

[17] J. Hadamard, "Sur l'itération et les solutions asymptotiques des équations différentielles," *Bull. Soc. Math. France*, vol. 29, pp. 224–228, 1901.

[18] Y. B. Pesin, "CHARACTERISTIC LYAPUNOV EXPONENTS AND SMOOTH ERGODIC THEORY," *Russian Mathematical Surveys*, vol. 32, pp. 55–114, aug 1977.

[19] G. A. Hedlund, "The dynamics of geodesic flows," *Bulletin of the American Mathematical Society*, vol. 45, no. 4, pp. 241–260, 1939.

[20] E. Hopf, *Statistik der geodätischen Linien in Mannigfaltigkeiten negativer Krümmung*, vol. 91. 1939.

[21] D. V. Anosov, "Geodesic flows on closed riemannian manifolds of negative curvature," *Trudy Matematicheskogo Instituta Imeni VA Steklova*, vol. 90, pp. 3–210, 1967.

[22] A. Hammerlindl, B. Krauskopf, G. Mason, and H. M. Osinga, "Global manifold structure of a continuous-time heterodimensional cycle," *arXiv preprint arXiv:1906.11438*, 2019.

[23] S. Smale *et al.*, "Differentiable dynamical systems," *Bulletin of the American mathematical Society*, vol. 73, no. 6, pp. 747–817, 1967.

[24] A. Katok and B. Hasselblatt, *Introduction to the Modern Theory of Dynamical Systems*. Encyclopedia of Mathematics and its Applications, Cambridge University Press, 1995.

[25] E. N. Lorenz, "Deterministic nonperiodic flow," *Journal of atmospheric sciences*, vol. 20, no. 2, pp. 130–141, 1963.

[26] D. Ruelle and F. Takens, "On the nature of turbulence," *Communications in Mathematical Physics*, vol. 20, no. 3, pp. 167–192, 1971.

[27] T.-Y. Li and J. A. Yorke, "Period three implies chaos," *The American Mathematical Monthly*, vol. 82, no. 10, pp. 985–992, 1975.

[28] G. Benettin, L. Galgani, A. Giorgilli, and J.-M. Strelcyn, "Lyapunov characteristic exponents for smooth dynamical systems and for hamiltonian systems; a method for computing all of them. part 1: Theory," *Meccanica*, vol. 15, no. 1, pp. 9–20, 1980.

[29] L. Barreira and Y. Pesin, *Nonuniform Hyperbolicity: Dynamics of Systems with Nonzero Lyapunov Exponents*. Encyclopedia of Mathematics and its Applications, Cambridge University Press, 2007.

[30] C. Bonatti, "Survey towards a global view of dynamical systems, for the c1-topology," *Ergodic Theory and Dynamical Systems*, vol. 31, no. 4, pp. 959–993, 2011.

[31] C. Bonatti, L. J. Díaz, and M. Viana, *Dynamics beyond uniform hyperbolicity: A global geometric and probabilistic perspective*, vol. 3. Springer Science & Business Media, 2004.

[32] W. Zhang, B. Krauskopf, and V. Kirk, "How to find a codimension-one heteroclinic cycle between two periodic orbits," *Discrete & Continuous Dynamical Systems*, vol. 32, no. 8, p. 2825, 2012.

[33] B. Hasselblatt and A. Katok, *A first course in dynamics: with a panorama of recent developments*. Cambridge University Press, 2003.

[34] J.-P. Eckmann and D. Ruelle, "Ergodic theory of chaos and strange attractors," *The theory of chaotic attractors*, pp. 273–312, 1985.

[35] E. Ott, *Chaos in dynamical systems*. Cambridge university press, 2002.

[36] H. J. S. Smith, "On the integration of discontinuous functions," *Proceedings of the London Mathematical Society*, vol. 1, no. 1, pp. 140–153, 1874.

[37] P. Grassberger, "Generalized dimensions of strange attractors," *Physics Letters A*, vol. 97, no. 6, pp. 227–230, 1983.

[38] P. Grassberger and I. Procaccia, "Characterization of strange attractors," *Physical review letters*, vol. 50, no. 5, p. 346, 1983.

[39] H. G. E. Hentschel and I. Procaccia, "The infinite number of generalized dimensions of fractals and strange attractors," *Physica D: Nonlinear Phenomena*, vol. 8, no. 3, pp. 435–444, 1983.

[40] A. Rényi, *Probability theory*. Courier Corporation, 2007.

[41] G. D. Birkhoff, "Proof of the ergodic theorem," *Proceedings of the National Academy of Sciences*, vol. 17, no. 12, pp. 656–660, 1931.

[42] K. E. Petersen, *Ergodic theory*, vol. 2. Cambridge University Press, 1989.

[43] D. Ruelle, "A measure associated with axiom-a attractors," *American Journal of Mathematics*, pp. 619–654, 1976.

[44] V. Baladi, *Positive transfer operators and decay of correlations*, vol. 16. World scientific, 2000.

[45] A. Lasota and M. C. Mackey, *Chaos, fractals, and noise: stochastic aspects of dynamics*, vol. 97. Springer Science & Business Media, 1998.

[46] G. Froyland, "Extracting dynamical behavior via markov models," in *Nonlinear dynamics and statistics*, pp. 281–321, Springer, 2001.

[47] A. Tantet, V. Lucarini, F. Lunkeit, and H. A. Dijkstra, "Crisis of the chaotic attractor of a climate model: a transfer operator approach," *Nonlinearity*, vol. 31, no. 5, p. 2221, 2018.

[48] A. Tantet, F. R. van der Burgt, and H. A. Dijkstra, "An early warning indicator for atmospheric blocking events using transfer operators," *Chaos: An Interdisciplinary Journal of Nonlinear Science*, vol. 25, no. 3, p. 036406, 2015.

[49] G. Froyland, K. Padberg, M. H. England, and A. M. Treguier, "Detection of coherent oceanic structures via transfer operators," *Physical review letters*, vol. 98, no. 22, p. 224503, 2007.

[50] S. M. Ulam, *Problems in modern mathematics*. Courier Corporation, 2004.

[51] G. Froyland and M. Dellnitz, "Detecting and locating near-optimal almost-invariant sets and cycles," *SIAM Journal on Scientific Computing*, vol. 24, no. 6, pp. 1839–1863, 2003.

[52] G. Froyland, "Approximating physical invariant measures of mixing dynamical systems in higher dimensions," *Nonlinear Analysis: Theory, Methods and Applications*, vol. 32, no. 7, pp. 831–860, 1998.

[53] R. Livi and P. Politi, *Nonequilibrium statistical physics: a modern perspective*. Cambridge University Press, 2017.

[54] A. Pikovsky and A. Politi, *Lyapunov exponents: a tool to explore complex dynamics*. Cambridge University Press, 2016.

[55] A. Pikovsky and A. Politi, *Lyapunov exponents: a tool to explore complex dynamics*. Cambridge University Press, 2016.

[56] V. I. Oseledets, "A multiplicative ergodic theorem. characteristic ljapunov, exponents of dynamical systems," *Trudy Moskovskogo Matematicheskogo Obshchestva*, vol. 19, pp. 179–210, 1968.

[57] H. D. I. Abarbanel, R. Brown, and M. B. Kennel, "Variation of lyapunov exponents on a strange attractor," *Journal of Nonlinear Science*, vol. 1, no. 2, pp. 175–199, 1991.

[58] E. N. Lorenz, "Predictability: A problem partly solved," in *Proc. Seminar on predictability*, vol. 1, 1996.

[59] M. Cencini and F. Ginelli, "Lyapunov analysis: from dynamical systems theory to applications," *Journal of Physics A: Mathematical and Theoretical*, vol. 46, no. 25, p. 250301, 2013.

[60] E. Kalnay, *Atmospheric modeling, data assimilation and predictability*. Cambridge university press, 2003.

[61] C. Nicolis, "Dynamics of model error: The role of the boundary conditions," *Journal of the atmospheric sciences*, vol. 64, no. 1, pp. 204–215, 2007.

[62] C. Nicolis, R. A. Perdigao, and S. Vannitsem, "Dynamics of prediction errors under the combined effect of initial condition and model errors," *Journal of the atmospheric sciences*, vol. 66, no. 3, pp. 766–778, 2009.

[63] S. Vannitsem, "Predictability of large-scale atmospheric motions: Lyapunov exponents and error dynamics," *Chaos: An Interdisciplinary Journal of Nonlinear Science*, vol. 27, no. 3, p. 032101, 2017.

[64] B. Legras and M. Ghil, "Persistent anomalies, blocking and variations in atmospheric predictability," *Journal of Atmospheric Sciences*, vol. 42, no. 5, pp. 433–471, 1985.

[65] S. Schubert and V. Lucarini, "Dynamical analysis of blocking events: spatial and temporal fluctuations of covariant lyapunov vectors," *Quarterly Journal of the Royal Meteorological Society*, vol. 142, no. 698, pp. 2143–2158, 2016.

[66] S. Vannitsem and C. Nicolis, "Lyapunov vectors and error growth patterns in a t21l3 quasigeostrophic model," *Journal of the atmospheric sciences*, vol. 54, no. 2, pp. 347–361, 1997.

[67] J. L. Kaplan and J. A. Yorke, "Chaotic behavior of multidimensional difference equations," in *Functional differential equations and approximation of fixed points*, pp. 204–227, Springer, 1979.

[68] P. Frederickson, J. L. Kaplan, E. D. Yorke, and J. A. Yorke, "The liapunov dimension of strange attractors," *Journal of Differential Equations*, vol. 49, no. 2, pp. 185–207, 1983.

[69] H. Poincaré, *Les méthodes nouvelles de la mécanique céleste: Méthodes de MM. Newcomb, Glydén, Lindstedt et Bohlin. 1893*, vol. 2. Gauthier-Villars it fils, 1893.

[70] P. Cvitanović, "Periodic orbits as the skeleton of classical and quantum chaos," *Physica D: Nonlinear Phenomena*, vol. 51, no. 1-3, pp. 138–151, 1991.

[71] C. Grebogi, E. Ott, and J. A. Yorke, "Unstable periodic orbits and the dimensions of multifractal chaotic attractors," *Physical Review A*, vol. 37, no. 5, p. 1711, 1988.

[72] R. Bowen, "ω-limit sets for axiom a diffeomorphisms," *Journal of differential equations*, vol. 18, no. 2, pp. 333–339, 1975.

[73] R. Artuso, E. Aurell, and P. Cvitanovic, "Recycling of strange sets: Ii. applications," *Nonlinearity*, vol. 3, no. 2, p. 361, 1990.

[74] M. C. Gutzwiller, *Chaos in classical and quantum mechanics*, vol. 1. Springer Science & Business Media, 2013.

[75] D. Ruelle, *Thermodynamic formalism: the mathematical structure of equilibrium statistical mechanics*. Cambridge University Press, 2004.

[76] D. Ruelle, "Smooth dynamics and new theoretical ideas in nonequilibrium statistical mechanics," *Journal of Statistical Physics*, vol. 95, no. 1, pp. 393–468, 1999.

[77] A. Katok and B. Hasselblatt, *Introduction to the modern theory of dynamical systems*. No. 54, Cambridge university press, 1997.

[78] R. Bowen, "Periodic orbits for hyperbolic flows," *American Journal of Mathematics*, vol. 94, no. 1, pp. 1–30, 1972.

[79] D. Auerbach, P. Cvitanović, J.-P. Eckmann, G. Gunaratne, and I. Procaccia, "Exploring chaotic motion through periodic orbits," *Physical Review Letters*, vol. 58, no. 23, p. 2387, 1987.

[80] R. Artuso, E. Aurell, and P. Cvitanovic, "Recycling of strange sets: I. cycle expansions," *Nonlinearity*, vol. 3, no. 2, p. 325, 1990.

[81] B. Eckhardt and G. Ott, "Periodic orbit analysis of the lorenz attractor," *Zeitschrift für Physik B Condensed Matter*, vol. 93, no. 2, pp. 259–266, 1994.

[82] V. Lucarini, "Evidence of dispersion relations for the nonlinear response of the lorenz 63 system," *Journal of Statistical Physics*, vol. 134, no. 2, pp. 381–400, 2009.

[83] A. Gritsun, "Unstable periodic trajectories of a barotropic model of the atmosphere.," *Russian Journal of Numerical Analysis and Mathematical Modelling*, vol. 23, no. 4, 2008.

[84] A. Gritsun, "Statistical characteristics, circulation regimes and unstable periodic orbits of a barotropic atmospheric model," *Philosophical Transactions of the Royal Society A: Mathematical, Physical and Engineering Sciences*, vol. 371, no. 1991, p. 20120336, 2013.

[85] A. Gritsun and V. Lucarini, "Fluctuations, response, and resonances in a simple atmospheric model," *Physica D: Nonlinear Phenomena*, vol. 349, pp. 62–76, 2017.

[86] D. Faranda, G. Messori, M. C. Alvarez-Castro, and P. Yiou, "Dynamical properties and extremes of northern hemisphere climate fields over the past 60 years," *Nonlinear Processes in Geophysics*, vol. 24, no. 4, pp. 713–725, 2017.

[87] M. C. Krygier, J. L. Pughe-Sanford, and R. O. Grigoriev, "Exact coherent structures and shadowing in turbulent taylor–couette flow," *Journal of Fluid Mechanics*, vol. 923, p. A7, 2021.

[88] I. Shimada and T. Nagashima, "A numerical approach to ergodic problem of dissipative dynamical systems," *Progress of theoretical physics*, vol. 61, no. 6, pp. 1605–1616, 1979.

[89] G. Benettin and J.-M. Strelcyn, "Numerical experiments on the free motion of a point mass moving in a plane convex region: Stochastic transition and entropy," *Physical review A*, vol. 17, no. 2, p. 773, 1978.

[90] G. Benettin, L. Galgani, and J.-M. Strelcyn, "Kolmogorov entropy and numerical experiments," *Physical Review A*, vol. 14, no. 6, p. 2338, 1976.

[91] B. V. Chirikov, "Research concerning the theory of non-linear resonance and stochasticity," tech. rep., CM-P00100691, 1971.

[92] A. Wolf and J. Swift, "Progress in computing lyapunov exponents from experimental data," in *Statistical physics and chaos in fusion plasmas*, 1984.

[93] A. Brandstäter, J. Swift, H. L. Swinney, A. Wolf, J. D. Farmer, E. Jen, and P. Crutchfield, "Low-dimensional chaos in a hydrodynamic system," *Physical Review Letters*, vol. 51, no. 16, p. 1442, 1983.

[94] S. Lang, *Introduction to linear algebra*. Springer Science & Business Media, 2012.

[95] T. Parker and L. Chua, "Practical numerical algorithms for chaotic systems. new york: Spring 2 verlag," 1989.

[96] G. Froyland, K. Judd, and A. I. Mees, "Estimation of lyapunov exponents of dynamical systems using a spatial average," *Physical Review E*, vol. 51, no. 4, p. 2844, 1995.

[97] K. Geist, U. Parlitz, and W. Lauterborn, "Comparison of different methods for computing lyapunov exponents," *Progress of theoretical physics*, vol. 83, no. 5, pp. 875–893, 1990.

[98] J. Miller and J. Yorke, "Finding all periodic orbits of maps using newton methods: sizes of basins," *Physica D: Nonlinear Phenomena*, vol. 135, no. 3-4, pp. 195–211, 2000.

[99] K. T. Hansen, "Alternative method to find orbits in chaotic systems," *Physical Review E*, vol. 52, no. 3, p. 2388, 1995.

[100] O. Biham and W. Wenzel, "Characterization of unstable periodic orbits in chaotic attractors and repellers," *Physical review letters*, vol. 63, no. 8, p. 819, 1989.

[101] O. Biham and W. Wenzel, "Unstable periodic orbits and the symbolic dynamics of the complex hénon map," *Physical Review A*, vol. 42, no. 8, p. 4639, 1990.

[102] T. S. Parker and L. Chua, "Practical numerical algorithms for chaotic systems," 2012.

[103] K. Pyragas, "Continuous control of chaos by self-controlling feedback," *Physics letters A*, vol. 170, no. 6, pp. 421–428, 1992.

[104] E. Kazantsev, "Unstable periodic orbits and attractor of the barotropic ocean model," *Nonlinear processes in Geophysics*, vol. 5, no. 4, pp. 193–208, 1998.

[105] Y. Lan and P. Cvitanović, "Variational method for finding periodic orbits in a general flow," *Physical Review E*, vol. 69, no. 1, p. 016217, 2004.

[106] E. Kazantsev, "Sensitivity of the attractor of the barotropic ocean model to external influences: approach by unstable periodic orbits," *Nonlinear processes in Geophysics*, vol. 8, no. 4/5, pp. 281–300, 2001.

[107] S. Kato and M. Yamada, "Unstable periodic solutions embedded in a shell model turbulence," *Physical Review E*, vol. 68, no. 2, p. 025302, 2003.

[108] L. Van Veen, S. Kida, and G. Kawahara, "Periodic motion representing isotropic turbulence," *Fluid dynamics research*, vol. 38, no. 1, p. 19, 2006.

[109] C. J. Crowley, J. L. Pughe-Sanford, W. Toler, M. C. Krygier, R. O. Grigoriev, and M. F. Schatz, "Turbulence tracks recurrent solutions," *Proceedings of the National Academy of Sciences*, vol. 119, no. 34, p. e2120665119, 2022.

[110] C. T. Kelley, *Iterative methods for linear and nonlinear equations*. SIAM, 1995.

[111] Y. Saad and M. Schultz, "G mre s: A generalized minimum residual algorithm for solving nonsymmetric linear systems, sia m j," *Scienti fi c and Stat. Comp*, vol. 7, no. 8, pp. 56–8, 1986.

[112] G. Yalniz, B. Hof, and N. B. Budanur, "Coarse graining the state space of a turbulent flow using periodic orbits," *Phys. Rev. Lett.*, vol. 126, p. 244502, Jun 2021.

[113] G. Froyland, "Statistically optimal almost-invariant sets," *Physica D: Nonlinear Phenomena*, vol. 200, no. 3-4, pp. 205–219, 2005.

[114] T. Caby, D. Faranda, S. Vaienti, and P. Yiou, "On the computation of the extremal index for time series," *Journal of Statistical Physics*, vol. 179, pp. 1666–1697, 2020.

[115] A. J. McNeil, "Extreme value theory for risk managers," *Departement Mathematik ETH Zentrum*, vol. 12, no. 5, pp. 217–37, 1999.

[116] D. Faranda, M. C. Alvarez-Castro, G. Messori, D. Rodrigues, and P. Yiou, "The hammam effect or how a warm ocean enhances large scale atmospheric predictability," *Nature communications*, vol. 10, no. 1, p. 1316, 2019.

[117] D. Faranda, G. Messori, and P. Yiou, "Dynamical proxies of north atlantic predictability and extremes," *Scientific reports*, vol. 7, no. 1, pp. 1–10, 2017.

[118] W. Tucker, "The lorenz attractor exists," *Comptes Rendus de l'Académie des Sciences-Series I-Mathematics*, vol. 328, no. 12, pp. 1197–1202, 1999.

[119] Z. Galias and P. Zgliczyński, "Computer assisted proof of chaos in the lorenz equations," *Physica D: Nonlinear Phenomena*, vol. 115, no. 3-4, pp. 165–188, 1998.

[120] W. Tucker, "A rigorous ode solver and smale's 14th problem," *Foundations of Computational Mathematics*, vol. 2, no. 1, pp. 53–117, 2002.

[121] V. Franceschini, C. Giberti, and Z. Zheng, "Characterization of the lorentz attractor by unstable periodic orbits," *Nonlinearity*, vol. 6, no. 2, p. 251, 1993.

[122] Y. Saiki and M. Yamada, "Reply to "comment on 'time-averaged properties of unstable periodic orbits and chaotic orbits in ordinary differential equation systems'"," *Physical Review E*, vol. 81, no. 1, p. 018202, 2010.

[123] Y. Saiki and M. Yamada, "Time-averaged properties of unstable periodic orbits and chaotic orbits in ordinary differential equation systems," *Physical Review E*, vol. 79, no. 1, p. 015201, 2009.

[124] Y. Saiki, "Numerical detection of unstable periodic orbits in continuous-time dynamical systems with chaotic behaviors," *Nonlinear Processes in Geophysics*, vol. 14, no. 5, pp. 615–620, 2007.

[125] R. Barrio, A. Dena, and W. Tucker, "A database of rigorous and high-precision periodic orbits of the lorenz model," *Computer Physics Communications*, vol. 194, pp. 76–83, 2015.

[126] D. Viswanath, "Symbolic dynamics and periodic orbits of the lorenz attractor," *Nonlinearity*, vol. 16, no. 3, p. 1035, 2003.

[127] Z. Galias and W. Tucker, "Symbolic dynamics based method for rigorous study of the existence of short cycles for chaotic systems," in *2009 IEEE International Symposium on Circuits and Systems*, pp. 1907–1910, IEEE, 2009.

[128] C. C. Maiocchi, V. Lucarini, and A. Gritsun, "Decomposing the dynamics of the lorenz 1963 model using unstable periodic orbits: Averages, transitions, and quasi-invariant sets," *Chaos: An Interdisciplinary Journal of Nonlinear Science*, vol. 32, no. 3, p. 033129, 2022.

[129] R. Bowen, "Topological entropy and axiom a," in *Proc. Sympos. Pure Math*, vol. 14, pp. 23–41, 1970.

[130] T. Palmer, "Extended-range atmospheric prediction and the lorenz model," *Bulletin of the American Meteorological Society*, vol. 74, no. 1, pp. 49–65, 1993.

[131] P. Gaspard, "Chaos, scattering and statistical mechanics," *Chaos*, 2005.

[132] D. Lucas and R. R. Kerswell, "Recurrent flow analysis in spatiotemporally chaotic 2-dimensional kolmogorov flow," *Physics of Fluids*, vol. 27, no. 4, p. 045106, 2015.

[133] M. C. Krygier, J. L. Pughe-Sanford, and R. O. Grigoriev, "Exact coherent structures and shadowing in turbulent taylor-couette flow," *arXiv preprint arXiv:2105.02126*, 2021.

[134] P. Cvitanović and J. Gibson, "Geometry of the turbulence in wall-bounded shear flows: periodic orbits," *Physica Scripta*, vol. 2010, no. T142, p. 014007, 2010.

[135] T. Kreilos and B. Eckhardt, "Periodic orbits near onset of chaos in plane couette flow," *Chaos: An Interdisciplinary Journal of Nonlinear Science*, vol. 22, no. 4, p. 047505, 2012.

[136] P. Gaspard, "Chaos, scattering and statistical mechanics," *Chaos*, 2005.

[137] C. Sparrow, "The lorenz equations," *Edited by Arun V. Holden*, p. 111, 1982.

[138] S. M. Zoldi and H. S. Greenside, "Comment on "optimal periodic orbits of chaotic systems"," *Phys. Rev. Lett.*, vol. 80, pp. 1790–1790, Feb 1998.

[139] D. Lasagna, "Sensitivity analysis of chaotic systems using unstable periodic orbits," *SIAM Journal on Applied Dynamical Systems*, vol. 17, no. 1, pp. 547–580, 2018.

[140] D. Lasagna, "Sensitivity of long periodic orbits of chaotic systems," *Physical Review E*, vol. 102, no. 5, p. 052220, 2020.

[141] V. Lucarini, "Response operators for markov processes in a finite state space: Radius of convergence and link to the response theory for axiom a systems," *Journal of Statistical Physics*, vol. 162, no. 2, pp. 312–333, 2016.

[142] G. Froyland and K. Padberg, "Almost-invariant sets and invariant manifolds—connecting probabilistic and geometric descriptions of coherent structures in flows," *Physica D: Nonlinear Phenomena*, vol. 238, no. 16, pp. 1507–1523, 2009.

[143] G. Froyland and K. Padberg-Gehle, "Almost-invariant and finite-time coherent sets: directionality, duration, and diffusion," in *Ergodic Theory, Open Dynamics, and Coherent Structures*, pp. 171–216, Springer, 2014.

[144] M. Dellnitz and O. Junge, "On the approximation of complicated dynamical behavior," *SIAM Journal on Numerical Analysis*, vol. 36, no. 2, pp. 491–515, 1999.

[145] M. Dellnitz and O. Junge, "Almost invariant sets in chua's circuit," *International Journal of Bifurcation and Chaos*, vol. 7, no. 11, pp. 2475–2485, 1997.

[146] G. Froyland, "Unwrapping eigenfunctions to discover the geometry of almost-invariant sets in hyperbolic maps," *Physica D: Nonlinear Phenomena*, vol. 237, no. 6, pp. 840–853, 2008.

[147] P. Cvitanović, "Dynamical averaging in terms of periodic orbits," *Physica D: Nonlinear Phenomena*, vol. 83, no. 1-3, pp. 109–123, 1995.

[148] B. R. Hunt and E. Ott, "Optimal periodic orbits of chaotic systems," *Phys. Rev. Lett.*, vol. 76, pp. 2254–2257, Mar 1996.

[149] T.-H. Yang, B. R. Hunt, and E. Ott, "Optimal periodic orbits of continuous time chaotic systems," *Phys. Rev. E*, vol. 62, pp. 1950–1959, Aug 2000.

[150] L. A. Smith, C. Ziehmann, and K. Fraedrich, "Uncertainty dynamics and predictability in chaotic systems," *Quarterly Journal of the Royal Meteorological Society*, vol. 125, no. 560, pp. 2855–2886, 1999.

[151] T. D. Sauer, "Shadowing breakdown and large errors in dynamical simulations of physical systems," *Phys. Rev. E*, vol. 65, p. 036220, Feb 2002.

[152] E. Kalnay, *Atmospheric {Modeling, Data Assimilation and Predictability}*. Cambridge: Cambridge University Press, 2003.

[153] M. Ghil and V. Lucarini, "The physics of climate variability and climate change," *Rev. Mod. Phys.*, vol. 92, p. 035002, Jul 2020.

[154] T. N. Palmer, "Predicting uncertainty in forecasts of weather and climate," *Reports on Progress in Physics*, vol. 63, pp. 71–116, jan 2000.

[155] J. Slingo and T. Palmer, "Uncertainty in weather and climate prediction," *Philosophical Transactions of the Royal Society A: Mathematical, Physical and Engineering Sciences*, vol. 369, no. 1956, pp. 4751–4767, 2011.

[156] A. Carrassi, M. Bocquet, L. Bertino, and G. Evensen, "Data assimilation in the geosciences: An overview of methods, issues, and perspectives," *WIREs Climate Change*, vol. 9, no. 5, p. e535, 2018.

[157] Y. Wu, Z. Shen, and Y. Tang, "A flow-dependent targeted observation method for ensemble kalman filter assimilation systems," *Earth and Space Science*, vol. 7, no. 7, p. e2020EA001149, 2020. e2020EA001149 2020EA001149.

[158] Y. Chen, A. Carrassi, and V. Lucarini, "Inferring the instability of a dynamical system from the skill of data assimilation exercises," *Nonlinear Processes in Geophysics*, vol. 28, no. 4, pp. 633–649, 2021.

[159] L. De Cruz, S. Schubert, J. Demaeyer, V. Lucarini, and S. Vannitsem, "Exploring the lyapunov instability properties of high-dimensional atmospheric and climate models," *Nonlinear Processes in Geophysics*, vol. 25, no. 2, pp. 387–412, 2018.

[160] S. Vannitsem and V. Lucarini, "Statistical and dynamical properties of covariant lyapunov vectors in a coupled atmosphere-ocean model—multiscale effects, geometric degeneracy, and error dynamics," *Journal of Physics A: Mathematical and Theoretical*, vol. 49, no. 22, p. 224001, 2016.

[161] S. Vannitsem and W. Duan, "On the use of near-neutral backward lyapunov vectors to get reliable ensemble forecasts in coupled ocean–atmosphere systems," *Climate Dynamics*, vol. 55, no. 5, pp. 1125–1139, 2020.

[162] P. Laloyaux, M. Balmaseda, D. Dee, K. Mogensen, and P. Janssen, "A coupled data assimilation system for climate reanalysis," *Quarterly Journal of the Royal Meteorological Society*, vol. 142, no. 694, pp. 65–78, 2016.

[163] T. J. O'Kane, P. A. Sandery, D. P. Monselesan, P. Sakov, M. A. Chamberlain, R. J. Matear, M. A. Collier, D. T. Squire, and L. Stevens, "Coupled data assimilation and

ensemble initialization with application to multiyear enso prediction," *Journal of Climate*, vol. 32, no. 4, pp. 997 – 1024, 2019.

[164] E. N. Lorenz, "Designing Chaotic Models," *Journal of the Atmospheric Sciences*, vol. 62, pp. 1574–1587, 05 2005.

[165] D. L. van Kekem and A. E. Sterk, "Travelling waves and their bifurcations in the lorenz-96 model," *Physica D: Nonlinear Phenomena*, vol. 367, pp. 38 – 60, 2018.

[166] D. L. van Kekem and A. E. Sterk, "Wave propagation in the lorenz-96 model," *Nonlinear Processes in Geophysics*, vol. 25, no. 2, pp. 301–314, 2018.

[167] D. Wilks, "Effects of stochastic parametrizations in the Lorenz '96 system," *Quarterly Journal of the Royal Meteorological Society*, vol. 131, no. 606, pp. 389–407, 2005.

[168] H. M. Arnold, I. M. Moroz, and T. N. Palmer, "Stochastic parametrizations and model uncertainty in the lorenz system," *Philosophical Transactions of the Royal Society A: Mathematical, Physical and Engineering Sciences*, vol. 371, no. 1991, p. 20110479, 2013.

[169] G. Vissio and V. Lucarini, "A proof of concept for scale-adaptive parametrizations: the case of the Lorenz '96 model," *Quarterly Journal of the Royal Meteorological Society*, vol. 144, pp. 63–75, 2018.

[170] A. Chattopadhyay, P. Hassanzadeh, and D. Subramanian, "Data-driven predictions of a multiscale lorenz 96 chaotic system using machine-learning methods: reservoir computing, artificial neural network, and long short-term memory network," *Nonlinear Processes in Geophysics*, vol. 27, no. 3, pp. 373–389, 2020.

[171] D. J. Gagne II, H. M. Christensen, A. C. Subramanian, and A. H. Monahan, "Machine learning for stochastic parameterization: Generative adversarial networks in the lorenz '96 model," *Journal of Advances in Modeling Earth Systems*, vol. 12, no. 3, p. e2019MS001896, 2020. e2019MS001896 10.1029/2019MS001896.

[172] M. Gelbrecht, V. Lucarini, N. Boers, and J. Kurths, "Analysis of a bistable climate toy model with physics-based machine learning methods," *The European Physical Journal Special Topics*, vol. 230, no. 14, pp. 3121–3131, 2021.

[173] R. Blender and V. Lucarini, "Nambu representation of an extended lorenz model with viscous heating," *Physica D: Nonlinear Phenomena*, vol. 243, no. 1, pp. 86 – 91, 2013.

[174] A. E. Sterk and D. L. van Kekem, "Predictability of extreme waves in the lorenz-96 model near intermittency and quasi-periodicity," *Complexity*, vol. 2017, p. 9419024, 2017.

[175] G. Hu, T. Bódai, and V. Lucarini, "Effects of stochastic parametrization on extreme value statistics," *Chaos: An Interdisciplinary Journal of Nonlinear Science*, vol. 29, no. 8, p. 083102, 2019.

[176] A. Trevisan and F. Uboldi, "Assimilation of standard and targeted observations within the unstable subspace of the observation–analysis–forecast cycle system," *Journal of the atmospheric sciences*, vol. 61, no. 1, pp. 103–113, 2004.

[177] J. Brajard, A. Carrassi, M. Bocquet, and L. Bertino, "Combining data assimilation and machine learning to emulate a dynamical model from sparse and noisy observations: A case study with the lorenz 96 model," *Journal of Computational Science*, vol. 44, p. 101171, 2020.

[178] D. S. Wilks, "Comparison of ensemble-mos methods in the lorenz '96 setting," *Meteorological Applications*, vol. 13, no. 3, p. 243–256, 2006.

[179] W. Duan and Z. Huo, "An Approach to Generating Mutually Independent Initial Perturbations for Ensemble Forecasts: Orthogonal Conditional Nonlinear Optimal Perturbations," *Journal of the Atmospheric Sciences*, vol. 73, pp. 997–1014, 02 2016.

[180] S. Hallerberg, D. Pazo, J. M. Lopez, and M. A. Rodriguez, "Logarithmic bred vectors in spatiotemporal chaos: Structure and growth," *Physical Review E*, vol. 81, no. 6, p. 066204, 2010.

[181] M. Carlu, F. Ginelli, V. Lucarini, and A. Politi, "Lyapunov analysis of multiscale dynamics: the slow bundle of the two-scale lorenz 96 model," *Nonlinear Processes in Geophysics*, vol. 26, no. 2, pp. 73–89, 2019.

[182] R. V. Abramov and A. J. Majda, "New approximations and tests of linear fluctuation-response for chaotic nonlinear forced-dissipative dynamical systems," *Journal of Nonlinear Science*, vol. 18, no. 3, pp. 303–341, 2008.

[183] V. Lucarini and S. Sarno, "A statistical mechanical approach for the computation of the climatic response to general forcings," *Nonlinear Processes in Geophysics*, vol. 18, no. 1, pp. 7–28, 2011.

[184] V. Lucarini, "Stochastic perturbations to dynamical systems: A response theory approach," *Journal of Statistical Physics*, vol. 146, no. 4, pp. 774–786, 2012.

[185] G. Gallavotti and V. Lucarini, "Equivalence of non-equilibrium ensembles and representation of friction in turbulent flows: the lorenz 96 model," *Journal of Statistical Physics*, vol. 156, no. 6, pp. 1027–1065, 2014.

[186] Vissio, Gabriele and Lucarini, Valerio, "Mechanics and thermodynamics of a new minimal model of the atmosphere," *Eur. Phys. J. Plus*, vol. 135, no. 10, p. 807, 2020.

[187] P. Grassberger and I. Procaccia, "Measuring the strangeness of strange attractors," *Physica D: Nonlinear Phenomena*, vol. 9, no. 1, pp. 189–208, 1983.

[188] R. Barrio, A. Dena, and W. Tucker, "A database of rigorous and high-precision periodic orbits of the lorenz model," *Computer Physics Communications*, vol. 194, pp. 76–83, 2015.

[189] D. Pazó, J. M. López, and A. Politi, "Universal scaling of lyapunov-exponent fluctuations in space-time chaos," *Phys. Rev. E*, vol. 87, p. 062909, Jun 2013.

[190] T. Laffargue, K.-D. N. T. Lam, J. Kurchan, and J. Tailleur, "Large deviations of lyapunov exponents," *Journal of Physics A: Mathematical and Theoretical*, vol. 46, p. 254002, jun 2013.

[191] R. Abraham and S. Smale, "Nongenericity of -stability," *Proc. Symp. Pure Math.*, vol. 14, p. 5 – 8, 1970. Cited by: 149.

[192] S. Dawson, C. Grebogi, T. Sauer, and J. A. Yorke, "Obstructions to shadowing when a lyapunov exponent fluctuates about zero," *Physical review letters*, vol. 73, no. 14, p. 1927, 1994.

[193] F. J. Romeiras, C. Grebogi, E. Ott, and W. Dayawansa, "Controlling chaotic dynamical systems," *Physica D: Nonlinear Phenomena*, vol. 58, no. 1-4, pp. 165–192, 1992.

[194] E. J. Kostelich, I. Kan, C. Grebogi, E. Ott, and J. A. Yorke, "Unstable dimension variability: A source of nonhyperbolicity in chaotic systems," *Physica D: Nonlinear Phenomena*, vol. 109, no. 1, pp. 81–90, 1997. Proceedings of the Workshop on Physics and Dynamics between Chaos, Order, and Noise.